UNIVERSITI TEKNOLOGI MALAYSIA

BORANG PENGESAHAN
LAPORAN AKHIR PENYELIDIKAN

TAJUK PROJEK: COMPRESSIBILITY CHARACTERISTICS OF PEAT SOIL USING LARGE STRAIN CONSOLIDOMETER

Saya NURLY GOFAR

(HURUF BESAR)

Mengaku membenarkan **Laporan Akhir Penyelidikan** ini disimpan di Perpustakaan Universiti Teknologi Malaysia dengan syarat-syarat kegunaan seperti berikut:

1. Laporan Akhir Penyehdikan ini adalah hakmilik Universiti Teknologi Malaysia.
2. Perpustakaan Universiti Teknologi Malaysia dibenarkan membuat salinan untuk tujuan rujukan sahaja.
3. Perpustakaan dibenarkan membuat penjualan salinan Laporan Akhir Penyeliclikan ini bagi kategori TIDAK TERHAD.
4. Sila tandakan (/)

☐	SULIT	(Mengandungi maklumat yang berclarjah keselamatan atau Kepentingan Malaysia seperti yang termaktub di dalam AKTA RAHSIA RASMI 1972).
☐	TERHAD	(Mengandungi maklumat TERHAD yang telah ditentukan oleh Organisasi/badan di mana penyehdikan dijalankan).
☑	TIDAK TERHAD	

TANDATANGAN KETUA PENYELIDIK

DR. NURLY GOFAR
PENSYARAH
FAKULTI KEJURUTERAAN AWAM
UNIVERSITI TEKNOLOGI MALAYSIA

Nama dan Cop Ketua Penyelidik

Tarikh : 28 Feb 2006

CATATAN : ** Jika Laporan Akhir Penyelidikan ini SULIT atau TERHAD, sila lampirkan surat daripada pihak berkuasa/organisasi berkenaan dengan menyatakan sekali sebab dan tempoh laporan ini perlu dikelaskan sebagai SULIT dan TERHAD.*

STUDY OF COMPRESSIBILITY CHARACTERISTICS OF PEAT SOIL USING LARGE STRAIN CONSOLIDOMETER

NURLY GOFAR

Laporan Projek Penyelidikan Fundamental
Vot 75137

Faculty of Civil Engineering
Universiti Teknologi Malaysia

FEBRUARY 2005

IN THE NAME OF ALLAH THE BENEFICENT THE MERCIFUL.

ACKNOWLEDGEMENT

The author would like to convey her sincere appreciation to the Research Management Center (RMC) of Universiti Teknologi Malaysia for the provision of the research grant (vot 75137) amounting to RM 43,000.00 to carry out this fundamental research. Special gratitude is dedicated to the Faculty of Civil Engineering and the staff of the Geotechnical Laboratory for their support and encouragement. The author is also indebted to his co-researcher Assoc. Prof. Dr. Khairul Anuar Kassim and research assistants (Yulindasari, Wong Leong Sing, Eng Chun Wei, Bong Ting Ting) for their assistances and sharing of ideas. Appreciations are also conveyed to those who contributed in one way or another that brought this research work to a success.

ABSTRACT

Peat has been identified as one of the major group of soil in Malaysia. The area covered by peat deposit is about 3.0 million hectare or 8% of the total area of Malaysia. Among them, 6300 Ha of peat deposit is found in West Johore i.e.: Pontian, Batu Pahat, and Muar. Despite of this fact, not much research has been focused on compression characteristics and behavior of peat.

The study was conducted to gain a better understanding on the compression behavior peat soil by using samples of peat from Kampung Bahru, Pontian, a location of peat deposit closed to UTM. Generalization of research data was not attempted in this research since it is fully understood that the properties of peat soil are uniquely site specific.

The study focuses on the analysis of compressibility characteristics of peat soil based on the time-compression curves obtained from Oedometer and Rowe consolidation tests and the effects of surcharge on the behavior of peat soil.

The sampling of the peat soil was designed and executed in such a way that disturbance could be minimized. Preliminary laboratory test was conducted to identify the soil and to compare the results to published data especially on Malaysia's peat. Oedometer test was done to establish the bases for the selection of range of pressure to be applied to the hydraulic consolidation test. The evaluation on compressibility parameters was made based on the results of large strain consolidation test. Analysis of settlement was performed for a hypothetical problem.

The results showed that the peat soil found in Kampung Bahru, Pontian can be classified as fibrous peat with a very high organic content which is typical of peat soil in Peninsular Malaysia. Degree of decomposition according to von Post scale is H_4. Undrained shear strength is very low (2 - 3 kPa); the fact discourages the construction work to take place on the deposit. Initial permeability is 1.20×10^{-4} m/s which is similar to that of sand and it is decreases significantly with pressure.

The results of both oedometer test and large strain consolidation test indicate that the secondary settlement is dominant in fibrous peat under study. However, the analysis of settlement showed that the large portion of settlement is still due to primary consolidation owing to the high initial void ratio and the time required for the completion pore water pressure dissipation. The results also showed that the secondary consolidation can be better evaluated by large strain consolidation test.

ABSTRAK

Tanah gambut dikenalpasti sebagai salah satu kumpulan utama tanah di Malaysia. Kawasannya meliputi lebih kurang 3 juta hektar atau 8 % jumlah dari kawasan Malaysia, diantaranya 6300 hektar dijumpai di Johor bahagian barat iaitu Pontian, Batu Pahat dan Muar. Walaupun demikian, tidak banyak kajian telah dibuat mengenai ciri kemampatan tanah gambut.

Kajian ini dilakukan untuk mendapatkan pengertian yang lebih baik tentang kelakuan kemampatan tanah gambut menggunakan contoh tanah gambut dari Kampung Bahru, Pontian yang mana kedudukannya berdekatan dengan UTM. Keputusan kajian bgi kawasan tersebut tidak akan dijadikan sebagai kesimpulan umum memandangkan sifat-sifat gambut adalah sensitif dan khusus terhadap sesuatu tempat atau lokasi.

Kajian ini tertumpu kepada analisis ciri kebolehmampatan tanah gambut berdasarkan lengkung masa-kebolehmampatan yang terhasil daripada ujian Oedometer dan Rowe dan kesan surcaj terhadap sifat tanah gambut.

Pensampelan tanah gambut direkabentuk dan dibuat supaya gangguan yang ada dapat diminimumkan. Ujikaji awal di makmal dilakukan untuk mengenalpasti tanah dan membandingkan dengan data sedia ada terutama data-data tanah gambut di Malaysia. Ujian Oedometer dilakukan untuk menghasilkan julat tekanan untuk digunakan pada ujian pengukuhan terikan besar atau Rowe. Penilaian kepada parameter kebolehmampatan dibuat berdasarkan keputusan ujian pengukuhan terikan besar. Analisis enapan dibuat berdasarkan problem rekaan.

Keputusan-keputusan menunjukan bahawa tanah gambut yang dijumpai di Kampung bahru, Pontian dapat dikelompokkan sebagai tanah gambut gentian yang mengandungi bahan organik yang tinggi yang merupakan ciri khas tanah gambut di Semenanjung Malaysia. Darjah penghuraian berdasarkan von Post adalah H_4. Kekuatan ricih tak tersalir hanya 2 - 3 kPa saja; ini menunjukkan kerja-kerja pembinaan tidak dapat dilakukan di kawasan tersebut. Ciri keboleh telapan tanah adalah sama dengan pasir iaitu 1.20×10^{-4} m/s tetapi akan berkurang selepas berlakunya tekanan.

Keputusan dari ujian oedometer dan ujian pengukuhan terikan besar menunjukkan enapan yang besar disebabkan oleh pengukuhan pertama dan pemampatan kedua. Analisis enapan menunjukkan bahawa pengukuhan pertama mangambil masa yang cukup panjang sehingga kesan surcaj kepada pengukuhan kedua sangat kecil. Keputusan ujian juga menunjukkan bahawa ujian pengukuahan terikan besar adalah lebih baik bagi mendapatkan ciri pemampatan tanah gambut.

TABLE OF CONTENTS

LIST OF TABLES

LIST OF FIGURES

LIST OF SYMBOLS

A	-	Area of sample
a	-	Primary compressibility (based on rheological model)
AC	-	Ash content
B	-	Pore pressure parameter
b	-	Coefficient of secondary compressibility (based on rheological model)
c_c	-	Compression index
c_r	-	Recompression index
c_v	-	Coefficient of rate of consolidation
$c_{\alpha\infty}$ $c_{\alpha 1}$	-	Coefficient of secondary compression
$c_{\alpha 2}$	-	Coefficient of tertiary compression
D	-	Diameter of sample
e	-	Void ratio
e_o	-	Initial void ratio
e_{op}	-	Void ratio at the beginning of secondary consolidation
FC	-	Fiber content
G_s	-	Specific gravity
H	-	Initial thickness of consolidating soil layer
H	-	Head loss due to the height of water in the burette
i	-	Hydraulic gradient
k	-	Coefficient of permeability
k_v	-	Vertical coefficient of permeability

k_{vo}	-	Initial vertical coefficient of permeability
L	-	Longest drainage path in consolidating soil layer; equal to half of H with top and bottom drainage, and equal to H with top drainage only
λ/b	-	Rate of secondary compression (based on rheological model)
M	-	Secondary compression factor
m_v	-	Coefficient of volume compressibility
OC	-	Organic content
p'	-	Consolidation pressure
p_o	-	Initial pressure
p_1	-	Inlet pressure
p_2	-	Outlet pressure
Q	-	Cumulative flow
q	-	Rate of flow
r	-	Radius of sample
T_v	-	Vertical theoretical time factor
t	-	Time
t_s	-	Time to reach end of secondary compression
t_p	-	Time to reach end of primary consolidation
t_{100}	-	Time at 100% degree of consolidation
U_r	-	Average degree of consolidation due to radial drainage
U_v	-	Average degree of consolidation due to vertical drainage
u	-	Excess pore water pressure at any point and any time
u_o	-	Initial excess pore water pressure
w	-	Natural moisture content

ΔH_s	-	Change in height of soil layer due to secondary compression from time, t_1 to time, t_2
ΔH_t	-	Change in height of soil layer due to tertiary compression from time, t_3 to time, t_4
Δp	-	Pressure difference
ε_i	-	Instantaneous strain
ε_p	-	Primary strain
ε_s	-	Secondary strain
ε_t	-	Tertiary strain
γ_w	-	Unit weight of water
σ'_v	-	Effective vertical stress
δ	-	Total compression
δ_p	-	Primary consolidation settlement
δ_s	-	Secondary compression

LIST OF APPENDICES

CHAPTER 1

INTRODUCTION

1.1 Background

Peat has been identified as one of the major groups of soils found in Malaysia. In fact, 3.0 million hectares or 8% of the area is covered with peat (Huat, 2004). Some 6300 Ha of the peat-land is found in Pontian, Batu Pahat and Muar, West Johore area. On the west coast of Malaysian peninsular, the peat deposits are formed in depressions consisting predominantly of marine clay deposits or a mixture of marine and river deposits especially in areas along river courses. There are two types of peat deposit, the shallow deposit usually less than 3 m thick while the thickness of deep peat deposit in Malaysia exceeds 5 m.

Currently the utilization of peat-land in Malaysia is quite low although construction on marginal land such as peat has become increasingly necessary for economic reasons. Engineers are reluctant to construct on peat because of difficulty to access the site and other problems related to unique characteristics of peat. Thus, not much research has been focused on the behavior of peat and the development of soil improvement method for construction on peat soil.

In general, peat is grouped into two categories; amorphous peat and fibrous peat. Amorphous peat is the peat soil with fiber content less than 20%. It contains mostly particles of colloidal size (less than 2 microns), and the pore water is absorbed around the particle surface. Previous researches have found that the behavior of amorphous peat is similar to clay soil, thus evaluation of its

compressibility characteristics can be made based on Terzaghi one-dimensional theory of consolidation. Fibrous peat is the one having fiber content more than 20% and posses two types of pore i.e.: macro-pores (pores between the fiber) micro-pores (pores inside the fiber itself). The behavior of fibrous peat is very different from clay due to the existence of the fiber in the soil.

Researchers have examined fibrous peat soils from different parts of the world and their findings differ from one and another mainly due to different content of peat soils. This indicates that in term of content, fibrous peat soil differs from location to location and detailed soil investigation need to be conducted for fibrous peat soil at a particular site where a structure is intended to be constructed. The difference becomes particularly apparent especially at low vertical stresses i.e., for shallow peat deposits or in early load increments in the laboratory

One of the most important characteristics of peat is the compression behavior. Fibrous peat typically has high organic and fiber content and thus, it does not exhibit the basic tenets of the conventional clay compression behavior (Edil, 2003). Several compression models have been proposed to predict the compressibility of fibrous peat. Extension of Casagrande's curve was used for the evaluation of time compression curve derived from consolidation tests (Dhowian and Edil, 1980). Development of theory based on the test results are made by several researchers (Mesri and Choi 1985a, Mesri and Lo 1986, Mesri and Lo 1991, Mesri et al. 1994). den Haan (1996) presents "a simple and effective" model for calculating the deformation of non-brittle soft clays and peat called an "*abc*" method. The other method was based on rheological model of soil consisting of mass-spring-dashpot (Gibson and Lo (1961), and Berry and Poskit (1972)).

Most of the methods for prediction of compressibility characteristics of soil are developed based on the results of laboratory consolidation test. Several test methods have been used to study the compressibility of different type of soil including peat. The oldest and the most popular is the conventional oedometer test. More advanced testing methods have been developed for example the Rowe cell or large strain consolidometer, and constant rate of strain (CRS) test.

1.2 Objectives of Study

Based on the uniqueness of the properties of fibrous peat and the importance of compressibility of the peat in the evaluation of its response to loading, the following objectives were set for the study:

1. To identify the type of peat found in Kampung Bahru Pontian, West Johore
2. To study the compressibility characteristics of the fibrous peat based on the results of consolidation test using large stain consolidometer (Rowe Cell).
3. To evaluate the response of peat to surcharge as one method of soil improvement methods for constructions on fibrous peat.

1.3 Scope of Project

The study focuses on the compressibility characteristics of peat soil found in Kampung Bahru Pontian, West Johore and the effects of surcharge on the behavior of the peat. Thus, the interpretation of the results of the study waslimited to:

1. Peat soil found in Kampung Bahru, Pontian, West Johore.
2. Samples were obtained using block sampling method (procedure outlined in Appendix A).
3. Identification of index properties of soil include: water content, specific gravity, sieve analysis, and acidity.
4. Classification of peat was made based on degree of humification (von Post) and fiber and organic content.
5. Evaluation of shear strength of the peat was made by vane shear (field) and Direct shear tests (laboratory)
6. Use of Oedometer test data to determine the range of pressure and estimate on Time-Compression curve to be used in Hydraulic consolidation test (Rowe Cell).

7. Evaluation of compressibility characteristics was made based on the results of Hydraulic consolidation test (Rowe Cell).
8. Evaluation on the effect of surcharge was also made based on the results of Hydraulic consolidation test (Rowe Cell).

CHAPTER 2

LITERATURE REVIEW

2.1 Peat Soil

Peat is a mixture of fragmented organic material formed in wetlands under appropriate climatic and topographic conditions. The deposit is generally found in thick layers on limited areas. The soil is known for its low shear strength and high compressibility which often results in difficulties when construction work has to take place on peat deposit. These characteristics put the peat soil in a problematic category. The low strength often causes stability problem and consequently the applied load is limited or the load has to be placed in stages. Large deformation may occur during and after construction period both vertically and horizontally, and the deformation may continue for a long time due to creep.

In general peat is grouped into two categories: amorphous granular peat and fibrous peat. Amorphous peat is the peat soil with fiber content less than 20%. It contains mostly particles of colloidal size (less than 2 microns), and the pore water is absorbed around the particle surface. The behavior of amorphous granular peat is similar to clay soil. Fibrous peat is the one having fiber content more than 20% and posses two types of pore i.e.: macro-pores (pores between the fibers) micro-pores (pores inside the fiber itself). The behavior of fibrous peat is very different from clay due to the fiber in the soil. Fibrous peat is a mixture of fragmented organic material formed in wetlands under appropriate climatic and topographic conditions. The soil has essentially an open structure with interstices filled with a secondary structural arrangement of non-woody, fine fibrous material (Dhowian and Edil, 1980). Fibrous

peat differs from amorphous peat in that it has a low degree of decomposition, fibrous structure, and easily recognizable plant structure. The compressibility of fibrous peat is very high and so the rate of consolidation.

2.1.1 Sampling of Peat

Sampling of fibrous peat involves a lot of difficulties related to the high water table and the nature of the fiber. Sampling methods vary with the peat texture, water content, and the expected use of samples. In general, there are two types of samples; disturbed and undisturbed samples.

Disturbed samples can be used for identification purpose. Block sampling and piston sampler can be used to obtain samples at shallow depth (Noto, 1991). For deeper elevation, screw augers and split spoon sampler can provide disturbed sample. The success rate of samplers in the standard penetration test (split spoon sampler or Raymond sampler) is about 90 % for peat containing some clay, but can be as low as 68-89 % for typical peat. The reliability of sampling method is sometimes further reduced and may be zero because of dropping off.

It is virtually impossible to obtain undisturbed samples of any type of soil, including peat. Both physical intrusions of the sampler and the removal of *in situ* stresses can cause disturbance. However, using certain sampling techniques, disturbance can be minimized. There was a reasonably well-established understanding of the causes of disturbance during sampling, transport, and handling of inorganic clays and corresponding accepted practices for sampling of soils. However, for sampling of peat, additional factors such as compression while forcing the sampler into the ground, tensile resistance of fibers near the sampler edge during extraction of the sampler, and drainage and internal redistribution of water must be considered.

Kogure and Ohira (1977) pointed out the difficulties associated with the use of most standard soil samplers because of the presence of fibers in peat. During sampling, most samplers do not cut the peat fibers causing a great distortion and

compression of the peat structure. Therefore the sharpness of cutting edge is very important to ensure the quality of sample. Additional disturbance takes place from water drainage while extracting the peat sample, thus extraction of sample should be done with extra care to minimize the loss of water.

Undisturbed samples can be obtained at shallow depth by block sampling method, while large diameter tube sampler modified by adding sharp cutting edge may be used to obtain sample at depth. Lefebvre (1984) claimed that both methods give good quality samples for obtaining engineering characteristics of peat.

For block sampling method, typically a pit is excavated and blocks of peat are removed from the pit wall. Other way is to excavate the surroundings of a sampling site so that samples can be removed from the perimeter.

Landva et al. (1983) attributed the disturbance during sampling to the loss of volume with the presence of gas, the loss of moisture, and the deformation of the peat structure. Large block samples (250 mm-square) can be obtained from below the ground and groundwater surface (down to a depth of 175 mm) using a block sampler for peat. Large-size down-hole block samplers such as Sherbrooke sampler (250-mm. in diameter) and Laval sampler (200-mm in diameter) that have been developed for sampling clays can also be used for organic soils and probably for peat. They also suggested that large diameter (> 100 mm) thin walled fixed piston sampler can be used in the same way as in soft clay when obtaining undisturbed peat sampler. This is especially useful for obtaining deeper sample. Recovery ratio is above 95% except for fibrous peat containing tough fibers (Noto, 1991).

Hobbs (1986) stated that even-though block sampling is ideal for minimizing peat sample disturbance; it is only feasible for shallow deposits. He recommended using tube samples with double barrel cutters to reduce disturbance an applying a correction to the void ratio as follows:

$$e_c = e_o = (e_m + \varepsilon_s) \times (1 - \varepsilon_s) \qquad (2.1)$$

where e_c, is the corrected void ratio, ε_s, is the measured compression strain during sampling, and e_m is the measured void ratio. It is not easy, however, to measure the compression strain during sampling.

2.1.2 Physical and Chemical Properties

Peat soils own a wide range of physical properties such as texture, color, water content, density, and specific gravity. Table 2.1 and 2.2 present the results of previous researches on the physical properties of peat around the world.

The texture of fibrous peat is coarse when compared to clay. This has an implication on the geotechnical properties of peat related to the particle size and compressibility behavior of peat.

Fibrous peat generally has very high natural water content due to its natural water-holding capacity. Soil fabric, characterized by organic coarse particles, holds a considerable amount of water because the coarse particles are generally very loose, and the organic particle itself is hollow and largely full of water. Previous researches have indicated that the average water content of fibrous peat is about 600%. High water content results in high buoyancy and high pore volume leading to low bulk density and low bearing capacity. The water content of peat researched in West Malaysia ranges from 200 to 700 % (Huat, 2004).

Unit weight of peat is typically lower compared to inorganic soils. The average unit weight of fibrous peat is about equal to or slightly higher than the unit weight of water. Previous researches suggested that the average unit weight of fibrous peat is about 10.5kN/m^3 (Berry, 1983). A range of 8.3–11.5 kN/m^3 is common for unit weight of fibrous peat in West Malaysia (Huat, 2004). Specific gravity of fibrous peat soil ranges from 1.3 to 1.8 with an average of 1.5. The low specific gravity is due to low mineral content of the soil. Natural void ratio of peat is generally higher than that of inorganic soils indicating their higher capacity for compression. Natural void ratio of 5-15 is common and a value as high as 25 have been reported for fibrous peat (Hanharan, 1954).

Table 2.1 Important physical and chemical properties for some peat deposits (Ajlouni, 2000)

Peat type	ω_o %	Bulk density Mg/m^3	Specific Gravity	Acidity pH	Ash content %	Reference
Fibrous-woody	484-909	-	-	-	17	Colley 1950
Fibrous	850	0.95-1.03	1.1-1.8	-	-	Hanrahan 1954
Peat	520	-	-	-	-	Lewis 1956
Amorphous and fibrous	500-1500	0.88-1.22	1.5-1.6	-	-	Lea and Browner1963
	200-600	-	1.62	4.8-6.3	12.2-22.5	Adams 1965
	355-425	-	1.73	6.7	15.9	
Amorphous to fibrous	850	-	1.5	-	14	Keene and Zawodniak 1968
Fibrous	605-1290	0.87-1.04	1.41-1.7	-	4.6-15.8	Samson and LaRochell 1972
Coarse Fibrous	613-886	1.04	1.5	4.1	9.4	Berry and Vickers 1975
Fibrous sedge	350	-	-	4.3	4.8	Levesque et al. 1980
Fibrous Sphagnum	778	-	-	3.3	1	
Coarse Fibrous	202-1159	1.05	1.5	4.17	14.3	Berry 1983
Fine Fibrous	660	1.05	1.58	6.9	23.9	NG and Eischen 1983
Fine Fibrous	418	1.05	1.73	6.9	9.4	
Amorphous Granular	336	1.05	1.72	7.3	19.5	
Peat Portage	600	0.96	1.72	7.3	19.5	Edil and Mochtar 1984
Peat Waupaca	460	0.96	1.68	6.2	15	
Fibrous Peat Middleton	510	0.91	1.41	7	12	
Fibrous Peat Noblesville	173-757	0.84	1.56	6.4	6.9-8.4	Edil and Mochtar 1984
Fibrous	660-1590	-	1.53-1.68	-	0.1-32.0	Levebre et al. 1984
Fibrous Peat	660-890	0.94-1.15	-	-	-	Olson 1970
Amorphous Peat	200-875	1.04-1.23	-	-	-	
Peat	125-375	0	1.55-1.63	5-7	22-45	Yamaguchi et al. 1985
Peat	419	1	1.61	-	22-45	Jones et al. 1986
Peat	490-1250	-	1.45	-	20-33	Yamaguchi et al. 1987
Peat	630-1200	-	1.58-1.71	-	22-35	Nakayama et al. 1990
Peat	400-1100	0.99-1.1	1.47	4.2	5-15	Yamaguchi 1990
Fibrous	700-800	~1.00	-	-	-	Hansbo 1991
Peat (Netherlands)	669	0.97	1.52	-	20.8	Termatt and Topolnicki 1994
Fibrous (Middleton)	510-850	0.99-1.1	1.47-1.64	4.2	5-7	Ajlouni, 2000
Fibrous (James Bay)	1000-1340	0.85-1.02	1.37-1.55	5.3	4.1	

Table 2.2 Physical Properties of Peat based on Location (Huat, 2004)

Soil deposits	Natural water content(w_o %)	γ (KN/m^3)	Specific gravity (Gs)	Organic content (%)
Quebec fibrous peat	370-450	8.7-10.4	-	-
Antoniny fibrous peat, Poland	310-450	10.5-11.1	-	65-85
Co. Offaly fibrous peat, Ireland	865-1400	10.2-11.3	-	98-99
Cork amorphous peat, Ireland	450	10.2	-	80
Cranberry bog peat, Massachusetts	759-946	10.1-10.4	-	60-77
Austria peat	200-800	9.8-13.0	-	-
Japan peat	334-1320	-	-	20-98
Italy peat	200-300	10.2-14.3	-	70-80
America peat	178-600	-	-	-
Canada peat	223-1040	-	-	17-80
Hokkaido peat	115-1150	9.5-11.2	-	20-98
West Malaysia peat	200-700	8.3-11.5	1.38-1.70	65-97
East Malaysia peat	200-2207	8.0-12.0	-	76-98
Central Kalimantan peat	467-1224	8.0-14.0	1.50-1.77	41-99

Peat will shrink extensively when dried. The shrinkage could reach 50% of the initial volume. But the dried peat will not swell up upon re-saturation because dried peat cannot absorb water as much as initial condition; only 33% to 55% of the water can be reabsorbed (Mokhtar, 1998).

Generally, peat soils are very acidic with low pH values, often lies between 4 and 7 (Lea, 1956). Peat in Peninsular Malaysia is known to have very low pH values ranging from 3.0 to 4.5, and the acidity tends to decrease with depth (Muttalib et al. 1991).

The submerged organic component of peat is not entirely inert but undergoes very slow decomposition, accompanied by the production of methane and less amount of nitrogen and carbon dioxide and hydrogen sulfide. Gas content affects all

physical properties measured and field performance that relates to compression and water flow. The gas content is difficult to determine and no widely recognized method is yet available. A gas content of 5 to 10% of the total volume of the soil is reported for peat and organic soils (Muskeg Engineering Handbook 1969).

2.1.3 Classification

The physical, chemical and geotechnical characteristic commonly used for classification of inorganic soil may not be applicable to the characterization of peat. On the other hand, properties which are not pertinent to inorganic soil may be important for classification of peat. Furthermore, the ranges of values applied for some properties of inorganic soil may not be relevant for peat soil. Generally the classification of peat soil is developed based on (1) decomposition of fiber (2) the vegetation forming the organic content, and (3) organic content and fiber content.

The classification based on the degree of decomposition was proposed by Von Post (1922) in which the degree of decomposition is grouped into H_1 to H_{10}: the higher the number, the higher the degree of decomposition. Table 2.3 shows the classification of peat based on the degree of composition. The test was conducted by taking a handful of peat and when pressed in the hand, gives off marked muddy water. The pressed residue is some-what thick and the material remaining in the hand has fibrous structure. Fibrous peat with more than 60% fiber content is usually in the range of H_1 to H_4 (Halten and Wolski, 1996). The classification based on the vegetation forming the organic material is not usually adopted in engineering practice.

The most widely used classification system in engineering practice is based on organic content. A soil with organic content of more than 75% is classified as peat. Ash content is the percentage of ash to the weight of dried peat. Table 2.4 shows the classification of peat based on organic and fiber content. The ash content in most of the peat of the west coast of Peninsular Malaysia is less than 10%, showing a very high content of organic matter. This is indicated by a loss of ignition value exceeding 90 % (Muttalib et al., 1991). The peat is further classified based on

fiber content because the presence of fiber alters the consolidation process of peat from that of inorganic soil. The peat soil containing more than 20% fiber is classified as fibrous peat.

Table 2.3 Classification of Peat Based on Degree of Decomposition (von Post, 1922)

Condition of peat before squeezing				Condition of peat on sequeezing		
Degree of Humification	**Soil color**	**Degree of decomposition**	**Plant structure**	**Squeezed solution**	**Material extruded (passing between fingers)**	**Nature of Residue**
H1	White or yellow	None	Easily identified	Clear, color-less water	Nothing	Not pasty
H2	Very pale brown	Insignificant	Easily identified	Yellowish water/pale brown-yellow	Nothing	Not pasty
H3	Pale brown	Very slight	Still identified	Dark brown, muddy water not peat	Nothing	Not pasty
H4	Pale brown	Slight	Not easily identified	Very dark brown muddy water	Some peat	Some what pasty
H5	Brown	Moderate	Recogniza ble but vague	Very dark brown muddy water	Some peat	Strongly pasty
H6	Brown	Moderately strong	Indistinct (more distinct after squeezing)	Very dark brown muddy water	About one-third of peat squeezed out	Very strongly pasty
H7	Dark brown	Strong	Faintly recognizab le	Very dark brown muddy water	About one-half of peat squeezed out	Very strongly pasty
H8	Dark brown	Very strong	Very indistinct	Very dark brown pasty water	About two-third squeezed out	Very strongly pasty
H9	Very dark brown	Nearly complete	Almost recognizab le	Very dark brown muddy water	Nearly all the peat squeezed out as fairly uniform paste	Very strongly pasty
H10	Black	Complete	Not discernible	Very dark brown muddy paste	All the peat passes between the fingers;no free water visible	N/A

Table 2.4 Clasification of Peat based on organic and fiber content

Classification peat soil based on ASTM standards	
Fiber Content (ASTM D1997)	Fibric : Peat with greater than 67 % fibers
	Hemic : Peat with between 33 % and 67 % fibers
	Sapric : Peat with less than 67 % fibers
Ash Content (ASTM D2974)	Low Ash : Peat with less than 5 % ash
	Medium Ash : Peat with between 5% and 15 % ash
	High Ash : Peat with more than 15 % ash
Acidity (ASTM D2976)	Highly Acidic : Peat with a pH less than 4.5
	Moderately Acidic : Peat with a pH between 4.5 and 5.5
	Moderately Acidic : Peat with a pH between 4.5 and 5.5
	Slighly Acidic : Peat with a pH greater than 5.5 and less than 7
	Basic : Peat with a pH equal or greater than 7

Consistency or Atterberg limit is not generally used for classification of peat because plasticity gives little indication of the characteristics of peat (Hobbs, 1986), and the existence of fiber makes it difficult or impossible to run the test for determination of liquid limit and plastic limit of most peat. Nevertheless, some researchers have reported the liquid limit and plastic limit of peat soil (Huat, 2004)

2.1.4 Shear Strength

The shear strength of peat soil is very low; however, the strength could increase significantly upon consolidation. The rate of strength increase is almost one-fold as compared to soft clay with a rate of strength increase of 0.3 (Noto, 1991). The shear strength of these soils is also associated with several variables namely: origin of soil, water content, organic content and degree of decomposition.

Most peat is considered frictional or non- cohesive material (Adam, 1965) due to the fiber content, thus the shear strength of peat is determined based on drained condition as: $\tau_f' = \sigma' \tan \phi'$; however, the friction is mostly due to the fiber

and the fiber is not always solid because it is usually filled with water and gas. Thus, the high friction angle does not actually reflect the high shear strength of the soil.

Direct shear and triaxial have been used to determine the shear strength of peat soil although the results of triaxial test on fibrous peat are difficult to interpret because fiber often act as horizontal reinforcement, so failure is seldom obtained in a drained test. In addition, triaxial test in drained condition may take several weeks for peat with low permeability. Shear box is the most common test for determining the drained shear strength of fibrous peat and triaxial test under consolidated-undrained condition is common for laboratory evaluation of undrained shear strength of peat (Noto, 1991).

Previous studies indicated that the effective internal friction ϕ' of peat is generally higher than inorganic soil i.e: 50° for amorphous granular peat and in the range of 53° – 57° for fibrous peat (Edil and Dhowian, 1981). Landva (1983) indicated the range of undrained friction angle of 27° – 32° under a normal pressure of 3 to 50 kPa. The range of undrained friction angle of peat in West Malaysian is 3° – 25° (Huat, 2004).

Considering the presence of peat soil is almost always below the groundwater level, the determination of undrained shear strength is also important. This is usually done in-situ because sampling of peat for laboratory evaluation of undrained shear strength of fibrous peat is almost impossible. Some approaches to in situ testing in peat deposits are: vane shear test, cone penetration test, pressure-meter test, dilatometer test, plate load test and screw plate load tests (Edil, 2001). Among them, the vane shear test is the most commonly used; however, the interpretation of the test results must be handled with caution. An undrained shear strength of peat soil (S_u) obtained by vane shear test was in range of 3 –15 kPa, which is much lower than that of the mineral soils. A correction factor of 0.5 is suggested for the test results on organic soil with a liquid limit of > 200% (Hartlen and Wolsky, 1996).

2.1.5 Compressibility

The compression behavior of fibrous peat is different from that of clay soil. Fiber content is one of the dominant factors controlling the compressibility characteristics of peat. Others include natural water content, void ratio and initial permeability. Problems are raised when secondary compression is found as the more significant part of compression because the time rate is much slower than the primary consolidation. Subsequently the formulae used to estimate the amount of compression is different from that of clay soil.

Peat soils have unit weights close to that of water; thus, the in-situ effective stress (σ'_o) is very small and sometimes cannot be detected from the results of consolidation test. It is also very difficult to obtain the beginning of secondary consolidation t_p from the consolidation curve because the preliminary consolidation occurs rapidly. Furthermore, the secondary consolidation may start before the dissipation of excess pore water pressure is completed. The natural void ratio e_o is very high due to large pores. The e-log p' curves showed a steep slope indicating a high value of a_v and c_c. Published data on c_c ranges from 2 – 15. Ajlouni (2000) pointed out a pronounced decrease in c_v with load during consolidation due to large reduction in permeability. Ratio of c_α/c_c has been used widely to study the behavior of peat. Mesri et al. (1994) reported a range between 0.05 and 0.07 for c_α/c_c. Published data on the compressibility properties is given in Table 2.5.

2.1.6 Permeability

Permeability is one of the most important properties of peat because it controls the rate of consolidation and increase in the shear strength of soil (Hobbs, 1986). The permeability of peat depends on the void ratio, mineral content, degree of decomposition of the peat, chemistry and the presence of gas. A coefficient of permeability of 10^{-5} to 10^{-8} m/sec was obtained from previous studies (Colley, 1950 and Miyakawa, 1960).

Table 2.5 Compressibility Characteristics of some Peat Deposit (Ajlouni, 2000)

Peat	ω_o or e_o %	k_{vo} m/s	c_{vo} m^2/year	c_c	c_α/c_c	Reference
Fibrous peat	850	$4x10^{-6}$	-	10	0.06-0.1	Hanrahan 1954
Peat	520	-	-	-	0.061-0.078	Lewis 1956
Amorphous and fibrous peat	500-1500	10^{-7}-10^{-6}	14-14	2.5-5	0.035-0.083	Lea and Browner 1963
Canadian muskeg	200-600	10^{-5}	-	-	0.09-0.1	Adams 1965
Amorphous to fibrous peat	705	-	55.6	4.7-10.3	0.073-0.091	Keene and Zawodniak 1968
Peat	400-750	10^{-5}	-	-	0.075-0.085	Weber 1969
Amorphous granular peat	e_o=7	$4x10^{-7}$	64	2.6	0.05	Berry and Poskitt 1972
Fibrous peat	e_o=11	$8x10^{-7}$	16.1	4.4	0.05	
Fibrous peat	605-1290	10^{-6}	-	-	0.052-0.072	Samson and LaRochelle 1972
Fibrous peat	613-886	10^{-6}-10^{-5}	9.1	-	0.06-0.085	Berry and Vickers 1975
Fibrous peat	600	10^{-6}	-	-	0.042-0.083	Dhowian and Edil 1980
Coarse fibrous	202-1159	$1.1x10^{-6}$	-	6.4	0.055-0.064	Berry 1983
Fibrous peat	660-1590	$5x10^{-6}$-$5x10^{-5}$	-	4.5-15	0.06	Lefebvre et al. 1984
Fibrous peat	200-875	-	27.2	-	-	Olson. 1970
Amorphous peat	125-375	-	3.79	-	-	
Peat	419	$3x10^{-8}$	>6.4	-	-	Jones et al. 1986
Fibrous peat	700-800	10^{-6}	3-6	-	0.042-0.083	Hansbo 1991
Fibrous peat	370	$1.4x10^{-12}$	-	-	0.06	Den Haan 1994
Fibrous peat (Middleton)	510-850	$3x10^{-8}$-10^{-6}	20-150	6-9	0.053	Ajlouni (2000)
Fibrous peat	1000-1340	$4x10^{-7}$- $7x10^{-6}$	30-300	10-12	0.059	

Anisotropy problem is often pronounced in fibrous peat. This type of soil is known to have higher permeability in the horizontal direction as compared to the vertical direction (Edil and Dhowian, 1980) because of the orientation of fiber content in the soil. Constant head permeability and Rowe consolidation cells have been used to determine the vertical and horizontal coefficient of permeability.

2.2 Soil Compressibility

In general, the compressibility of a soil consists of three stages, namely initial compression, primary consolidation and secondary compression. While initial compression occurs instantaneously after the application of load, the primary and secondary compressions are time dependent. The initial compression is due partly to the compression of small pockets of gas within the pore spaces, and partly to the elastic compression of soil grains. Primary consolidation is due to dissipation of excess pore water pressure caused by an increase in effective stress whereas secondary compression takes place under constant effective stress after the completion of dissipation of excess pore water pressure.

The time required for the water to dissipate from the soil depends on the permeability of the soil itself. In granular soil, the process is very fast and hardly noticeable due to its high permeability. On the other hand, the consolidation process may take years in clay soil. For peat, the primary consolidation occurs rapidly due to high initial permeability and secondary compression takes a significant part of compression.

2.2.1 One-dimensional Consolidation

One-dimensional theory of consolidation developed by Terzaghi in 1925 carries an assumption that primary consolidation is due to dissipation of excess pore water pressure caused by an increase in effective stress whereas secondary compression takes place under constant effective stress after the completion of the dissipation of excess pore water pressure. Other important assumptions attached to

the Terzaghi consolidation theory are that the flow is one-dimensional and the rate of consolidation or permeability is constant throughout the consolidation process.

Consolidation characteristics of soil can be represented by consolidation parameters such as coefficient of compressibility a_v, coefficient of volume compressibility m_v, compression index c_c, and recompression index c_r. Another important characteristic of soil compressibility is the pre-consolidation pressure (σ_c'). The soil that has been loaded and unloaded will be less compressible when it is reloaded again, thus; settlement will not usually be great when the applied load remains below the pre consolidation pressure. These parameters can be estimated from a curve relating void ratio (e) at the end of each increment period against the corresponding load increment in linear scale (Figure 2.1) or log scale (Figure 2.2).

Consolidation is a result of gradual dissipation of excess pore water pressure from a clay layer. The time rate of consolidation, and subsequently the time required for a certain degree of consolidation to take place, can be obtained based on plot of compression against time for each load increment. The Hydrodynamic equation governing the Terzaghi one-dimensional consolidation is:

$$c_v \frac{\partial^2 u_e}{\partial z^2} = \frac{\partial u_e}{\partial t} \tag{2.2}$$

where u_e is the excess pore water pressure at time t and depth z, and c_v is the coefficient of rate of consolidation (m^2/year or m^2/sec) which contains the material properties that govern the consolidation process.

$$c_v = \frac{k_v}{\gamma_w} \frac{1+e_o}{a_v} \tag{2.3}$$

General solution to Equation 1 is given by Taylor (1948) in terms of a Fourier series expansion of the form:

$$\mu = (\sigma_2' - \sigma_1') \sum_{n=0}^{n=\infty} f_1(Z) f_2(T_v) \tag{2.4}$$

where Z and T_v are non-dimensional parameters. Z is geometry factor, which is equal to z/H, and T_v is Time factor, in which:

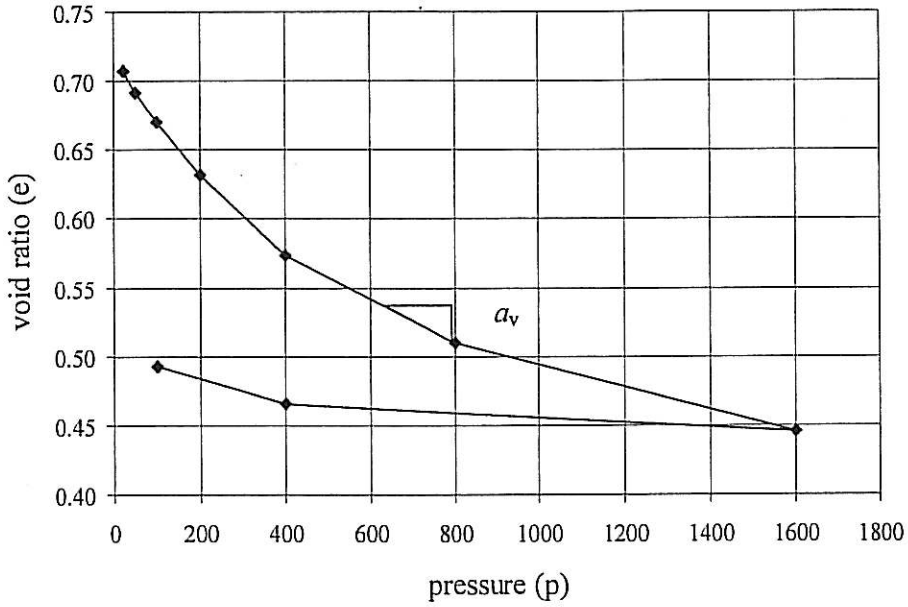

Figure 2.1 Plot of Void ratio vs. pressure in linear scale

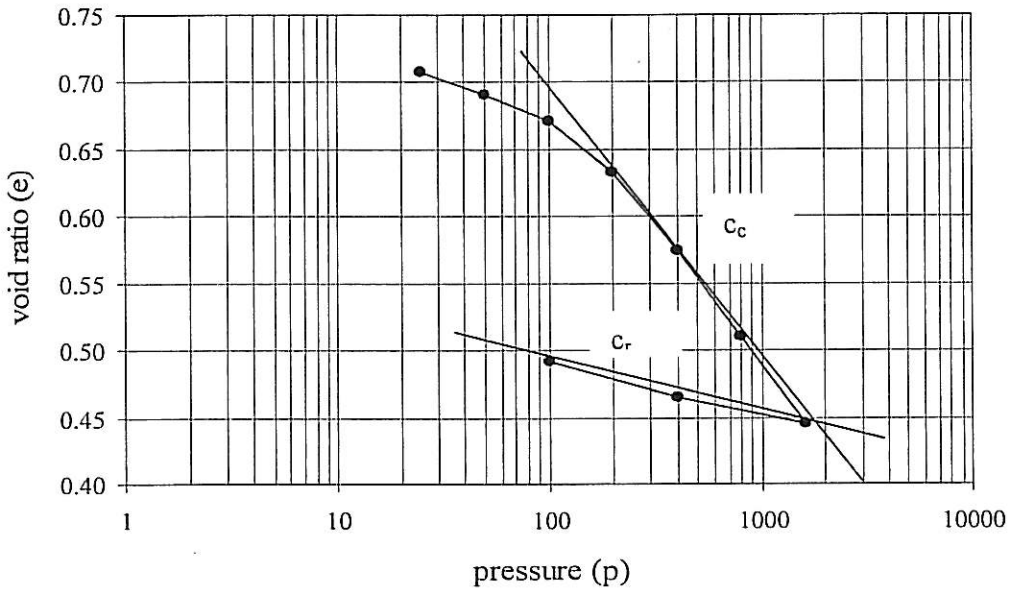

Figure 2.2 Plot of void ratio vs. pressure in logarithmic scale

$$T_v = \frac{c_v\, t}{H_d^{\,2}} \qquad (2.5)$$

The relationship between the average degree of consolidation U_{avg} and T_v can be observe from Figure 2.3 or the following formulas:

For $U < 60\%$ $T = (\pi/4)\, U^2 = (\pi/4)\, (U\%/100)^2$ (2.6a)

For $U > 60\%$ $T = -0.933 \log (1-U) - 0.085 = 1.781 - 0.933 \log (100 - U\%)$ (2.6b)

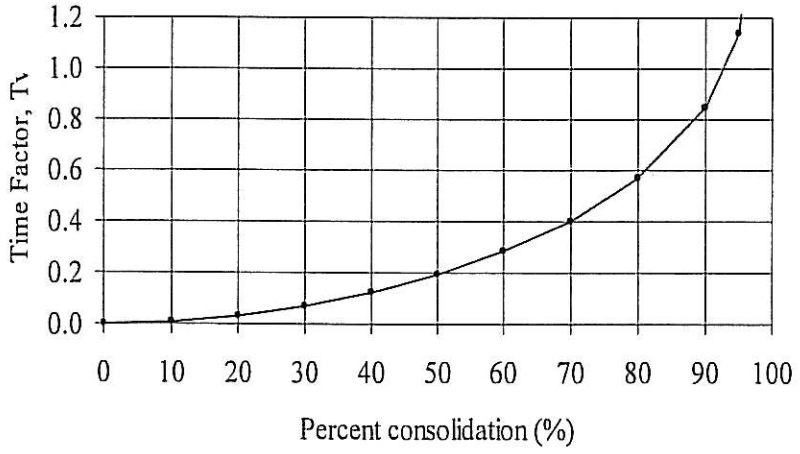

Figure 2.3 Consolidation curve (T_v vs U%) for two-way vertical drainage

The value of c_v for a particular pressure increment in oedometer test can be determined by *curve fitting* methods. There are two methods commonly used to determine the value of c_v i.e the logarithmic time (Cassagrande's) method, and the square root time (Taylor's) method. These empirical procedures were developed to fit approximately the observed laboratory test data to the Terzaghi theory of consolidation. The procedures as explained in Head (1982) are given in Appendix F.

2.2.2 Secondary Compression

For some soils, especially those containing organic material, the compression does not cease when the excess pore water pressure has completely dissipated but continues at a gradually decreasing rate under constant effective stress. Thus, it is common to differentiate the two processes as primary and secondary compression.

Secondary compression, also referred as creep, is thought to be due to the gradual readjustment of the clay particles into a more stable configuration following the structural disturbance caused by the decrease in void ratio, especially if the clay is laterally confined.

Previous researchers have shown that both primary and secondary compressions can take place simultaneously. However, it is assumed that the secondary compression is negligible during primary compression, and is identified after primary consolidation is completed. Secondary compression of soil is conveniently assumed to occur at a slower rate after the end of primary consolidation. The rate of secondary compression in the oedometer test can be defined by the slope (c_a) of the final part of the void ratio versus log time curve (Figure 2.4).

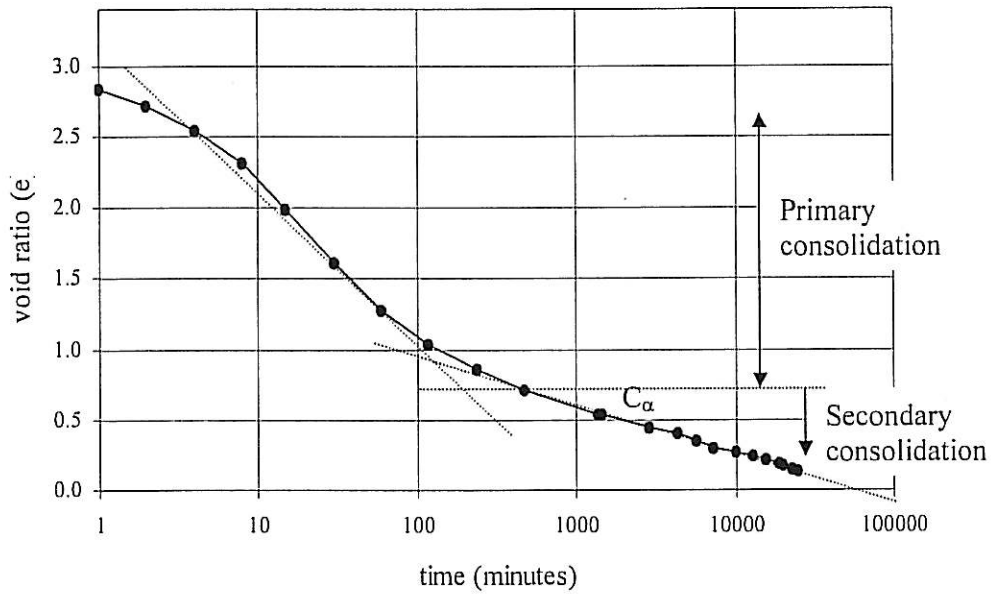

Figure 2.4 void ratio vs log time curve

Cassagrande defined the slope as:

$$C_a = \frac{\Delta e}{\Delta \log t} = \frac{\Delta e}{\log \frac{t_f}{t_p}} \qquad (2.7)$$

and the rate of secondary compression can be expressed as:

$$C_{\alpha\varepsilon} = \frac{C_\alpha}{1+e_o} \tag{2.8}$$

where Δe is the change of void ratio from t_p to t_f. t_p denotes the time of the completion of primary consolidation, while t_f is the time for which the secondary consolidation settlement is required. The void ratio at time t_p is denoted as e_o. This estimate is based on assumptions that c_α is independent of time, thickness of compressible layer and applied pressure. Research showed that the ratio of c_α/c_c is almost constant and varies from 0.025 to 0.1 for normally consolidated soil (Holtz and Kovacs, 1981).

2.3 Consolidation of Fibrous Peat

The predictions of settlement based on Terzaghi's theory of consolidation have been in reasonable agreement with a large number of laboratory tests results. However, in many other cases, the theory has not accurately predicted the laboratory and field results for highly compressible clays and organic soils. Subsequently, many theories of consolidation have been developed mainly as modifications to Terzaghi's theory. Such modifications, mostly intended for soft clays and silts, include the decrease in permeability with the progress of consolidation, the changes in compressibility during consolidation, time-related compressibility during and after the primary consolidation phase, the finite value of strains, and the effect of self weight. Among these theories, few were developed solely to model consolidation of fibrous peat. Table 2.6 presents the basic assumptions in the development of the compressibility theories for peat. These methods can be summarized in four categories: (1) based on time – compression curve derived from one-dimensional consolidation test, (2) based on finite strain model, and (3) based on rheological model of soil and (4) 'abc' model.

Table 2.6 Theories of Consolidation for Peat and their Basic Assumptions (Ajlouni, 2000)

Reference	c_v	Permeability	Strain	$e - \sigma'$	Self weight	Time effects
Terzaghi (1923)	constant	Constant	small	a_v constant	no	not included
Berry & Poskitt (1969)	variable	c_k constant	finite	c_c constant	no	Included during primary consolidation only
Mesri & Choi (1985)	variable	c_k constant	finite	c_c variable	no	included
Lan (1992)	variable	c_k constant	finite	$\sigma' = f(e,e')$	no	Included
den Haan (1996)	variable	c_k constant	finite	$\frac{\ln(1+e)}{\ln p}$ constant	no	included

2.3.1 Time-Compression curve

Figure 2.5 shows three types of time-compression curve derived from laboratory test (Leonards and Girault, 1961). Type I curve is defined by Terzaghi's theory with S-shaped curve. The separation of primary and secondary compression from Type I curve is relatively easy because it follows that the secondary compression occurs at a slower rate after the dissipation of pore water pressure. Identification of the beginning of secondary consolidation (t_p) and the rate of secondary compression (c_α) for type I curve can be estimated based on Cassagrande method by taking two straight lines from compression - log time curve and the point of intersection is identified as the end of primary consolidation ($t_p = t_{100}$). The procedures as given in Head (1986) are given in Appendix F.

Researches showed that the time compression curves derived from results of one-dimensional consolidation test on fibrous peat soil do not follow the type I curve. They resemble the type II curve in which the primary consolidation is very rapid and secondary compression does not vary linearly with logarithmic of time and tertiary compression is actually observed after secondary compression. Therefore the quantification of secondary compression based on conventional (Cassagrande) method frequently under-estimate the settlement. Dhowian and Edil (1980) extended

the Cassagrande method to include the nonlinearity of secondary compression of fibrous peat by a coefficient of secondary compression, $c_{\alpha 1}$, and coefficient of tertiary compression, $c_{\alpha 2}$ (Figure 2.6). In this case, time of secondary compression (t_s) should be identified in addition to the time for primary consolidation (t_p). The term 'tertiary strain' is introduced as a soil strain to designate the increasing coefficient of secondary compression with time. The procedure for determination of the consolidation parameters is detailed in Appendix F.

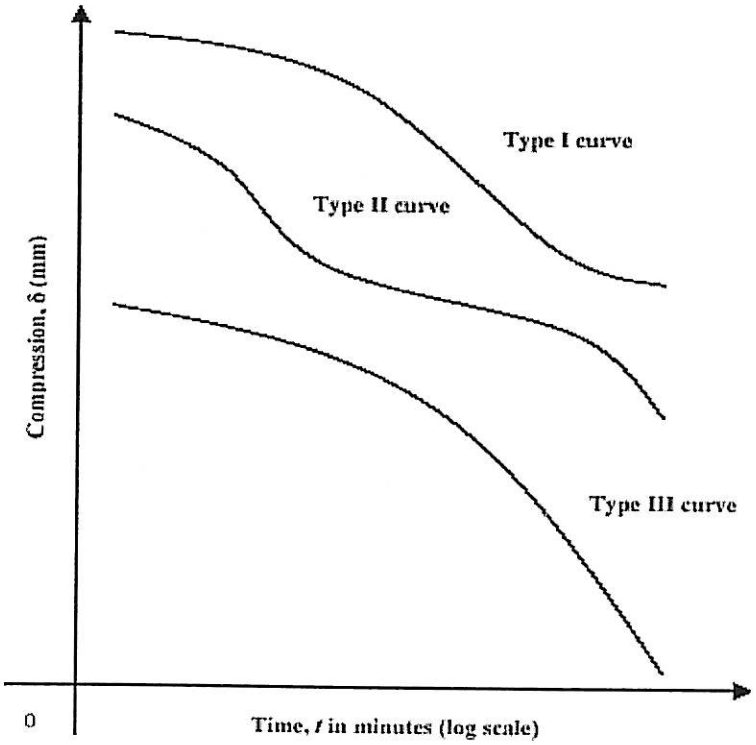

Figure 2.5 Types of time-compression curve derived from consolidation test (after Leonards and Girault, 1961)

Identification of the beginning and rate of secondary compression from Type I and Type II curves can also be made based on logarithmic of compression - logarithmic of time (logδ - log t) as proposed by Sridharan and Prakash (1998) (Figure 2.7). This relationship yields two linear portions in which the point of intersection between the two linear portions is regarded as the end of primary consolidation (t_p) or the beginning of secondary compression. An advantage of this

method is that the variation of secondary compression can be linearized over a wider extend of time. Procedure to obtain consolidation parameters by this method is described in Appedix F.

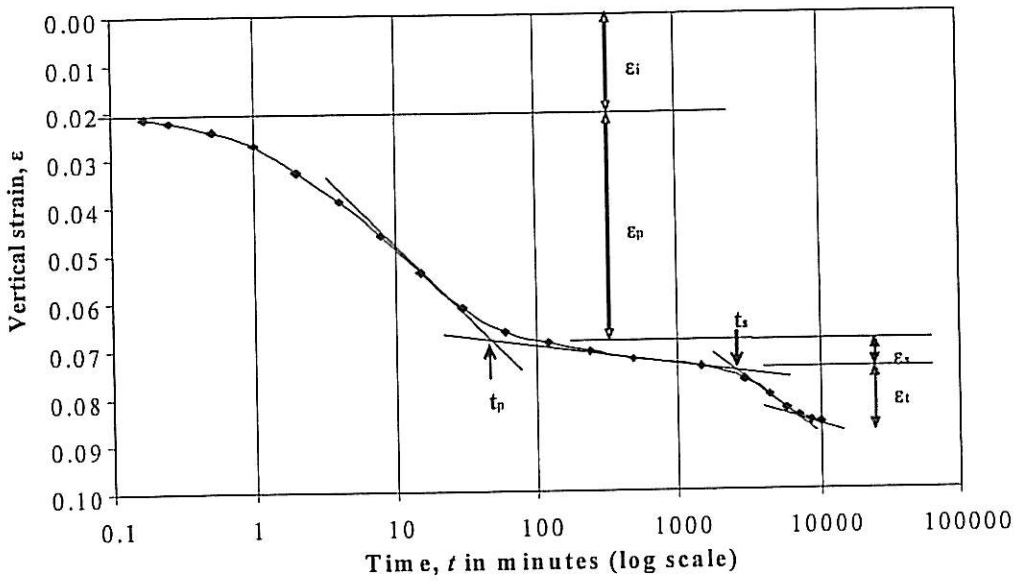

Figure 2.6: Log time-compression curve of fibrous peat soil for one-dimensional consolidation

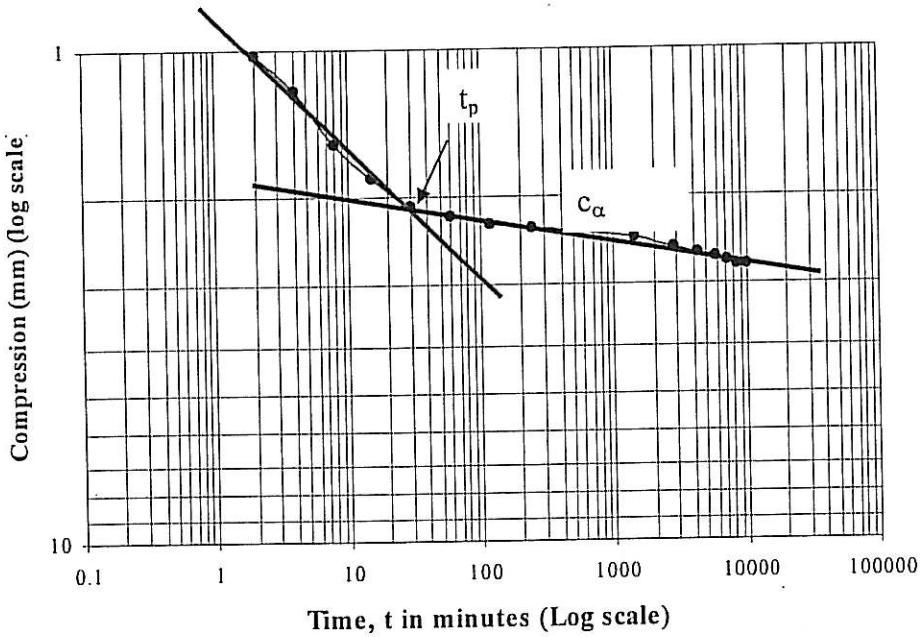

Figure 2.7 Sridharan and Prakash log δ log t curve

It is evident that the both Cassagrande and Sridharan & Prakash methods assumed that the secondary compression begins at the completion of pore-water pressure ($t_p = t_{100}$). The methods also assumed that the secondary compression occurs at a slower rate then the primary consolidation, thus t_p is obtained at the inflexion point in the curve. Therefore, the methods cannot evaluate secondary compression of soils exhibiting Type III curve (Figure 2.5) because the curve does not show an inflection point. Furthermore, previous researchers (e.g. Robinson, 1997) found that the secondary compression actually starts during the dissipation of excess pore-water pressure from the soil. Based on Terzaghi's one dimensional consolidation theory, the relationship between dissipation of excess pore water pressure and compression during primary consolidation can be represented by a straight line. Thus, Robinson (2003) suggested a method for separating the primary consolidation and secondary compression that occur during the consolidation process. The method uses a graph relating the compression and the degree of consolidation calculated from pore-water measurement from laboratory test (Figure 2.8). It should be noted that this method cannot be applied for the results of consolidation test whereby pore-water pressure was not measured during the test. The procedure is described in Appendix F.

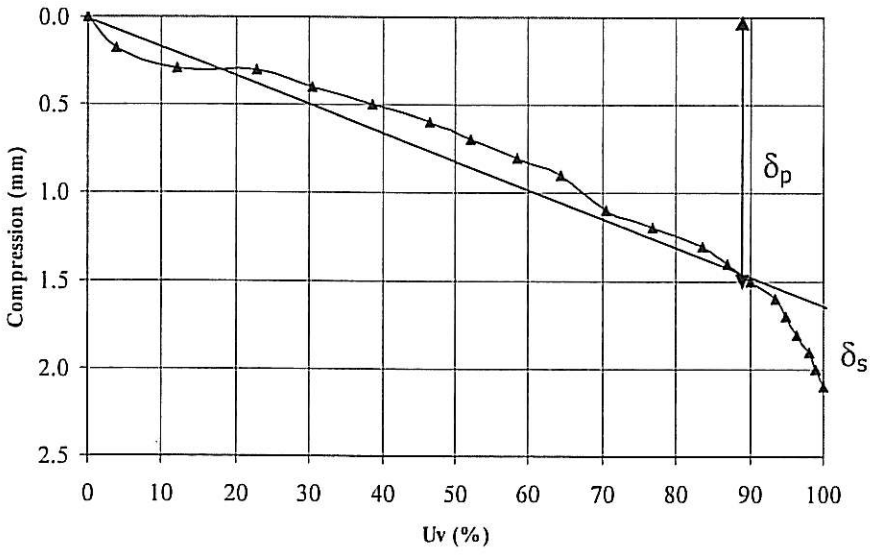

Figure 2.8 Robinson (2003) compression - degree of consolidation curve

2.3.2 Finite Strain model

Mesri and Rokhsar (1974) developed a theory of consolidation based on assumptions for soil properties that were more realistic than those in the original Terzaghi theory of one-dimensional consolidation. The assumptions were that (1) soil undergoes a finite strain; (2) the compressibility and the permeability of the soil are variable during consolidation; (3) the soil may display recompression to compression behavior with σ'_p; and (4) that soil has compressibility with effective stress and compressibility with time, both of which start to contribute at the application of a pressure increment. The time related compressibility during the primary consolidation stage was assumed to be equal to the degree of compression β multiplied by the secondary compression index c_α, measured during secondary consolidation stage.

Mesri and Choi (1985b) modified the theory of consolidation introduced by Mesri and Rokhsar (1974) to include a nonlinear relationship between void ratio and the logarithm of effective vertical stress. Another modification was that the time related compressibility was related to both the degree of compression β and the compression index c_c.

The theory was incorporated in a computer program ILLICON which was used successfully to predict time-rate of settlement and pore-water pressure dissipation during primary consolidation (Ajlouni, 2000).

2.3.3 Rheological Model

Another approach to modeling the consolidation process of peat soils is by assuming that the structure of soils exhibiting secondary compression can be evaluated based on rheological model consisting of mass-spring dashpot as shown in Figure 2.9. (Gibson and Lo 1961, Barden 1965, Barden 1968, Berry and Poskitt 1972). In this approach, the structural viscosity was assumed to be linier.

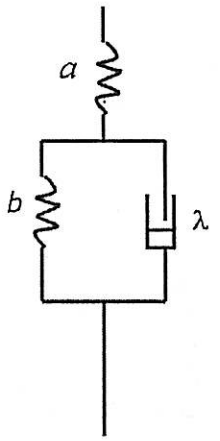

Figure 2.9 Rheological model used for soil undergoing secondary compression

Based on this model, the time-dependent strain $\varepsilon(t)$ for large values of time (t), may be written as :

$$\varepsilon(t)=\Delta\sigma\left[a-b\left(1-e^{(\lambda/b)t}\right)\right] \qquad (2.9)$$

where $\Delta\sigma$ is the increase in load, t is the time of interest, a is the primary consolidation factor, b is the secondary consolidation factor, and λ/b is the rate of secondary consolidation. Parameters a, b, and λ can be determined from the evaluation of log strain ($d\varepsilon/dt$) against time curve derived from the results of laboratory consolidation test (Edil and Dhowian, 1979). If the soil behaves as suggested by the rheological model, then the relationship of ($d\varepsilon/dt$) with time will form a straight within the range of secondary compression (Figure 2.10). The detailed procedures for estimation of a, b, and λ parameters as well as settlement calculation are given in Appendix F.

Researches have shown that there are some problems related Gibson and Lo model especially that a parameter is very sensitive to initial settlement of the soil. Both a and b are influenced by initial stress in the soil and stress applied during the test and time. Furthermore, the rate of strain ($d\varepsilon/dt$) obtained in the laboratory is usually lower than that obtained in the field, thus the values should be reduced to get actual value of λ/b. Mokhtar (1988) provided procedures to improve the accuracy of the estimation of settlement on peat soil based on Gibson & Lo model.

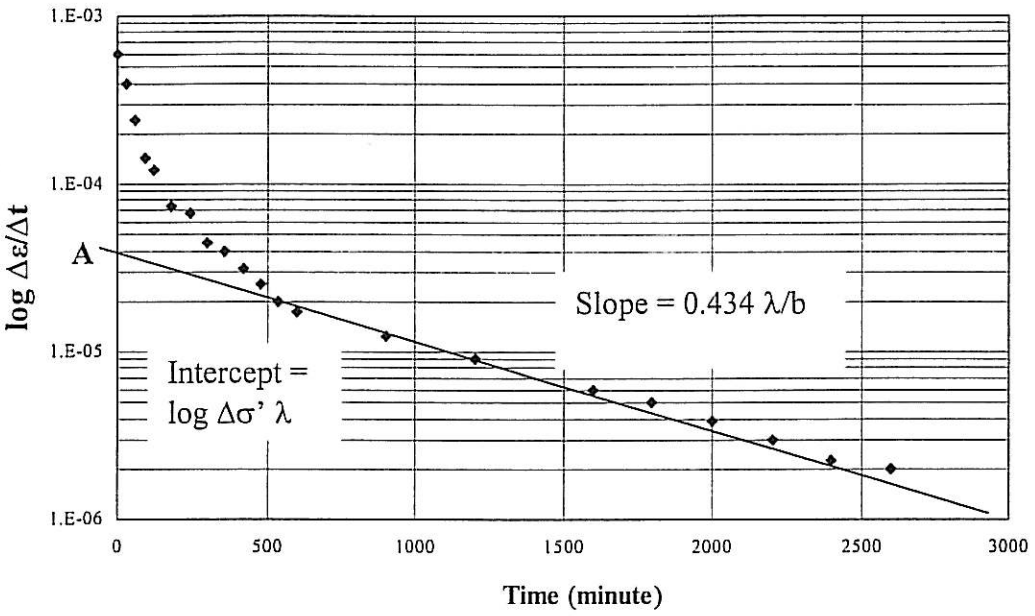

Figure 2.10: Theoretical log strain ($d\varepsilon/dt$) against time curve for Gibson and Lo model (Mokhtar, 1997)

Berry and Poskitt (1972) proposed two different rheological models to symbolize the consolidation of amorphous and fibrous peat. The models consider peat properties such as: (1) finite strain, (2) the linear relationship between void ratio and the logarithm of effective stress, (3) the linear relationship between void ratio and logarithm coefficient of permeability, and (4) the presence of time-related compressibility. The consolidation equation was solved for a single homogenous layer subjected to an increment of pressure and the solution was presented in the form of a non-dimensional graphical solution. Theoretical results that were obtained and compared with experimental data on amorphous and fibrous peat samples showed a general agreement, however: the procedure for obtaining the theoretical results includes curve fitting and arbitrary assumptions. In order to obtain the necessary parameters, the secondary part of deformation - log time relationship had to be of a constant slope. Five rheological parameters to be obtained by non conventional engineering means make it very difficult to apply this theory to data on peat.

2.3.4 "abc" model

den Haan (1996) presents "a simple and effective" model for calculating the deformation of non-brittle soft clays and peats. The constitutive model which makes use of natural strain, attributed to Hencky, and is designated by a superscript H, is defined as:

$$\varepsilon^H = -\int_{vo}^{v} \frac{dv}{v} = \ln \frac{v_o}{v} \tag{2.10}$$

where $v = 1+e$ is the specific volume, with strain measured from v_o. The relationship between the natural strain and the linear strain, attributed to Cauchy, is designated by the superscript C is:

$$\varepsilon^H = -\ln (1-\varepsilon^C) \tag{2.11}$$

Depending on the results of Butterfield (1979) and den Haan (1992), den Haan (1996) concluded that the linear relationship of In σ'_v', natural strain ε^H or the logarithm of the specific volume describe well the "virgin compression" behavior of many soils.

The model assumes that during secondary compression ε^H is linear with intrinsic time ($\tau = t-t_r$) where t is the linear time and t_r is time shift resulting from logarithmic transformation of time. τ is the time which will take the specimen to reach the present volume if the present increment had been applied to a freshly sediment state. Assuming the slope of ε^H - ln τ relationship is equal to c then

$$\varepsilon^H - \varepsilon_o^H = c \ln \frac{\tau}{\tau_o} \tag{2.12}$$

where subscript o designates the initial conditions on the intrinsic time line.

Natural strains are the summation of direct strains and secular strains as in the following:

$$\varepsilon^H = \varepsilon_d^H + \varepsilon_s^H \tag{2.13}$$

The rate of volume change is calculated as the sum of the rate of compression resulting from a stress increase, plus the creep (secular) rate, which is continuous during and after the primary stage.

$$\frac{d\varepsilon}{dt} = \varepsilon^H = \varepsilon_d^H + \varepsilon_S^H = \frac{a}{p}\frac{dp}{dt} + \frac{c}{\tau} \tag{2.14}$$

The outflow through an element of initial thickness dz applying Darcy's law yields:

$$q = -\frac{\partial}{\partial \xi}\left[k\frac{\partial}{\partial \xi}\left(\frac{u_e}{\lambda_w}\right)\right] = -\frac{v_o}{v}\frac{\partial}{\partial z}\left[k\frac{v_o}{v}\frac{\partial}{\partial z}\left(\frac{u_e}{\lambda_w}\right)\right] \tag{2.15}$$

where q is the net rate of outflow normalized by the volume v, $\partial\zeta = \frac{v_o}{v}dz$, u_e is the excess porewater pressure, and k is the permeability.

Using Terzaghi's effective stress equation to substitute for $\partial u_e/\partial z = \partial/\partial z(\sigma - p - u_s)$ where σ is the total stress and p is the applied effective stress, and u is the hydrostatic pore pressure, den Haan obtained:

$$\frac{\partial}{\partial z}(\sigma - u_e) = \frac{\gamma_S - \gamma_W}{\gamma_w} \tag{2.16}$$

where γ_s is unit weight of solids. Therefore, the hydrodynamic equation becomes:

$$q = -\frac{\gamma_S - \gamma_W}{\gamma_w}\frac{v_o}{v}\frac{\partial}{\partial z}\left(\frac{k}{v}\right) + \frac{1}{\gamma_w}\frac{v_o}{v}\frac{\partial}{\partial z}\left(k\frac{v_o}{v}\frac{\partial_P}{\partial z}\right) \tag{2.17}$$

Upon compression, the rate of volume loss resulting from the outflow of pore fluid is equated to the sum of the rate of direct strain and creep strain to obtain the constitutive equation:

$$\frac{dp}{dt} = \frac{p}{a}\left[\frac{\gamma_S - \gamma_W}{\gamma_w}\frac{v_o}{v}\frac{\partial}{\partial z}\left(\frac{k}{v}\right) + \frac{1}{\gamma_w}\frac{v_o}{v}\frac{\partial}{\partial z}\left(k\frac{v_o}{v}\frac{\partial_P}{\partial z}\right) - \frac{c}{\tau}\right] \tag{2.18}$$

The above is the consolidation equation which was solved by the finite difference technique for the boundary and initial condition, and the nonlinear permeability void ratio relationship. The solution was incorporated in a computer program called CONSEF (den Haan, 1996).

2.4 Large Strain Consolidation Test

The compressibility characteristics of a soil are usually determined from consolidation tests. General laboratory tests for measurement of compression and consolidation characteristics of a soil are: Oedometer consolidation test, Constant Rate of Strain (CRS) test, and Rowe Cell test. The procedures for these tests are fully described in BS 1377-6 and Head (1982, 1986).

2.4.1 Problems Related to Conventional Test

Although more sophisticated consolidation tests are now available, the oedometer test is still recognized as the standard test for determining the consolidation characteristics of soil. Oedometer cell can accommodate 50 mm diameter and 20 mm thick samples (Figure 2.11). Because of the relatively small specimen thickness, testing time is not excessively long and the test can be extended to a long-term test if secondary characteristics are required.

The test provides a reasonable estimate of the amount of settlement of structure on inorganic clay deposits. However, the rate of settlement is often underestimated, that is, the total settlement is reached in a shorter time than that predicted from the test data. This is largely due to the size of sample which does not represent soil fabric and its profound effect on drainage conditions. Besides the natural condition of the sample, sampling disturbance will have a more pronounced effect on the results of the test done on small samples. Furthermore, the boundary effect from the ring enhances the friction of the sample. Friction reduces the stress acted on the soil during loading and reduces swelling during unloading.

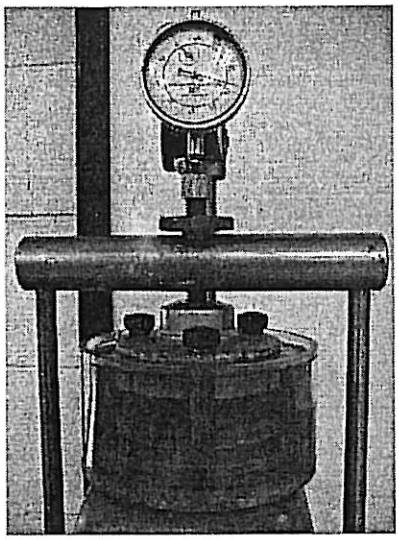

Figure 2.11 Oedometer Cell

For standard test, the samples were subjected to consolidation pressures with load increment ratio of 1. The load is applied through a mechanical lever arm system, thus: measurement can be easily affected by sudden shock. Excessive disturbance affects the e/log p plot and tends to obscure the effect of stress history; gives low values of pre-consolidation pressure and over-consolidation ratio, and gives high coefficient of volume compressibility at low stresses. Excessive disturbance also reduces the effect of secondary compression which is a very important characteristic of fibrous peat.

The other limitation of oedometer test is that there is no means of measuring excess pore-water pressures, the dissipation of which control the consolidation process. Therefore the estimation of compressibility is based solely on the change of height of the specimen.

2.4.2 Hydraulic Consolidation Test (Rowe Cell)

Rowe consolidation cell (Figure 2.12) was introduced by Rowe and Barden in 1966 to overcome the disadvantages of the conventional oedometer apparatus when

performing consolidation tests on non-uniform deposits such as fibrous peat. Rowe cell has many advantages over the conventional Oedometer consolidation apparatus. The main features responsible for these improvements are the hydraulic loading system; the control facilities and ability to measure pore water pressure, and the capability of testing samples of large diameter.

Through hydraulic loading system, the sample is less susceptible to vibration effects compared to the conventional oedometer cell. Pressures of up to 1000 kPa can be applied easily due to large sample size. Corrections required for the deformation of the loading system when subjected to pressure is negligible, except perhaps for very stiff soils. Furthermore, the hydraulic loading system enables samples of large diameter up to 254 mm diameter to be tested for practical purposes and allows for large settlement deformations.

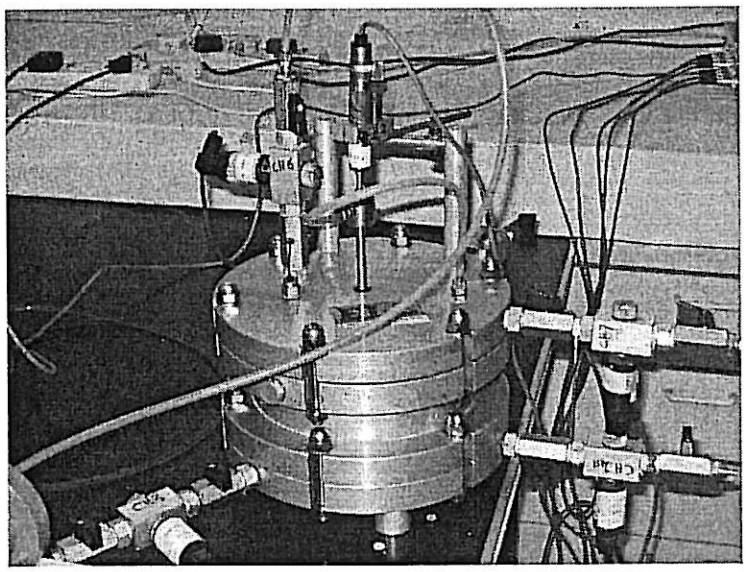

Figure 2.12 Rowe Consolidation cell

Three sizes of Rowe cell are commercially available i.e., 3 in (75 mm), 6 in (151) mm and 10 in (254 mm) diameters. The use of large samples enables the effect of the soil fabric (laminations, fissures, bedding planes) to be taken into account in the consolidation process, thereby enabling a realistic estimate of the rate of

consolidation to be made. Large samples (ie. 150 mm diameter and 50 mm thick, or larger) have been found to give higher and more reliable values of c_v, especially under low stresses, than conventional oedometer test samples (Head, 1986). Better agreement has been reported between predicted and observed rates of settlement, as well as their magnitude, may be partly due to the relatively smaller effect of structural viscosity and fabric in larger samples. Tests on high quality large diameter samples minimize the effect of sample disturbance and therefore provide more reliable data for settlement analysis than conventional one-dimensional oedometer tests on small samples.

The most important feature of Rowe cell is the ability to control drainage and to measure pore water pressure during the course of consolidation tests. Drainage of the sample can be controlled, and several different drainage conditions can be imposed on the sample. Control of drainage enables loading to be applied to the sample in the undrained condition, allowing full development of pore pressure. Consequently the initial immediate settlement can be measured separately from the consolidation settlement, which starts when the drainage line is opened.

Pore water pressure can be measured accurately at any time and with immediate response. Pore pressure readings enable the beginning and end of the primary consolidation phase to be positively established. The volume of water draining from the sample can be measured, as well as surface settlement.

The sample can be saturated by applying increments of back pressure until a B value of unity is obtained, or by controlling the applied effective stress, before starting consolidation. Tests can be carried out under an elevated back pressure, which ensures fully saturated conditions, gives a rapid p.w.p. response, and ensures reliable time relationships.

The sample can be loaded either by applying a uniform pressure over the surface (free strain), or through a rigid plate which maintains the loaded surface plane (equal strain). Fine control of loadings, including initial loads at low pressures, can be accomplished easily.

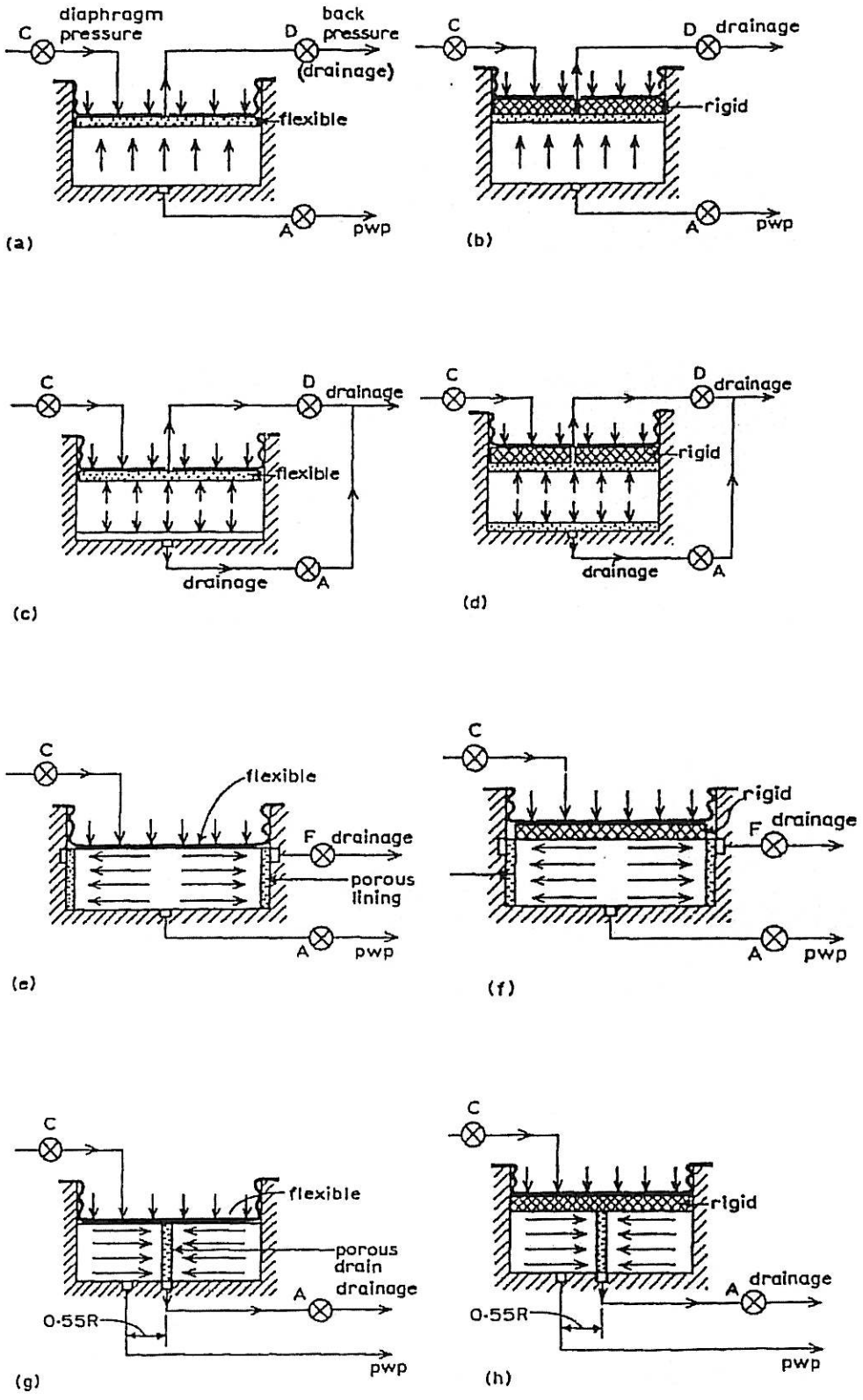

Figure 2.13 : Drainage and loading conditions for consolidations tests in Rowe cell: (a),(c), (e), (g) with 'free strain' loading, (b), (d), (f), (h) with 'equal strain' loading.

Several drainage conditions (vertical or horizontal) are possible, and back pressure can be applied to the sample. In this test, samples can be saturated and then tested under the application of back pressure. Consolidation and permeability tests can be successively conducted in Rowe cell providing data over a range of void ratios or strain. Figure 2.13 shows different type of consolidation tests using Rowe consolidometer.

2.5 Surcharging to Reduce Settlement

One of the most successful methods for accelerating the occurrence of primary settlement, and reducing and delaying the occurrence of secondary settlement is surcharging. Surcharging has long been used to reduce the secondary settlement of soft clays and peat deposits. Problems of differential settlement, and distortion and cracking in pavements were avoided by either preloading or surcharging. With all the mentioned success in implementing surcharging, no proven method is available to predict and design surcharging peculiarities for peat.

Laboratory and field work were conducted by many researchers in the past few decades in order to investigate the role of surcharging in reducing secondary compression such as Hanrahan (1954), Lea and Brawner (1963), Weber (1969), Samson and La Rochelle (1972), Samson (1985), Berry (1983), Mesri and Feng (1991), Mesri et al. (1997). They concluded that rate of settlement were reduced significantly due to surcharge and some of them related the reduction in the rate of settlement to the reduction of the water content in soil.

The effect of surcharge was studied in the laboratory consolidation test by loading – unloading – reloading sequence. Within the range of primary consolidation the stages showed a significant reduction in the compression of the peat sample. Fibrous peat did not show a significant swelling upon unloading. Beyond primary consolidation, most of the compression is due to the reorientation of the fiber in the soil or creep.

The application of surcharge is to reduce or to eliminate the stage of primary consolidation and to compensate for secondary consolidation. As discussed before, the consolidation process involves a readjustment of soil particles, especially for cohesive soil, as water is squeezed from the voids of the soil. Shear strength increased as pore water pressure decreased.

The reduction of settlement during primary consolidation can be explained as shown in Figure 2.14. The broken line represents the predicted consolidation settlement for the final height of the embankment. The solid line is the settlement versus time curve during and after surcharging. When the solid line (settlement with surcharge) reaches the final settlement of the embankment or actual structure, then it is the time for surcharge removal. It is important to emphasize that the design of pre-load should be considered as preliminary and the decision to remove the surcharge should be based on field monitoring.

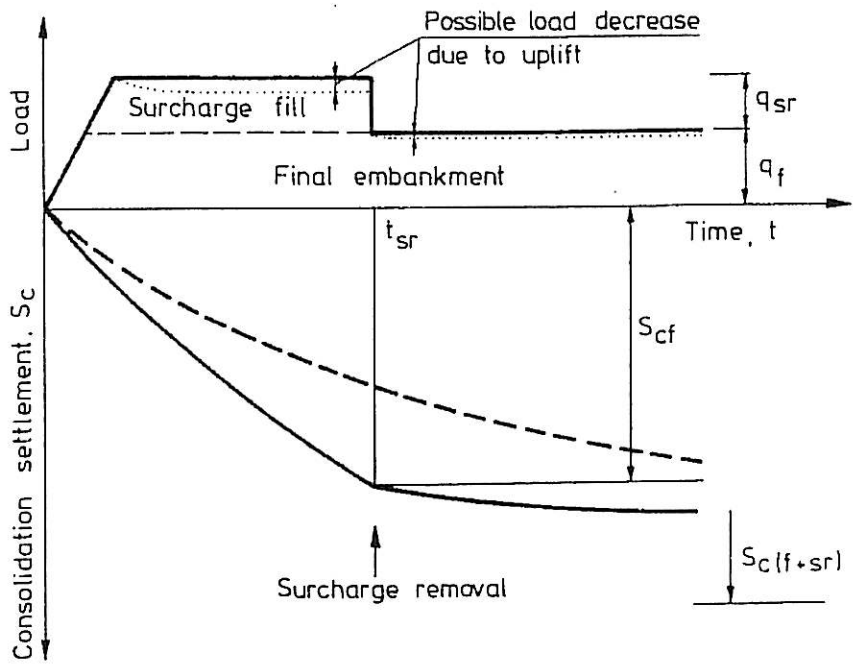

Figure 2.14 Effect of Surcharge to eliminate the primary settlement (Hartlen & Wolski, 1996).

The elimination of preliminary consolidation of peat is not very important because the duration of primary consolidation for peat deposit is short due to high initial permeability of peat which is almost equal to the permeability of sand. On the other hand, secondary compression may results in a significant settlement during the economic life of a construction. Figure 2.15 illustrates the compensation for secondary compression by temporary surcharging. It should be noted that the time for surcharge removal should be close to the end of primary consolidation of soil (t_p) because Larrson (1981) showed that the secondary settlement can take place as early as 80% degree of consolidation.

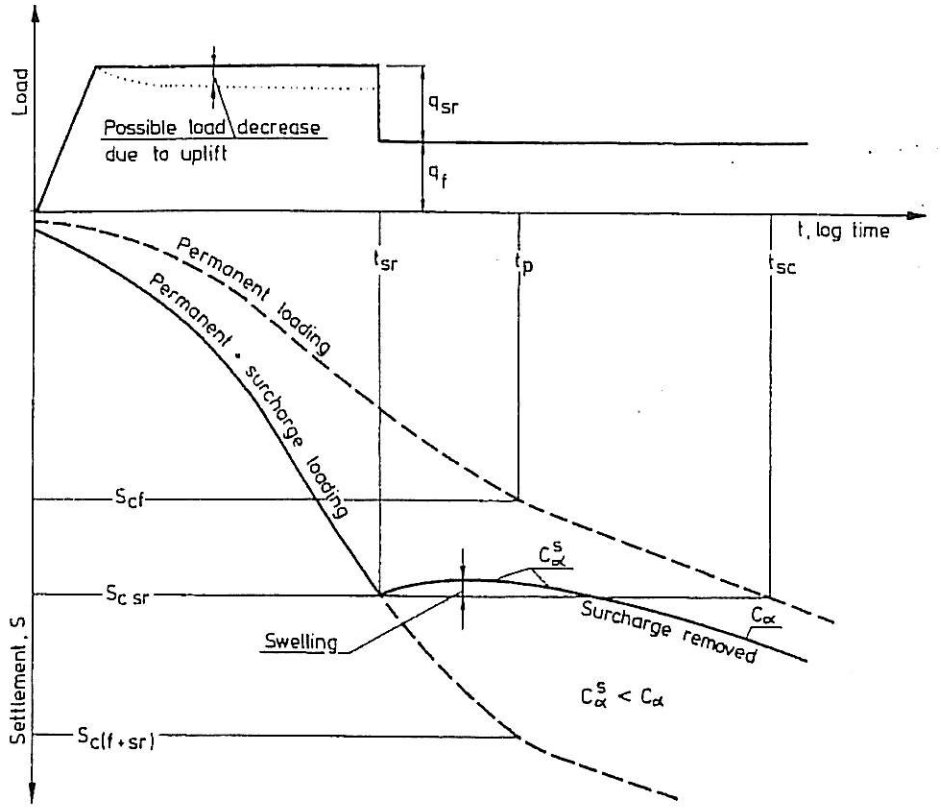

Figure 2.15 Compensation for secondary compression by temporary surcharging (Hartlen & Wolski, 1996)

The effect of surcharge on the secondary compression of peat was studied by Mesri et al. (1997) based on time-compression curve and the c_α/c_c concept presented by Mesri and Feng (1991) where total settlement without surcharging (S) is:

$$S = \frac{c_\alpha}{1+e_o} H \log \frac{t}{t_p} \qquad (2.19)$$

where H is the thickness of compressible layer, while all other parameters carry the same meaning as described in section 2.2. Total settlement with surcharge is

$$S = \frac{c''_\alpha}{1+e_o} H \log \frac{t}{t_f} \qquad (2.20)$$

in which $c''_\alpha = \Delta e / \Delta \log t$ is the post surcharge secant secondary compression index from t_1 to any time t where t_f can be obtained from Figure 2.16 as a function of R'_s and primary rebound after removal of surcharge t_{pr}. The parameter R'_s is defined in terms of effective surcharge ratio $R'_s = (\sigma'_{vs}/\sigma'_{vf}) - 1$, where σ'_{vs} is the maximum effective vertical stress reached before the removal of surcharge, and σ'_{vf} is the final effective vertical stress after the removal of surcharge (Mesri and Feng 1991). The value of t/t_f can also be obtained from Figure 2.17 if c''_α and R'_s are known.

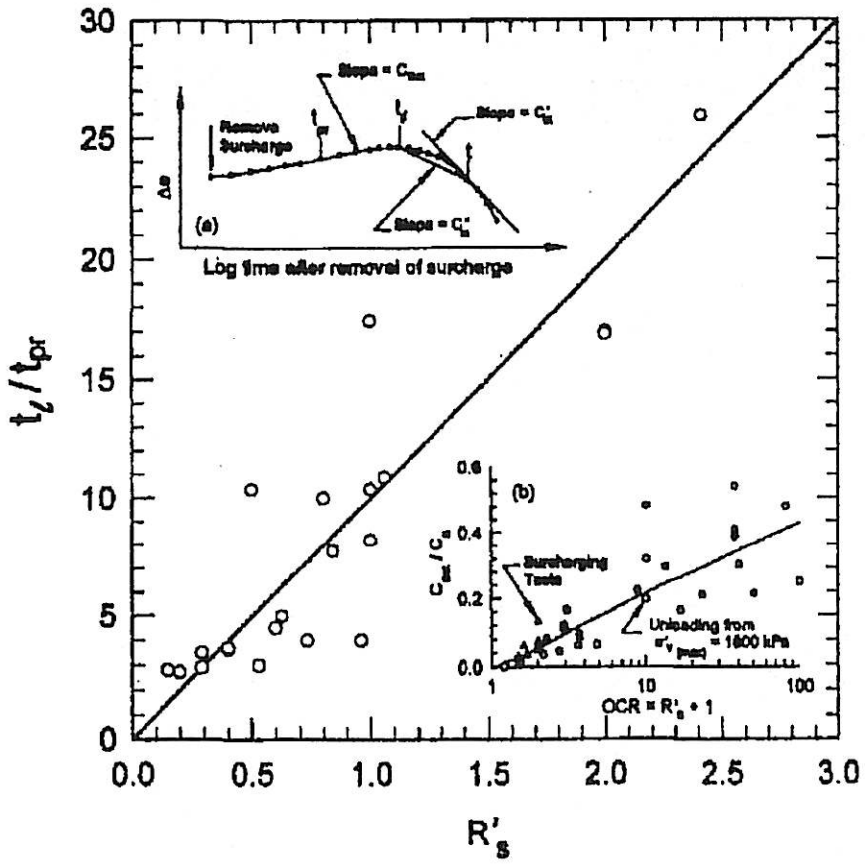

Figure 2.16 Relationship between t_f/t_{pr} vs R'_s for Middleton Peat (Mesri et al., 1997)

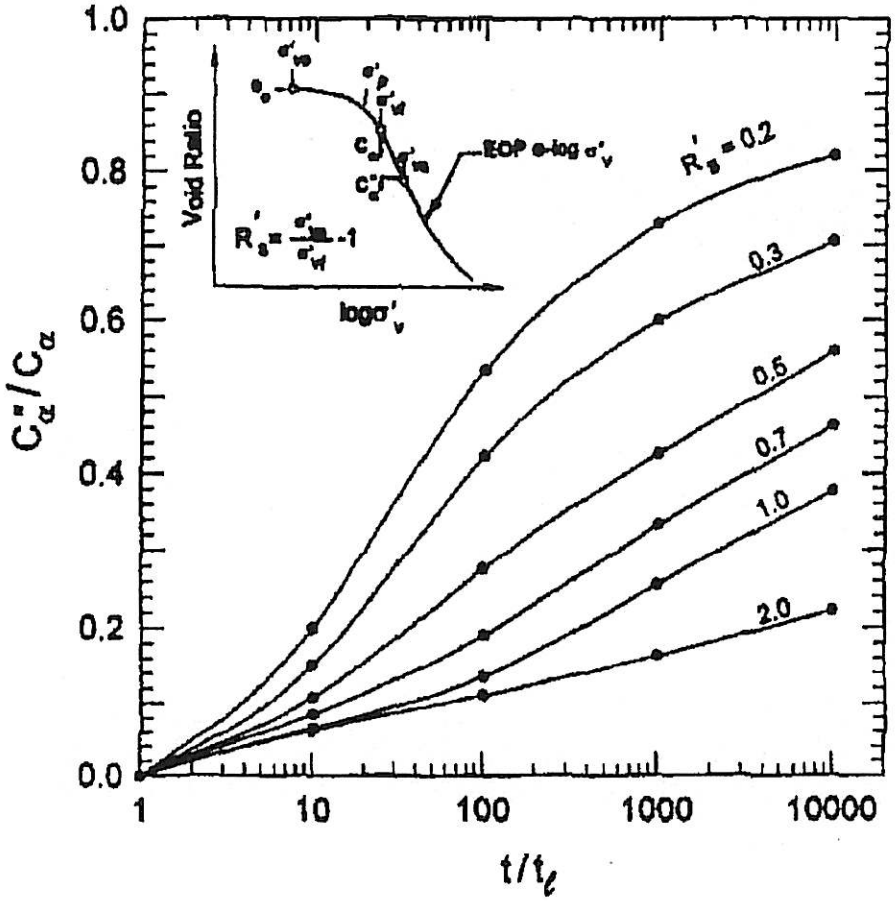

Figure 2.17 Ratio of c''_α/ c_α as Function of t/t_l, for Different Surcharging Efforts R'_s for Middleton Peat (Mesri et al, 1997)

Surcharging has been used to reduce secondary settlement of peat deposits (Lea and Brawner 1963; Samson and LaRochelle 1972; Samson 1985; Mesri, 1986; Jorgenson 1987 and Mesri and Feng 1991). According to laboratory and field post-surcharge compression measurements, explained and predicted by the c_α/c_c concept of compressibility, c'_α is expected to start with a small value and gradually increase. For practical settlement analyses, a secant secondary compression index, c''_α, is defined that allows the use of simple equation 2.20 for computing post-surcharge secondary settlements. The values of c''_α with surcharging are referenced to c_α without surcharging both defined at the same σ'_v .

Besides preloading with surcharge, improvement of fibrous peat soil is often done through staged construction. Staged construction consists in the filling of an embankment at a controlled rate so as not to cause failure but to permit an increase in shear strength due to consolidation (Hartlen and Wolski, 1996). In such a way, the obtained strengthening of the foundation soil should be sufficient to support safely the required load. Thus, in staged embankments, the pre-compression technique is used, which according to Johnson (1977) is defined as compressing the soil under an applied stress prior to placing or completing the structural load. In the case of the staged embankment, the first stage of embankment (preloading with first stage) compresses the subsoil prior to the filling of the second stage.

The improvement of compression behavior of peat by doing consolidation by staged construction can be modeled by doing consolidation settlement with constant load increment until final loading is reached.

CHAPTER 3

METHODOLOGY

3.1 Introduction

The methodology of the research is summarized in the flowchart shown in Figure 3.1. Literature study was done in this study to provide rationale of the research and to gather sufficient information on consolidation behavior of fibrous peat. Sampling for the study was carried out at Kampung Bahru, Pontian, Johor. Physical characteristics and classification of the soil were identified through laboratory tests. Engineering characteristics evaluated in this research include permeability and shear strength. Constant-head permeability tests were carried out to determine initial hydraulic conductivity of the peat. Direct shear test were performed to determine the shear strength characteristics of the peat while the evaluation of shear strength in-situ was made by field vane shear test. All laboratory test procedures are based on the manual of soil laboratory testing (Head, 1981, 1982, 1986) in accordance with the British (BS) and U.S. (ASTM) Standards.

The focus of the research was to evaluate the compressibility characteristics of fibrous peat. While data from oedometer consolidation tests were used to decide the range of consolidation pressures for hydraulic consolidation tests, and to observe the long term compression behavior of the peat, the research concentrate on the measurement of compressibility characteristics by large strain consolidometer (Rowe Cell) available in Geotechnics Laboratory, Faculty of Civil Engineering. The results from the large strain consolidation test were analyzed to develop the suitable model for predicting the compression behavior of fibrous peat under study. Comparisons

were made between the results of consolidation test using oedometer and Rowe cell. The test results were also compared with published data.

3.2 Sampling of Peat

Block sampling method was used in this study in order to obtain the samples of the fibrous peat soil from Kampung Bahru, Pontian, Johor. The method was selected because it is the best method for obtaining the most representative sample of peat at shallow depth. At the time of sampling, the groundwater table was found at depth of less then 1 m. Thus, the block sampling method was used to acquire the sample at a depth below ground water surface or between 1 to 1.5 m. The procedures for obtaining the samples is describe in Appendix A.

The soil was excavated to a depth of 1 m and then a tube of 300 mm-diameter and 300 mm high was pushed slowly into the soil. Then the surroundings of the sampler was excavated so that samples could be then cut at the base and a thin wooden plate was inserted at the bottom of the sample to cover the bottom of the sample before taking it to the surface. The quality of samples was maintained by ensuring the sharpness of the edge of the tube and knife used to cut the sample (Figure 3.2a). The top and bottom of the sample were covered by wax and wooden plate before they were transported to the laboratory. Eighteen samples were obtained from six different points, at least 2 meter apart in one location. Each samples was transported in a well cushioned wooden box and were kept in the laboratory under constant temperature (air conditioned room).

In addition to block samples, six samples were retrieved using piston sampler of diameter 105 mm and length 450 mm (Figure 3.2b). The samples were used for the determination of the natural water content and the initial permeability of the peat using the constant head permeameter.

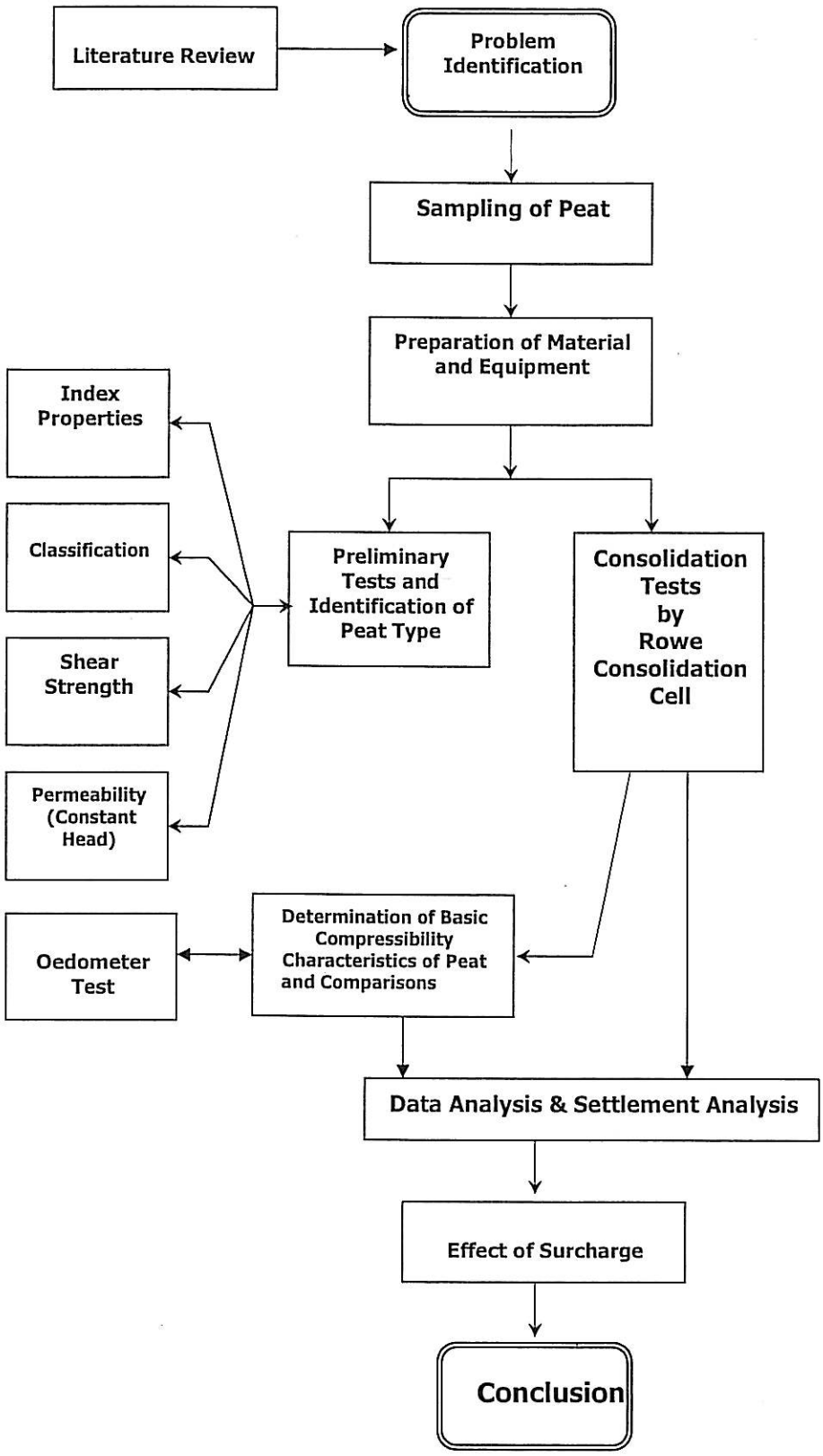

Figure 3.1 Flow chart of the study

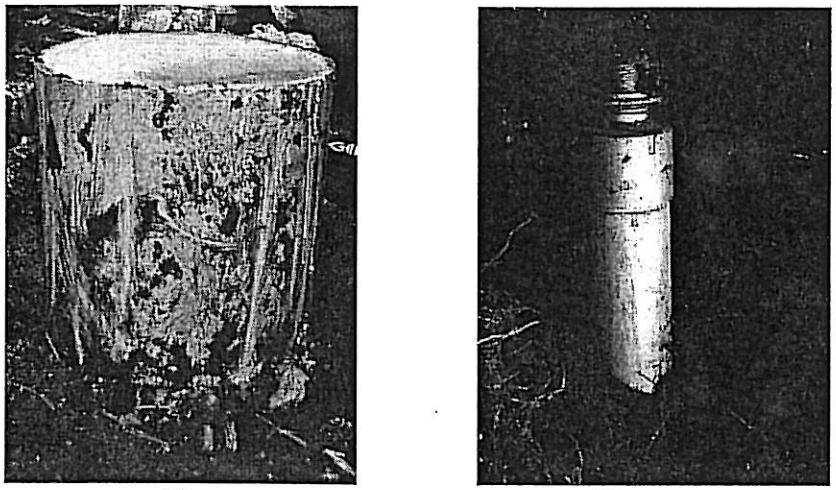

(a) (b)

Figure 3.2 Sampling methods (a) block sample, (b) piston sample

3.3 Preliminary Tests

3.3.1 Physical Properties and Classification

Several fundamental and classification tests were carried out to obtain engineering characteristics of peat. The tests for index properties included the water content (BS 1377-2), and unit weight (BS 1377-2). The determination of the specific gravity of peat soil was made using kerosene following (BS 1377-2).

The tests for classification of peat soil are Von Post degree of humification, sieve analysis (BS 1377-2). The organic content and the ash content were determined from the loss of ignition test whereby the oven dried mass of soil is further heated in muffle furnace at 440°C for 4 hours (BS1377-3). Fiber content was determined from dry weight of fibers retained on sieve no.100 sieve (> 0.15 mm opening size) as a percentage of oven-dried mass ((ASTM D1997-91). The acidity of the peat was determined from pH meter following (BS 1377-3).

3.3.2 Shear Strength

The assessment of in-situ shear strength of peat in this research was made by 65 mm diameter and 130 mm height field vane at depths of 1 and 2 m following standard procedure BS1377-9 (Figure 3.3). The smallest size vane available in the laboratory was selected in order to minimize the effect of fiber to the measured shear strength. Rotational speed of 0.1deg/sec is used in the test.

The drained shear strength of peat soil obtained in Pontian was measured by shear box test following standard procedure BS 1377-7 using normal stress of 8, 16, and 22 kPa. Determination of normal stresses used for the test is based on the estimation of overburden pressure on the soil at depth of 1 and 2 m. It should be noted that the test is in drained condition and the shear strength obtained from this test might not be an indication of the true shear properties of the peat in-situ.

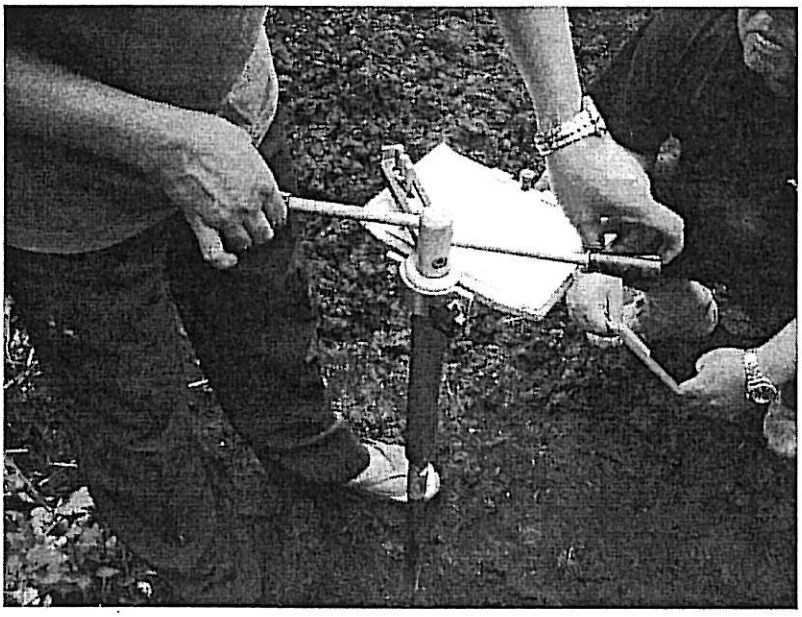

Figure 3.3 Vane shear test carried out at site.

3.3.3 Permeability

Since the peat soil can be as porous as sand, the constant head permeability test was chosen to evaluate the initial permeability of the soil. The constant head permeability test was done on sample obtained vertically and horizontally using piston sampler. The tests were performed following standard procedures of ASTM D2434 using a mould with 105.4 mm internal diameter and a height of 121.2 mm. The initial permeability of the soil was computed on the basis of the amount water that passes through the soil sample. The time for the water volume collected in a beaker from an immersion tank, with overflow was required for the computation of the rate of the permeability of the soil.

3.3.4 Standard consolidation tests

The standard consolidation tests were conducted as preliminary tests to determine the range of consolidation pressures that was suitable to be applied on the soil samples for the hydraulic consolidation tests. The procedures for the tests are based on BS 1377-5. Since the sample was taken from shallow depth (1 to 2 m), and subsequently the in-situ stress is very low, then the load applied for consolidation test started at a very low pressure. The applied loads were 12.5 kPa, 25 kPa, 50 kPa, 100 kPa, 200 kPa, and 400 kPa. Each load was maintained for two weeks or 20,000 minutes for loading stages during the first tests, but was modified to one week or 10,000 minutes upon determination of the end of primary consolidation (t_p) and secondary compression (t_s) of the soil.

3.4 Large Strain Consolidation Test (Rowe Cell)

Large strain consolidation tests were performed using Rowe consolidation cell (Figure 2.8) with internal diameter of 150 mm and height of 50 mm. Soil samples were subjected to hydraulic consolidation pressures of 25, 50, 100, and 200 kPa. This range of pressure was determined based on the results of oedometer test. The test was performed with two-way vertical drainage.

The designation of the hydraulic consolidation test with vertical drainage (two-way) is shown in Figure 3.4. In this type of test, drainage takes place from both top and bottom faces of the sample. A porous drainage disc is placed under the sample, and is connected to the same back pressure system as the top drainage line for the consolidation stages. In this type of test, drainage takes place vertically upwards and downwards while pore pressure is measured at the center of the base.

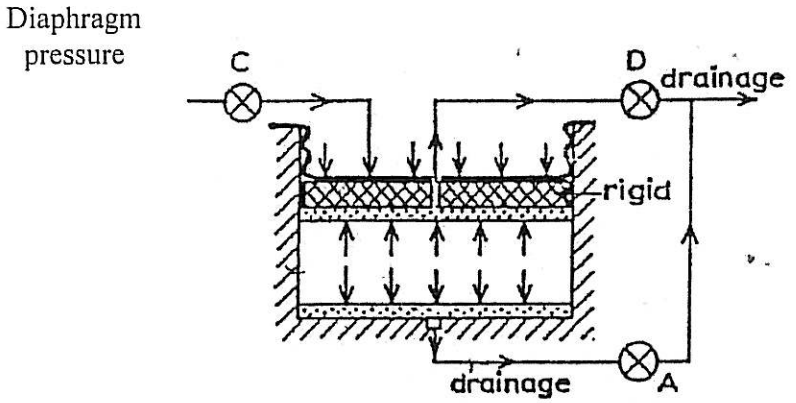

Figure 3.4: Two-way vertical drainage and loading condition for hydraulic consolidation test in Rowe cell with 'equal strain' loading (Head, 1986)

3.4.1 Cell assembly and Connections

Equipment & accessories needed for the large strain consolidation test are as follows:

1. Rowe cell (diameter 150 mm)
2. Sintered bronze porous disc 3 mm thick with typical permeability 4 x 10^{-4} m/s (the porous metal disc should be boiled after every test and carefully inspected in order to prevent a gradual build-up of fine particles).
3. Dial gage for measuring vertical settlement
4. Spare porous insert for measuring pore water pressure
5. Spare O Ring base seal
6. Spare Diaphragm
7. Flange sealing ring

8. Data Acquisition system for measurement of
    a. Diaphragm pressure
    b. Back pressure
    c. Pore water pressure
    d. Vertical settlement
    e. Volume of water draining out
    f. Time
9. Consumables: Silicone grease

The arrangement of the Rowe cell and connections are described in the following steps:

1. After covering the base with a film of water, place a saturated porous disc of sintered bronze on the cell base without entrapping any air.

2. Fit the cutting rings containing soil sample on top of the Rowe cell body (Figure 3.5). Place the sample into the Rowe cell body by slowly and steadily pushing the soil sample vertically downwards using a porous disc (Figure 3.6).

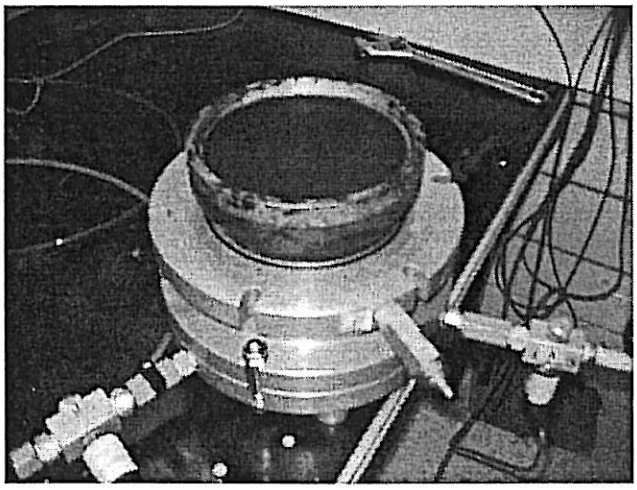

Figure 3.5: Cutting rings containing soil sample are fitted on top of the Rowe cell

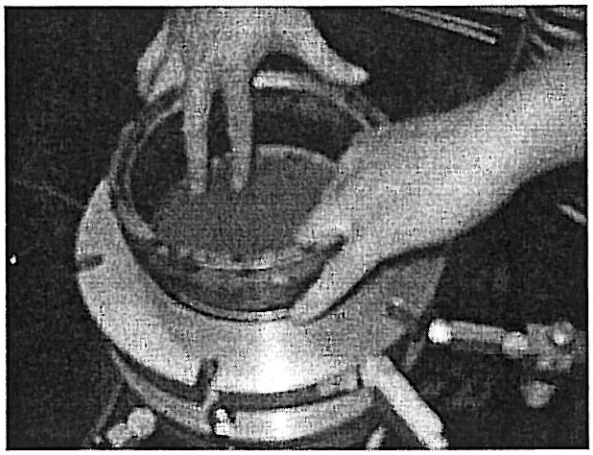

Figure 3.6: A porous disc is used to slowly and steadily push the soil sample vertically downward into the Rowe cell body

3. Flood the space at the top of the cell above the sample with de-aired water.

4. Place a saturated drainage disc through the water onto the sample by lowering into position using the lifting handle. Avoid trapping air under the plate. Ensure that there is a uniform clearance all round between the disc or discs and the cell wall.

5. Connect a tube to valve F and immerse the other end in a beaker containing de-aired water. The tube should be completely filled with de-aired water making sure that there are no entrapped air bubbles.

6. Support the cell top at three points so that it is level, and with more than enough clearance underneath for the settlement spindle attached to the diaphragm to be fully extended downwards. The cell top should be supported near its edge so that the flange of the diaphragm is not restrained. Fill the diaphragm with water using rubber tubing about one-third the volume. The way distilled water is filled into the diaphragm can be diagrammatically observed in Figure 3.7 and realistically observed in Figure 3.8. Open valve C.

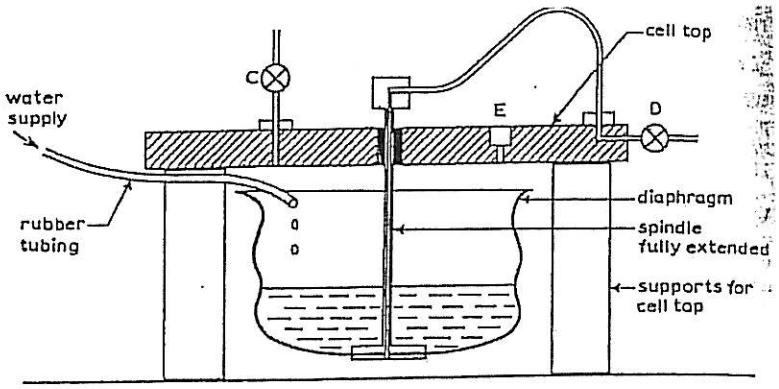

Figure 3.7: Schematic diagram of filling of distilled water into the diaphragm Head, 1986)

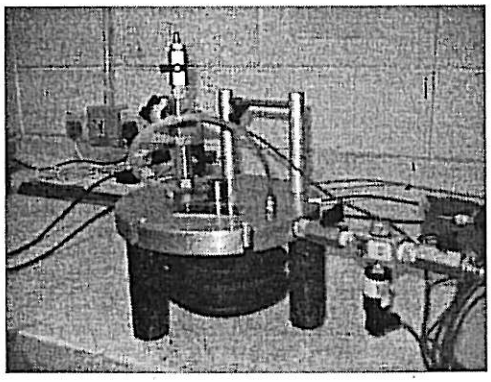

Figure 3.8: Realistic view of filling of distilled water into the diaphragm

7. Place three or four spacer blocks, about 30 mm high, on the periphery of the cell body flange. Lift the cell top, keeping it level, and lower it onto the spacers, allowing the diaphragm to enter the cell body. Bring the bolt holes in the cell top into alignment with those in the body flange.

8. Use rubber tube to add more water to the inside of the diaphragm so that the weight of water brings the diaphragm down and its periphery is supported by the cell body. Check that the cell body is completely filled with water. The whole of the extending portion of the diaphragm should be inside the cell body, and the diaphragm flange should lie perfectly flat on the cell body flange.

9. Hold the cell top while the supporting blocks are removed, then carefully lower it to seat onto the diaphragm flange without entrapping air or causing ruckling or pinching (Figure 3.9). Align the bolt holes. When correctly seated, the gap between top and body should be uniform all round and equal to a diaphragm thickness. Open valve F to permit escape of excess water from under the diaphragm.

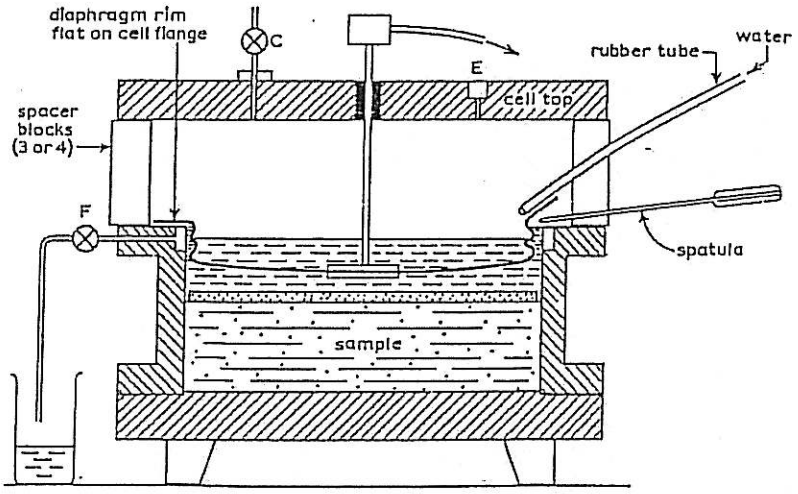

Figure 3.9: Diaphragm inserted into Rowe cell body (Head, 1986)

10. Tighten the bolts systematically (Figure 3.10). Ensure that the diaphragm remains properly seated, and that the gap between the metal ranges remains constant all round the perimeter.

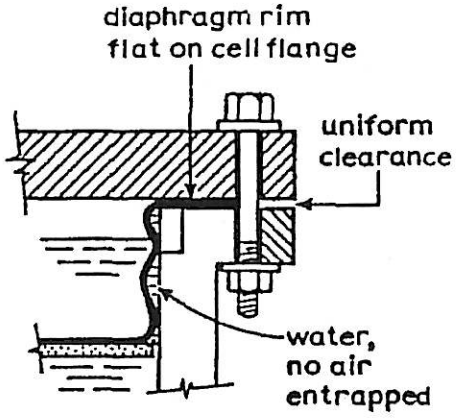

Figure 3.10: Diaphragm is correctly seated (Head, 1986)

11. Open valve D, and press the settlement stem steadily downwards until the diaphragm is firmly bedded on top of the plate covering the sample. Close valve D when no more water emerges.

12. Connect valve C to a header tank of distilled water having a free surface about 1.5 m above the sample.

13. Completely fill the space above the diaphragm with water through valve C with bleed screw E opened. Tilt the cell so that the last pocket of air can be displaced through E. Maintain the supply of water at C when subsequently replacing the bleed screw.

14. Maintain pressure at C, and as the diaphragm expands allow the remaining surplus water from above the sample to emerge through valve F. Open valve D for a moment to allow the escape of any further water from immediately beneath the diaphragm.

    Escape of water from F due to diaphragm expansion may take some considerable time because of the barrier formed by the folds of the diaphragm pressing against the cell wall.

15. Close valve F when it is evident that the diaphragm has fully extended. Observe the pore water pressure at the base of the sample, and when it has reached a constant value record it as the initial pore water pressure, u_o. This corresponds to the initial pressure p_o under the head of water connected to C. If the height from the top of the sample to the level of water in the header tank is h mm, then:

$$p_o = \frac{h \times 9.81}{1000} = \frac{h}{102} \text{ kPa} \qquad (3.1)$$

16. Maintain the pressure at C.

17. Connect the lead from the back pressure system to valve D without entrapping any air. Open valve F for a while to let out the bubble from back pressure line.

3.4.2 Test Procedure

The final arrangement of Rowe cell for two-way vertical drainage is diagrammatically shown in Figure 3.11. The test is described under the following stages: (A) Preliminaries, (B) Saturation, (C) Loading, (D) Consolidation, (E) Further load increments, (F) Unloading, (G) Conclusion, and (H) Measurements and Removal of the sample.

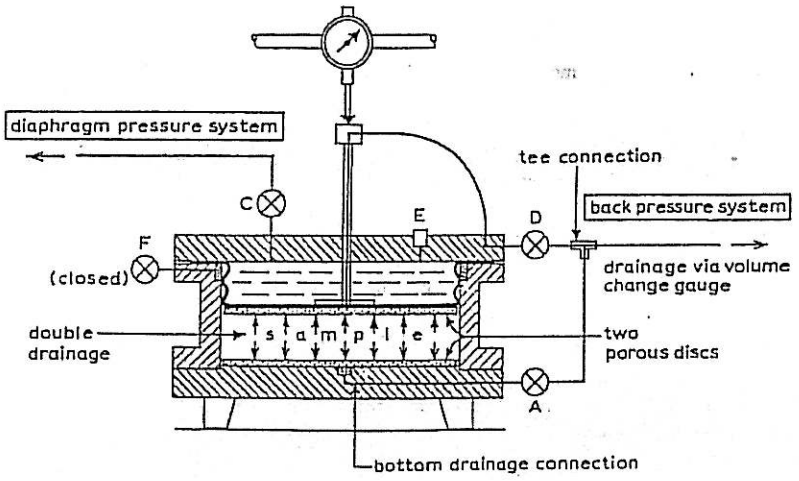

Figure 3.11 Arrangement of Rowe cell for consolidation test with two-way vertical drainage (Head, 1986)

3.4.2.1 Preliminaries

1. Close valve B to isolate the pore pressure transducer from the flushing system throughout the test.
2. Set the vertical movement dial gauge at a convenient initial reading near the upper limit of its travel, but allow for some upward movement if saturation is to be applied.
3. Record the reading as the zero (datum) value under the seating pressure p_o.
4. Set the back pressure to the required initial value, with valve D closed. The back pressure should be greater than the initial pore pressure (u_o) but it should be 10 kPa less than the first increment of cell pressure.
5. Record the initial reading of the volume gauge when steady.

3.4.2.2 Saturation

Saturation by the application of increments of back pressure is desirable for undisturbed samples taken from above water table. For this type of test, application of 10 kPa back pressure is used.

Saturation is generally accepted as being complete when the value of the pore pressure parameter *B* reaches about 0.96.

3.4.2.3 Loading Stage

1. With the drainage lines valve A and valve D closed and valve C open, increase the diaphragm pressure steadily to the first increment. Open valve A valve D when set.

   First increment of diaphragm pressure is taken as 50 kPa for this type of test.
2. Open valve F to allow excess water to escape from behind the diaphragm for a short time just to allow excess water from the top of the sample.
3. Wait until the pore pressure reaches a steady value equal to diaphragm pressure. If the sample is virtually saturated the increase in pore pressure should almost equal the pressure increment applied to the sample.
4. Record any settlement indicated by the dial gauge before starting consolidation.

3.4.2.4 Consolidation stage

Consolidation is started by opening the drainage outlets (valve A and valve D in Figure 3.12) and at the same instant starting the clock. Read the following data:

a. Vertical settlement
b. Pore water pressure
c. Volume change on back pressure line
d. Diaphragm pressure (check)

The primary consolidation phase is completed when the pore pressure has fallen to the value of the back pressure. Wait for secondary consolidation to take place.

3.4.2.5 Further load increments

1. Increase the diaphragm pressure to give the next value of effective stress. Allow excess water to drain from behind the diaphragm (valve F) if necessary.

2. The pore pressure should then be allowed to reach equilibrium before proceedings to the next consolidation stage.
3. Repeat the above steps for 100 kPa and 200 kPa consolidation pressures.

3.4.2.6 Unloading

Unloading is needed for evaluation of the effect of surcharge on the compressibility characteristics of peat. In this case, the sample was loaded to the pre-consolidation pressure (estimated based on oedometer test data, 30 kPa) and loaded to 100 kPa. At the end of consolidation test under 100 kPa, the soil was unloaded back to 30 kPa. For unloading stage, diaphragm pressure is reduced with valve D closed. It should be followed by swelling stage with valve D open, during which upward movement, volume increase and pore-pressure readings are taken in the same way as consolidation process. The pore-pressure should be allowed to reach equilibrium at the end of each stage before proceeding to the next stage of loading. The following stage of loading in this case is 100 kPa and 150 kPa.

3.4.2.7 Conclusion of test

1. Reduce the pressure to the initial seating pressure, p_o.
2. When equilibrium has been achieved, record the final settlement, volume change and pore pressure readings.
3. Close valve A and open valves C, D and F, allowing surplus water to escape. Unbolt and remove the cell top and place it on the bench supports.

3.4.2.8 Measurement and removal of sample

1. Remove the porous disc to expose the sample surface. Measure the diameter and height of the sample.
2. Remove the cell body from the base and remove the sample intact from the cell. Split the sample in two along a diameter.
3. Take two or more representative sample from one half of the sample for moisture content measurements.
4. Allow the other half to air-dry to reveal the fabric and any preferential drainage paths, which may have affected the test behavior.

5. Allow at least 4 hour before taking picture of the sample.

The cell components should be cleaned and dried before putting away, giving careful attention to the sealing ring at the base. Porous bronze and ceramic discs and inserts should be boiled and brushed; used porous plastic should be discarded. Connecting ports and valves should be washed out to remove any soil particles. Any corrosion growth on exposed metal surfaces should be scraped off, and the surface made smooth and lightly oiled.

3.4.3 Hydraulic Permeability Test

The hydraulic permeability measurements were carried out on a sample in a Rowe cell with laminar flow of water in the vertical direction (downwards). The designation of the hydraulic permeability test with vertical flow of water downwards is shown in Figure 3.12 while the arrangement of the Rowe cell for the permeability test with vertical drainage is shown in Figure 3.13.

3.4.3.1 Sample Preparation

The preparation of the sample and assembly of the cell are summarized as follows:

1. Fit a bottom drainage disc on the cell base.
2. Set up the sample in the cell by the method similar to that of Rowe cell consolidation test with vertical drainage (one-way).
3. Fit a porous stone on top of the sample.
4. Assemble the cell top.

Two independently controlled constant-pressure systems are required for the permeability test. One system is connected to valve C (Figure 3.13) to provide pressure on the diaphragm. One back pressure system is connected to valve D, and valve A is connected to an open burette.

Pore pressure readings are not required, except as a check on the B value if incremental saturation is applied before starting the test. Valve F remains closed. The difference between the inlet and outlet pressures should be appropriate to the vertical

permeability of the soil, and should be determined by trial until a reasonable rate of flow is obtained. The pressures are adjusted to give downward flow.

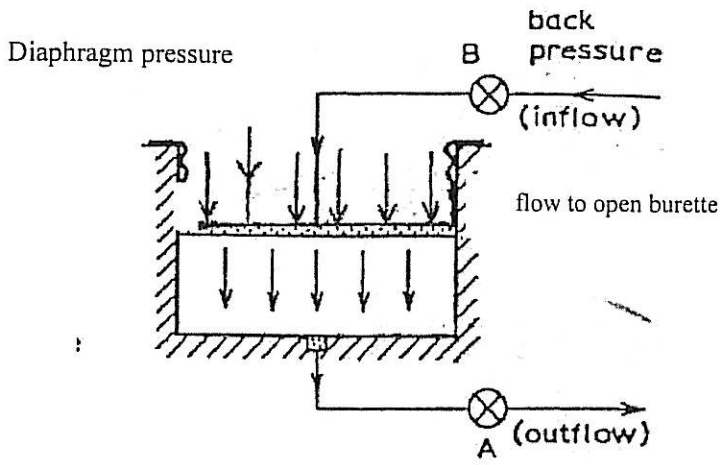

Figure 3.12: Downward vertical flow condition for hydraulic permeability test in Rowe cell (Head, 1986)

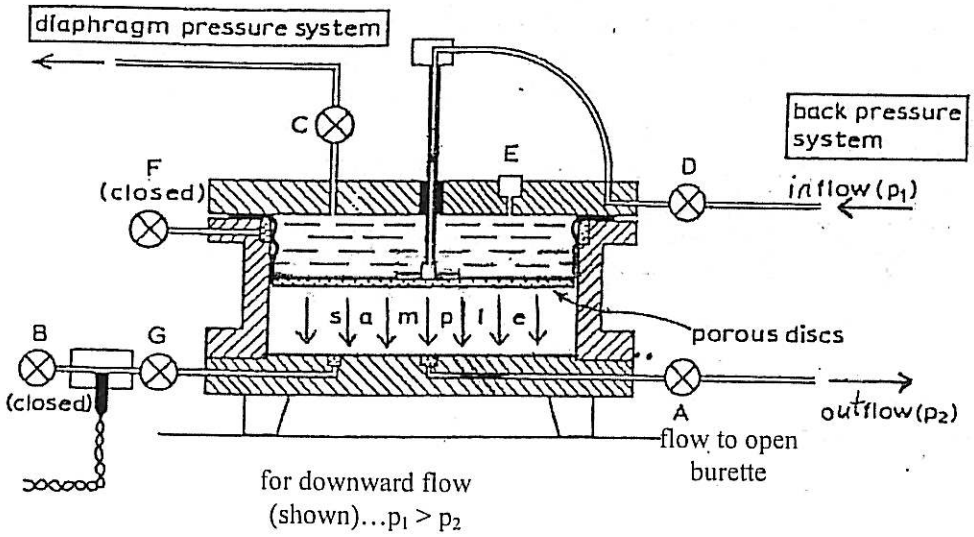

Figure 3.13: Arrangement of Rowe cell for permeability test with downwards vertical flow (Head, 1986)

3.4.3.2 Test Procedure

Permeability tests are carried out in Rowe consolidation cell under 'equal strain' conditions of known effective stress, with downward flow of water.

The arrangement of the cell and ancillary equipment is shown in Figure 3.13. Three independent constant pressure systems are required, one for applying the vertical stress, the other two on inlet and outlet flow lines but since, only two independent constant pressure systems are available, valve A at the base of the Rowe cell is connected to an open burette.

Since saturation by incremental back pressure is to be carried out initially, the pore pressure transducer housing should be connected to valve A. During the saturation stage, valve A should remain closed and water admitted to the sample through valve D as usual. Since only 2 constant pressure systems are available, the outlet from the sample is connected to an open burette via valve A whereas; the inlet to the sample is connected to a back pressure system via valve D. That means the direction of flow of water in the sample upon consolidation is downwards.

The arrangement shown in Figure 3.13 allows water to flow vertically through the sample under the application of a differential pressure between the base and top, while the sample is subjected to a vertical stress from the diaphragm pressure as in a consolidation test. Since the flow is to an open burette, the outlet pressure is zero if the free water surface in the burette is maintained at the same level as the sample face from which the water emerges.

The sample is first consolidated to the required effective stress by the application of diaphragm loading. Consolidation should be virtually completed, i.e. the excess pore pressure should be at least 95% dissipated before starting a permeability test.

The procedure for hydraulic permeability test using Rowe cell is as follows:

1. The test is first carried out by adjusting the pressure difference across the sample to provide a reasonable rate of flow through it. The hydraulic gradient required to induce flow should be ascertained by trial, starting with equal pressures on the inlet and outlet lines and progressively increasing the inlet pressure, which must never exceed the diaphragm pressure. Since only one back pressure system is used, the outlet drainage is connected to an open burette as shown in Figure 3.18.

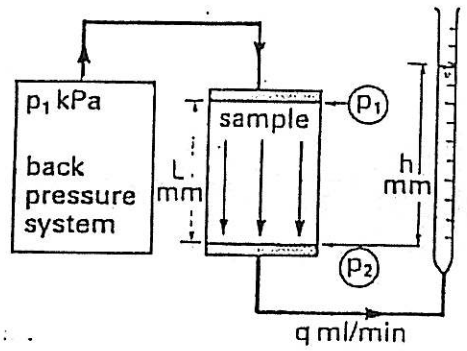

Figure 3.14: Arrangement for hydraulic vertical permeability test using one back pressure system for downward flow (Head, 1986)

2. When a steady rate of flow has been established, measure the time required for a given volume to pass through. The volume of water is measured from an open burette incorporated in the outlet of the soil sample via valve A.
3. Calculate the cumulative flow, Q (ml) up to the time of each reading, and plot a graph of Q against time, t (minutes), as the test proceeds. Continue the test until it can be seen that a steady rate of flow is reached, i.e. the graph is linear.
4. From the linear part of the graph, measure the slope to calculate the rate of flow, q (ml/minute); i.e. $q = \delta Q / \delta t$ (ml/minute).
5. Since the rate of flow is relatively small, the effect of head losses in the pipelines and connections can be neglected and the pressure difference across the soil sample is equal to $p_1 - p_2 = \Delta p$ where, $p_2 = 0$ since the free water surface in the burette is maintained at the same level as the sample face from which the water emerges.

The vertical coefficient of permeability is calculated from the following equation:

$$k_v = \frac{q_v}{60\,A\,i} = \frac{q_v\,H}{60\,A \times 102\,\Delta p} = \frac{q_v\,H}{6120\,A\,\Delta p} \qquad (3.2)$$

where, q_v is rate of vertical flow (ml/minute), t is time in minutes, A is the area of sample (mm^2) , i is the hydraulic gradient = $(102\ p_1 - h)/H$, Δp is the pressure difference (kPa) = $p_1 - p_2$, H is the height of sample (mm), p_1 and p_2 are inlet and

outlet pressure (kPa), h is the head loss due to the height of water in the burette, and k_v is the vertical coefficient of permeability (m/s).

3.5 Data Analysis

3.5.1 Analysis of Test Results

From each stage of a Rowe cell consolidation test, graphical plots are obtained of settlement, volume change and (in most cases) pore-water pressure, as a function of time. The graph should be kept up to date during each stage so that the progress of primary consolidation to reach 100% can be monitored. These graphs are used to determine the time corresponding to primary consolidation and secondary compression, from which the coefficient of consolidation can be calculated by using an equation with the appropriate multiplying factor.

Wherever possible, it is better to use the pore pressure dissipation graph rather than the settlement or volume change curve because the end points (0% and 100% dissipation) are both clearly defined and t_{50} or t_{90} can be read directly from the graph. The t_{50} point is preferable because the mid portion of the curve best fit to the theoretical curve. Settlement and volume-change measurements are governed by the deformation of the sample as a whole, and analysis is dependent on an overall 'average' behavior. A multiplying factor appropriate to the test conditions required for calculating the coefficient of rate of consolidation as shown in Table 3.1. For two-way vertical drainage, the coefficient of rate of consolidation can be calculated as

$$c_v = 0.131 \frac{T_v H^2}{t} \qquad (3.3)$$

where H is in mm and t is in minutes, while T_v is the theoretical time factor for 50% degree of consolidation for two-way vertical drainage or $T_{50} = 0.197$.

Table 3.1: Data for curve fitting (Head, 1986)

Test ref.	Drainage direction	Boundary strain	Consolidation location	Theoretical time factor T_{50}	Theoretical time factor T_{90}	Time function	Power curve slope factor	Measurements used	Coefficient of consolidation/year
(a) and (b)	Vertical, one way	Free and equal	Average	0.197 (T_v)	0.848	$t^{0.5}$	1.15	ΔV or ΔH* p.w.p.	$c_v = 0.526 \frac{T_v H^2}{t}$
			Centre of base	0.379	1.031				
(c) and (d)	Vertical, two way	Free and equal	Average	0.197 (T_v)	0.848	$t^{0.5}$	1.15	ΔV or ΔH*	$c_v = 0.131 \frac{T_v H^2}{t}$
(e)	Radial, outward	Free	Average	0.0632 (T_{ro})	0.335	$t^{0.465}$	1.22	$\Delta l'$ p.w.p.	$c_{ro} = 0.131 \frac{T_{ro} D^2}{t}$
			Central	0.200	0.479				
(f)		Equal	Average	0.0866 (T_{ro})	0.288	$t^{0.5}$	1.17	ΔV or ΔH p.w.p.	$c_{ro} = 0.131 \frac{T_{ro} D^2}{t}$
			Central	0.173	0.374				
(g)	Radial, inward†	Free	Average	0.771 (T_{ri})	2.631	$t^{0.5}$	1.17	$\Delta l'$ p.w.p.	$c_{ri} = 0.131 \frac{T_{ri} D^2}{t}$
			$r = 0.55R$	0.765	2.625				
(h)		Equal	Average	0.781 (T_{ri})	2.595	$t^{0.5}$	1.17	ΔV or ΔH p.w.p.	$c_{ri} = 0.131 \frac{T_{ri} D^2}{t}$
			$r = 0.55R$	0.778	2.592				

† Drain ratio 1/20
* ΔH with equal strain only
T_v, T_{ro}, T_{ri} = theoretical time factors
t = time (minutes)
H = sample height (mm)
D = sample diameter (mm)

Besides the time compression curve, a graph relating the void ratio at the end of each loading stage with the effective pressure on a linear or logarithmic scale was plotted for a complete set of consolidation test data. The e - p' curve is used to obtain coefficient of axial compressibility a_v and thus the coefficient of volume compressibility m_v, while the e – log p' is used to obtain compression and recompression indexes, c_c and c_r respectively. Pre-consolidation pressure can also be obtained if possible. These data are required for evaluation of the magnitude of primary settlement and to obtain the ratio of c_α/c_c for calculation of secondary compression.

3.5.2. Analysis of Time-Compression Curve

The time-compression curves derived from test results were analyzed based on suitable methods such as Cassagrande, Taylor, Sridharan & Prakash and Robinson methods. The secondary compression index as well as the beginning and end of secondary compression are among the parameters required for the analysis of secondary compression. Furthermore the coefficient of rate of consolidation c_v was calculated based on the curve.

The compression–log time curve was plotted for Cassagrande and Robinson methods, while the log compression–log time plot were needed for analysis using Sridharan & Prakash method and compression – square root of time plot is the basic of Taylor's method. Robinson method required the pore-water pressure–log time plot together with the compression–log time plot are used to develop compression - degree of consolidation graph. The detailed procedure for analysis of time – compression curve using various methods indicated above were presented in Appendix F.

The extended time compression curve based on the logarithmic of strain – log time plot was needed for evaluation of secondary compression based on Rheological model (Gibson and Lo, 1961). This method is used for comparison on the settlement estimation because the parameters are different from the previously discussed methods.

3.5.3 Settlement Analysis and Effect of Surcharge

A hypothetical problem of an embankment of 2.5 m high constructed over a 5 m thick deposit of fibrous peat (Figure 3.15) was used for the settlement analysis. The properties of fibrous peat deposit are based on the data obtained from the test results. The groundwater table is assumed to coincide with the ground surface. The embankment is constructed of sand fill over a geotextile layer so that uniform settlement can be expected. For the ease of calculation, the unit weight of the sand fill is taken as 20 kN/m^3, and the unit weight of water is 10 kN/m^3. The soil is improved by application of surcharge preloading in which the ratio of surcharge of 1.

Calculation of settlement for case with and without surcharge was made based on c_α/c_c concept and Gibson and Lo model.

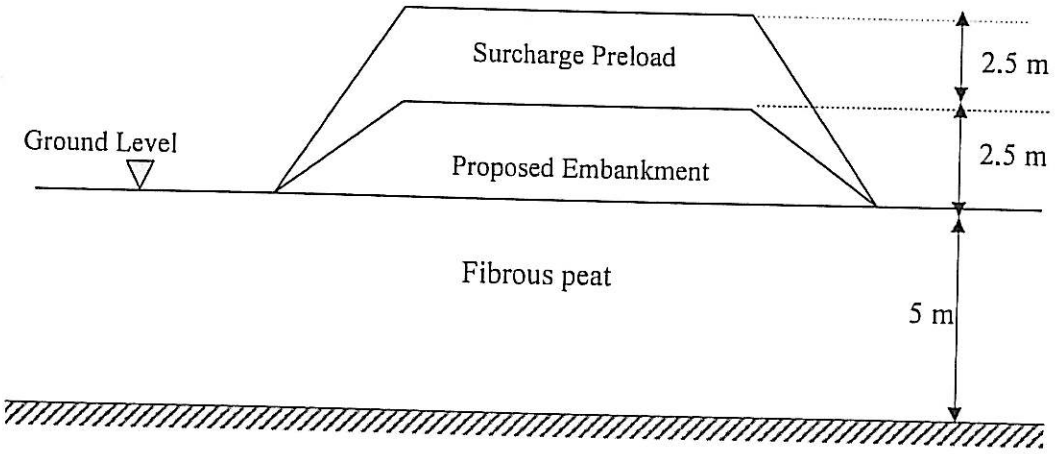

Figure 3.15 Hypothetical problem for analysis of settlement

CHAPTER 4

RESULTS AND DISCUSSION

4.1 Introduction

The discussion in this chapter will follow the stated objectives of the study mentioned in Chapter 1. Sections 4.2 and 4.3 will present the results of the laboratory test on the soil identification and engineering characteristics of the peat soil. The results and the analysis in these sections will answer the first objective of the study.

The second objective of the research was to study the compressibility characteristics of the fibrous peat based on the results of consolidation test. Section 4.4 and 4.5 discuss the compressibility characteristics obtained from consolidation test done on Oedometer and Rowe cells. The Oedometer test is currently regarded as the standard test for consolidation, thus; the results of large strain consolidation test using Rowe cell will be first compared to the results of Oedoemetr test. More detailed analysis was performed on the results of large strain consolidation test on Rowe cell. The other important compressibility characteristic of soil is the hydraulic permeability. The initial permeability and the effect of consolidation pressure on the permeability is discussed in Section 4.6.

Effect of surcharge on the secondary compressibility of peat was deliberated in Section 4.7 to answer the last objective of the study i.e. to evaluate the response of peat to surcharge as one method of soil improvement methods for constructions on fibrous peat. Section 4.8 illustrates the application of the results of the study on practical problems based on hypothetical problem.

4.2 Soil Identification

Data on the fundamental properties of the peat soil is summarized in Table 4.1. As shown in Table 4.1, the peat soil is acidic and has high organic and fiber contents. Moisture content of 608 % indicates that the peat soil has a high water-holding capacity. Based on the finding, it was found that the peat soil could be classified as fibrous peat with H_4 degree of humification according to von Post scale. Plant structures such as roots are easily recognizable from the soil. When squeezing a sample of the soil by hand, brown water comes out from the soil and the soil left on the hand has a large amount of fiber. The soil is acidic with pH of 3.24.

Table 4.1: The results of the study on the basic properties of soil in comparison to published data

	Parameters	Results from this study	Published data (ranges)
Index properties	Von Post humification of peat	H_4	H_1- H_4
	Natural water content (%)	608	200 – 700
	Bulk unit weight (kN/m^3)	10.02	8.30 – 11.50
	Dry unit weight (kN/m^3)	1.40	
	Specific Gravity (G_s)	1.47	1.30 – 1.80
	Initial void ratio (e_o)	8.92	3 – 15
	Acidity (pH)	3.24	3.0 – 4.5
Classification	% < 0.063 mm	2.74	
	Organic content (%)	97	> 90
	Ash content (%)	3	< 10
	Fiber content (%)	90	> 20

The test results also showed that the soil has organic and fiber content of 97 and 90%, respectively. These values are very high as compared to published data, but this is a typical fibrous peat obtained in West coast of Peninsular Malaysia with a very high organic and fiber contents, and very low pH (Muttalib, 1991 and Huat, 2004). The results of each index test and classification are presented in Appendix B.

4.3 Engineering Properties

4.3.1 Shear strength

The evaluation of the shear strength of peat was done in-situ by field vane shear test. A small size of vane (diameter 65 mm) and slow torque (0.1 mm/sec) were selected in order to minimize the effect of fiber in the measured undrained shear strength of peat (c_u). The undrained shear strength obtained from field vane shear test is very low compared to published data and it is increasing with depth i.e.: 1.90 kPa at 1 meter depth, and 3.20 kPa at 2 meter depth. The sensitivity of the peat is high i.e. 9.13 at 1 meter-depth, and 3.52 at 2 meter-depth, showing a tendency of decreasing shear strength upon remolding.

The laboratory evaluation of shear strength was made using shear box test, which gave drained shear strength of the soil. The shear box test is chosen because it is suitable for evaluating the shear strength of fibrous peat, even-though the high friction angle obtained from the test might not be an indication of the real strength of the soil. The results showed an average effective cohesion (c') of 3.32 kPa, and average effective angle of internal friction (ϕ') equal to 25°. The cohesion value is slightly lower compared to the published data on peat in West Malaysia (Huat, 2004). Result of shear box test is shown in Figure 4.1. The detailed results of field vane shear as well as shear box test for each sample are given in Appendix C.

4.3.2 Initial Permeability

The initial coefficients of permeability of the soil are measured by the constant head permeability tests in the soil's natural state. The samples for this test were obtained using piston sampler which size is similar with the size of samples required for the test. The results show that in the soil's initial state, the average vertical coefficient of permeability of the soil at standard temperature of 20°C, k_{vo} (20°) is 1.20 x 10^{-4} m/s which is within the range of permeability of clean sand. This indicates that at initial state, the soil has a good drainage characteristic.

Measurements also showed that the initial permeability of the soil varies from sample to sample. The effect of void ratio is significant as shown from the results shown in Figure 4.2. The variation of initial void ration is resulted from the natural soil imperfections or discontinuities, such as root holes, animal burrows, joints, fissures, seams, and soil cracks. These features, together with the presence of macro-pores and micro-pores within the fibrous peat soil, result in a high initial permeability of the soil.

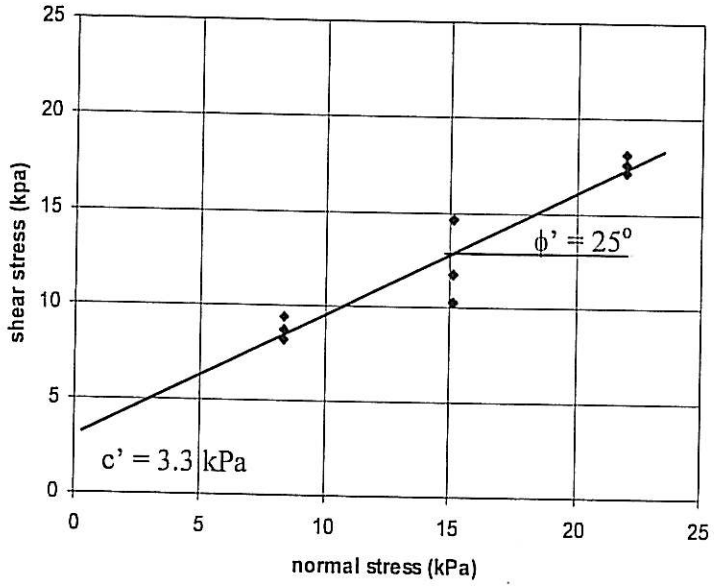

Figure 4.1 The typical results of the shear box test

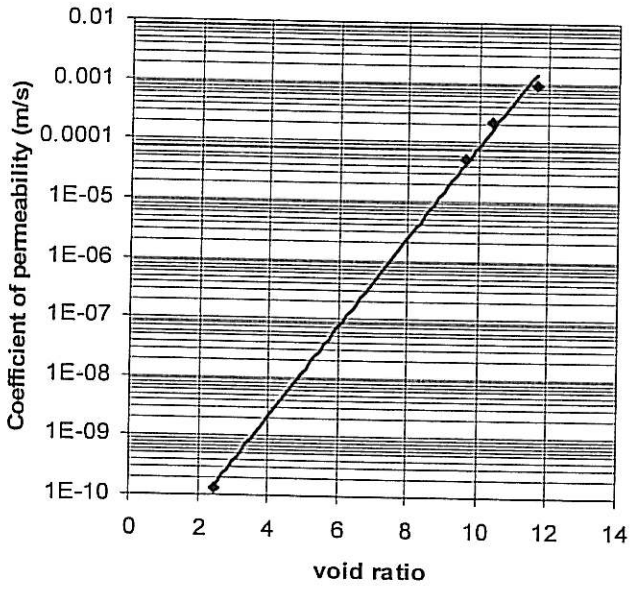

Figure 4.2 The relationship between the permeability and the void ratio

4.4 Standard consolidation tests

Three specimens of the fibrous peat soil sample were tested using oedometer. Each of the soil specimens has a thickness of about 20 mm, a diameter of 50 mm, and was subjected to consolidation pressures of 12.5 kPa, 25 kPa, 50 kPa, 100 kPa, 200 kPa, and 400 kPa. The time-compression curve derived from oedometer test is shown in Figure 4.3.

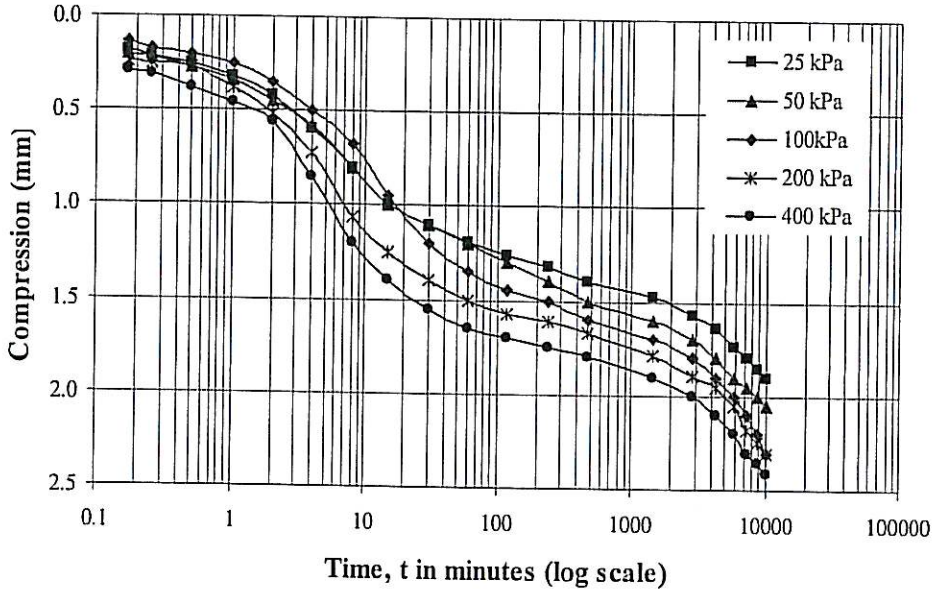

Figure 4.3: Log time-compression curves from oedometer test

The results from oedometer tests were mainly used to determine the range of consolidation pressures for hydraulic consolidation tests, and to evaluate the long-term compression behavior of the soil. The results were also used for comparison purposes.

Figure 4.3 shows that the plot of time-compression data follows the Type II curve in which the secondary compression varies non-linearly with time and tertiary compression was observed from all ranges of consolidation pressure. Therefore; extension of Cassagrande's and log δ–log time method were used to analyze the effect of tertiary compression on long term behavior of the peat soil under study. The beginning of secondary consolidation (t_p) and coefficient of secondary and

tertiary consolidation ($c_{\alpha 1}$, and $c_{\alpha 2}$) obtained from these analysis are summarized in Table 4.2.

Table 4.2: Consolidation Characteristics obtained from Oedometer test results

No	Consolidation Pressure (kPa)	Beginning of secondary compression, t_p(minutes)	Coefficient of secondary compression, $c_{\alpha 1}$	Beginning of tertiary Compression t_s (minutes)	Coefficient of tertiary compression $c_{\alpha 2}$	Coefficient of rate of consolidation c_v (m^2/yr)
1.	25	24	0.002	3167	0.003	2.673
2.	50	23	0.002	2900	0.003	1.821
3.	100	24	0.002	3133	0.003	1.345
4.	200	24	0.001	3600	0.003	0.902
5.	400	19	0.0005	2967	0.004	0.722

The results shown in Figure 4.3 and Table 4.2 indicate that the primary consolidation occurs relatively fast with an average t_p of about 23 minutes, while the secondary consolidation takes place for about 3000 minutes or 2 days. The results also shows that the time to reach the end of primary consolidation, t_p does not increase with increasing consolidation pressure. This can be explained by the fact that fibrous peat demonstrates unusual compression behavior in which the micro-pores within the soil's organic coarse particles tend to generate gas when compressed and this influences the shape of the consolidation curves.

The rate of secondary compression $c_{\alpha 1}$ decreases for higher consolidation pressure. On the other hand, the rate of tertiary compression increases with the pressure. This means that the higher the load applied to the soil, the higher the effect of tertiary compression. The coefficient of rate of consolidation c_v decreases as the consolidation pressure increases. The variation of c_v with pressure is shown in Figure 4.4.

The coefficient of rate of consolidation pressure for load increment of 100 kPa is 1.345 m^2/yr. The calculation made on a hypothetical example of compression of structure on 5 m depth of peat deposit with double drainage condition shows that

the 90% primary settlement occurs in about 2.5 years and the secondary settlement will last up to 250 years. This shows that the secondary consolidation is an important part of compression of fibrous peat and tertiary compression will not occur within the expected life of the structure, thus it is not important for evaluation.

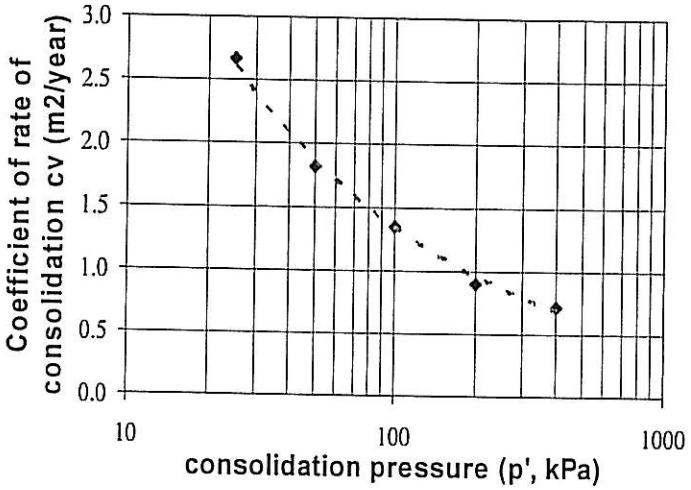

Figure 4.4 The variation of c_v with consolidation pressure p'

The e-log p'curve derived from oedometer test was constructed for raw data in which the compression is due to primary and secondary settlement and for the case where secondary settlement was excluded from analysis. Figure 4.5 shows the e-log p' curve for total settlement and primary settlement only. It can be seen from the figure that there is a difference in settlement, but the slope of the line remain almost the same. Evaluation of the curve indicates a compression index c_c about 3.772 if secondary compression is considered or 3.706 if secondary compression is excluded. The pre-consolidation pressure is estimated as 45 kPa. Based on this data, it was decided the starting pressure for the hydraulic consolidation test is 25 kPa, and subsequently followed by the load increment ratio (LIR) of one.

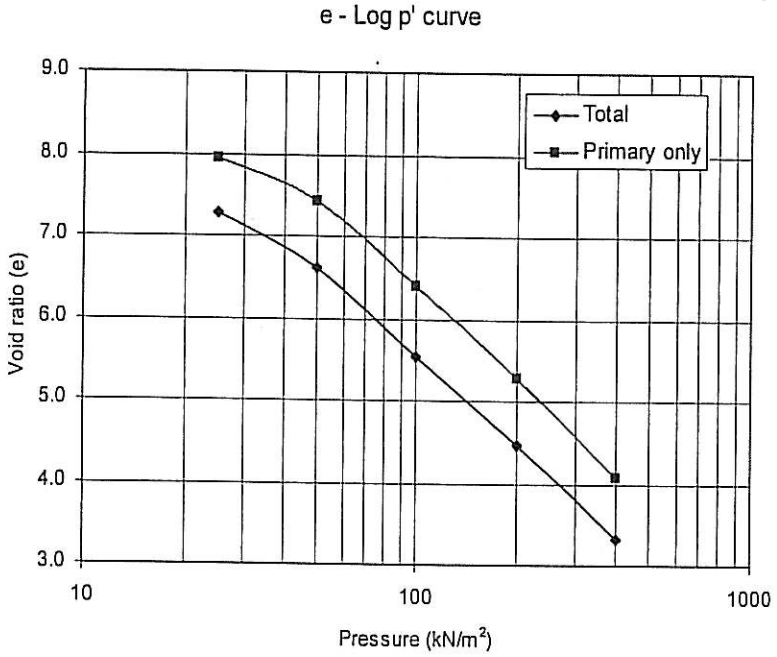

Figure 4.5 e-log p' curve from oedometer test

4.5 Hydraulic consolidation tests

Five series of hydraulic consolidation tests were done in order to evaluate the compressibility characteristics of the fibrous peat soil. The tests were performed using Rowe cell on a sample with thickness of about 50 mm and diameter of 151.4 mm. The sample was subjected to hydraulic consolidation pressures of 25, 50, 100, and 200 kPa. Drainage takes place from both top and bottom faces of the sample.

4.5.1 Evaluation of Time – Compression Curve

Time compression curve derived from hydraulic consolidation test is shown in Figure 4.6 and the data derived from the time-compression curve are presented in Table 4.3. The curve is similar in shape with the results of oedometer test (Figure 4.3). It was expected that the inflection point which indicate the completion of primary consolidation would occur at much longer time compared to the results of oedometer test due to the length of drainage path. However, as can be seen from Figure 4.5, the end of primary consolidation indicated by the inflection point occurs

at about 40 minutes which is only slightly longer than indicated by oedometer test results. The coefficient of rate of consolidation c_v varies with consolidation pressure and the value for the coefficient of rate of consolidation c_v at consolidation pressure 100 kPa is about 0.327 m^2/yr. The c_v is actually lower than that of calculated from the results of oedometer test due to the factor used in the analysis of consolidation test results using Rowe consolidometer (Head, 1986).

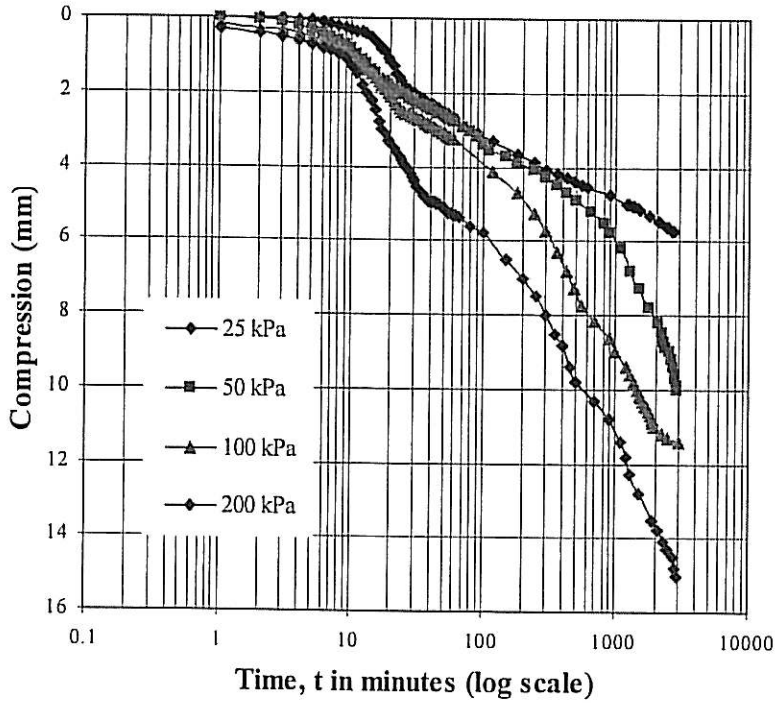

Figure 4.6: Log time-compression curves from hydraulic consolidation test

Table 4.3: Consolidation Characteristics obtained from Rowe test results

No	Consolidation Pressure (kPa)	Beginning of secondary compression, t_p(minutes)	Coefficient of secondary compression, $c_{\alpha 1}$	Beginning of tertiary Compression t_s (minutes)	Coefficient of tertiary compression $c_{\alpha 2}$	Coefficient of rate of consolidation c_v (m^2/yr)
1.	25	41	0.004	1180	0.009	0.573
2.	50	40	0.006	1130	0.015	0.393
3.	100	40	0.011	860	0.017	0.327
4.	200	38	0.011	800	0.018	0.209

It is also noted that the rate of secondary and tertiary settlement obtained from the hydraulic consolidation test is higher than that of the results obtained from oedometer test. Both $c_{\alpha 1}$ and $c_{\alpha 2}$ increases with increasing consolidation pressure while the beginning of secondary and the tertiary compression decreases with increasing consolidation pressure. The results of the hydraulic consolidation test are also analyzed based on Taylor, and Shridaran & Prakash methods.

In addition to the compression-log time curve, the results of the consolidation test using Rowe Cell can also be presented as pore-water pressure – log time curve (Figure 4.7). The evaluation of both curves is the basis of Robinson's method (Robinson, 2003) to evaluate the time and the degree of consolidation where the secondary compression starts. Table 4.4 shows the comparisons on the compressibility parameters obtained using these methods.

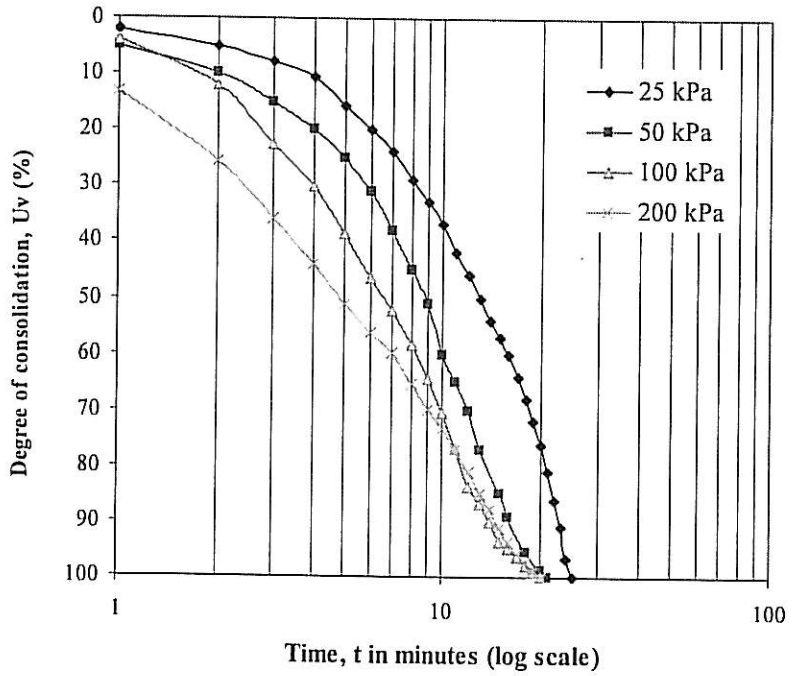

Figure 4.7 Degree of consolidation – log time curves based on Consolidation test using Rowe cell

Table 4.4 : The comparisons of consolidation parameters obtained from different methods

Method	Consolidation Pressure	25 kPa	50 kPa	100 kPa	200 kPa
Casagrande's method *(Dhowian & Edil, 1980)*	t_p	41	40	40	38
	t_s	1180	1130	860	800
	$c_{\alpha 1}$	0.004	0.006	0.011	0.011
	$c_{\alpha 2}$	0.009	0.015	0.017	0.018
	c_v	**0.573**	**0.393**	**0.327**	**0.209**
Taylor's method	c_v	**0.718**	**0.636**	**0.431**	**0.292**
log δ - log *t* method *(Sridharan and Prakash (1998)*	t_p	42	38	37	34
	$c_{\alpha 1}$	0.003	0.004	0.006	0.006
	c_v	**1.222**	**0.950**	**0.691**	**0.464**
Robinson's method *(Robinson, 2003)*	t_{100}	27	26	23	23
	U(%)	61	65	68	69
	t_p	18	15	13	13
	c_v	**0.676**	**0.685**	**0.631**	**0.540**

Note: c_v is in m^2/yr

As presented in Table 4.4, the beginning of the secondary consolidation predicted by Sridharan and Prakash is comparable to that predicted by Cassagrande method. Sridharan and Prakash predicted higher value of c_v compared to that of Cassagrande method, despite of comparable value of t_p. The method also predicted that the coefficient of the secondary consolidation increases with increasing consolidation pressure. Robinson predicted a much lower value because this method is based on pore water pressure dissipation, and therefore free of the effect of secondary consolidation. Robinson method also predicted a higher value for c_v due to the lower value of t_p. Variation of c_v predicted by different methods are shown in Figure 4.8.

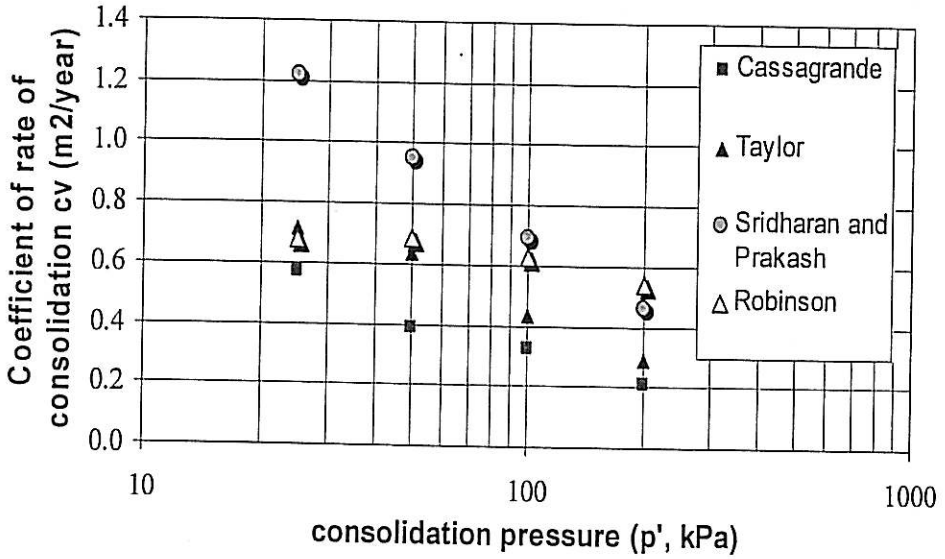

Figure 4.8 Variation of c_v analyzed using different methods

4.5.2 Evaluation of Compression Index

Figure 4.9 shows the e-log p' curve derived from hydraulic consolidation test. Figure 4.9a was constructed based on the raw data while Figure 4.9b was constructed for primary settlement only or the effect of secondary compression was excluded. The comparison of the two curves shows that the effect of secondary consolidation is not negligible. The result showed that the average compression index (c_c) obtained from the raw data is 4.025, while from primary consolidation data only, the compression index (c_c) is only 3.128. The results show that the effect of secondary consolidation can be better observed on the results of large strain consolidation test using Rowe cell than that of the oedometer test. The discrepancy is may be due to the constraint resulting from the size of the oedoemeter cell. The pre-consolidation pressure estimated from the graph is 41 kPa, which is slightly lower than that obtained from oedometer test. The higher pre-consolidation pressure observed in oedoemeter test may be due to the compression during trimming of the sample.

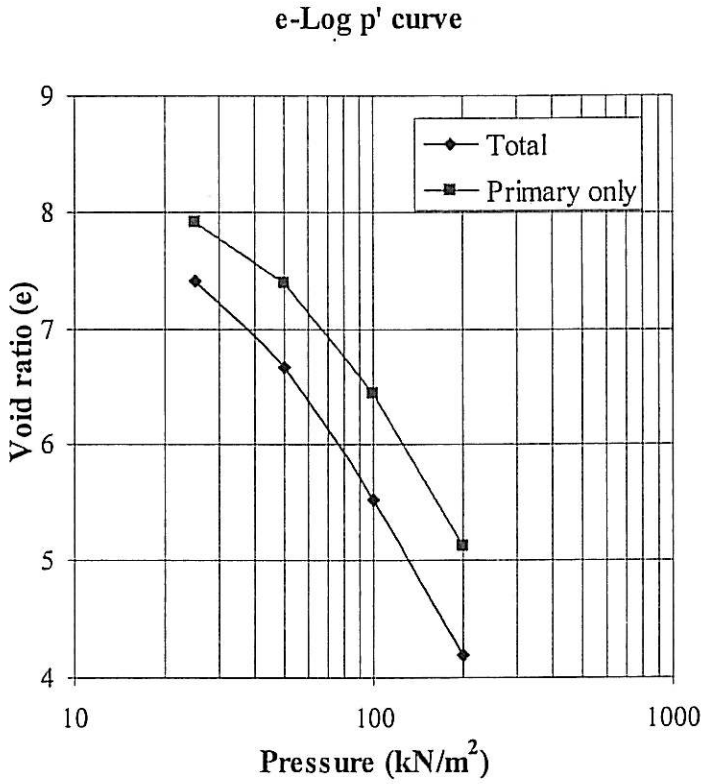

Figure 4.9 The e-log p' curve from hydraulic consolidation test

4.5.3 Rheological model parameters

For several cases presented by previous researches, the settlement of fibrous peat soil can be better estimated by the rheological model originally proposed by Gibson and Lo (1961). The evaluation is based on logarithmic of strain – logarithmic of time curve (Figure 4.10) and the parameters are actually greatly dependent on the stress increment applied to the sample. Table 4.5 presents the parameters obtained for each stress increment from hydraulic consolidation test. It can be seen from Table 4.5 that the primary compressibility parameter (a) does not vary with the stress increment and an average value close to 1 was obtained. The secondary compressibility parameter (b) value is strongly affected by the stress increment while the rate of secondary compression (λ/b) also increases with consolidation pressure.

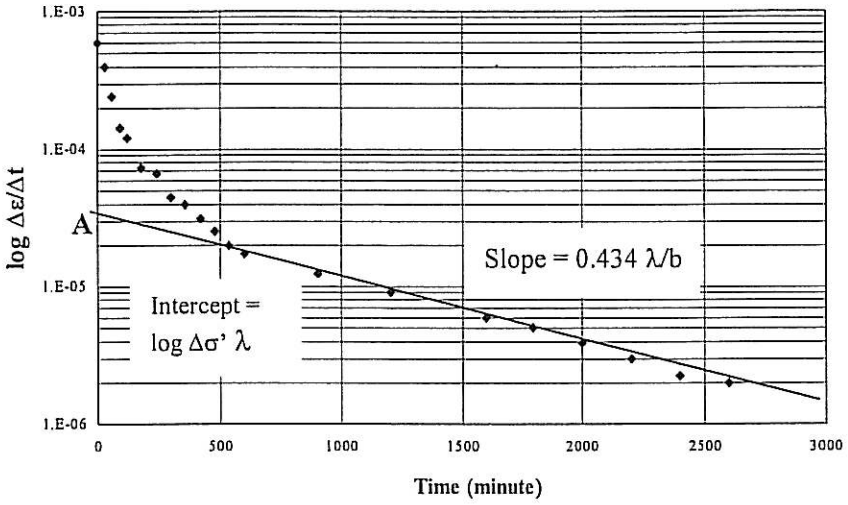

Figure 4.10 Typical plot of logarithmic of strain with log time from test results

Tabel 4.5: Rheological model parameters for settlement calculation

Parameter	25 kPa	50 kPa	100 kPa
a	0.996	0.994	0.997
b	0.096	0.2	0.48
λ/b	$1.17x10^{-4}$	$1.28x10^{-4}$	$2.80x10^{-4}$

4.6 Hydraulic Permeability

The rate of consolidation of the fully saturated and undisturbed fibrous peat soil is affected primarily by the permeability of the soil. Compression of the soil occurs rapidly when a new loading is applied and this is directly related to the high permeability of the soil. As such, it is important to evaluate the permeability of the soil, which is defined as the ability of water to flow through the soil. The permeability of the soil is characterized by the soil's permeability parameters, namely coefficient of permeability, k_v.

The hydraulic permeability test was carried out after the end of each hydraulic consolidation test or at a consolidation pressure of 200 kPa and an inlet

pressure of 180 kPa on the soil sample. The outlet pressure was determined by the height of the water collected by a burette connected to the outlet of water flow from the Rowe consolidometer. The burette has an internal diameter of 12.19 mm, an external diameter of 15.15 mm and a maximum volume capacity of 100 ml. All hydraulic permeability tests were conducted at a room temperature of 25°C.

The results of the hydraulic permeability tests on the soil samples indicate that at a consolidation pressure of 200 kPa, the average vertical coefficient of permeability of the soil at a standard temperature of 20°C, k_v (20°C) is 2.36 x 10^{-10} m/s. As mentioned in Section 4.3, the initial coefficient of permeability of the soil at standard temperature of 20°C, k_{vo} (20°) is 1.20 x 10^{-4} m/s which is within the range of permeability of clean sand. At a consolidation pressure of 200 kPa, the coefficient of permeability of the soil is reduced to values comparable to those of intact clay. This indicates that the change in permeability of the fibrous peat soil as a result of compression is drastic.

4.7 Laboratory Evaluation on the Effect of surcharge

The effect of the surcharge on the compressibility of fibrous peat was evaluated through the hydraulic consolidation test (Rowe cell) by loading and unloading phase. Three sets of hydraulic consolidation test with an effective surcharge ratio of 1 were done to investigate the effect of unloading on the secondary settlement of the fibrous peat. The sample is back-pressurized by a load equal to the pre-consolidation pressure, and then was loaded to 100 kPa. The sample was then unloaded to 50 kPa and reload to 100 kPa to look at the effect of loading – unloading – and reloading on time compression curve. The results of the test were evaluated following the procedure proposed by Mesri et al. (1997).

Figure 4.11 shows the loading curves for the first and second loading to 100 kPa. The time-compression curve for unloading stage to 50 kPa is shown in Figure 4.12. It is clear from Figure 4.11 that the unloading and reloading gives a significant effect of the compression behavior of the fibrous peat both in the primary and

secondary stages and even the tertiary stages was almost eliminated. Figure 4.12 shows that unlike other soil types, fibrous peat showed a short swelling stage, then followed by a compression stage.

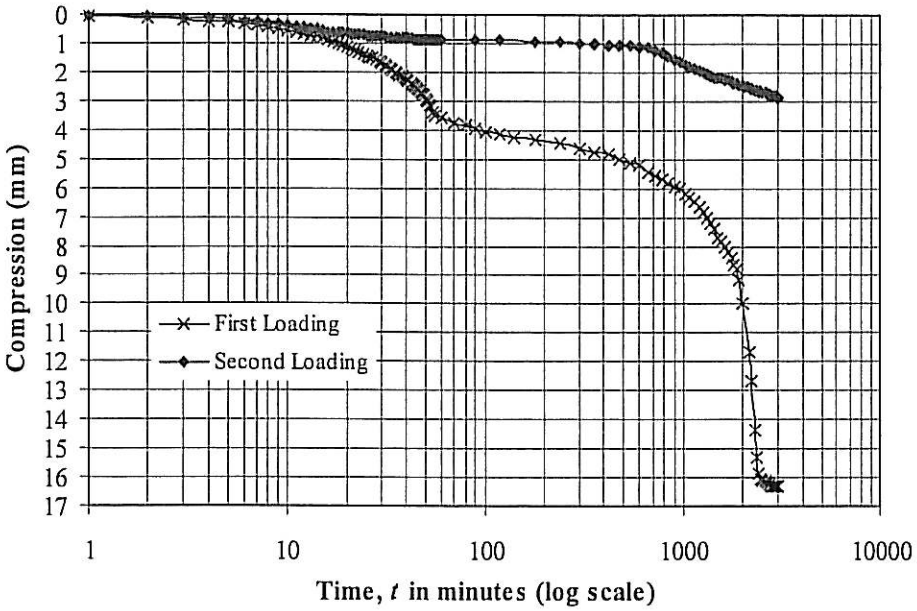

Figure 4.11 Time – compression curve for first and second loading to 100 kPa.

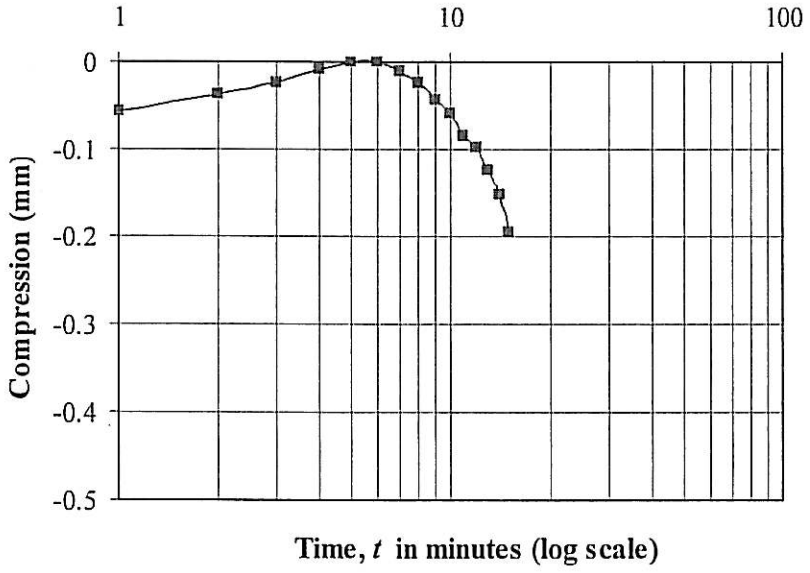

Figure 4.12 Time-compression curve for unloading stage.

The average c_α value obtained using Cassgrande's method for incremental loading to 100 kPa was 0.011. This gives a ratio of c_α/c_c equal to 0.0035. The coefficient of the secondary consolidation obtained from this series of loading-unloading-reloading test were 0.008 for first loading of 100 kPa and 0.001 for second loading to 100 kPa. It showed that the coefficient of secondary consolidation after unloading stage was only 13% of the loading case. The post-surcharge secant secondary compression index c''_α can be obtained from time-compression curve for unloading stage (Figure 4.12) and the average value for the three sets of test is 0.004 which is 50% of the first loading case.

4.8 Settlement Calculation

As mentioned in Chapter 3, the settlement calculation was made based on a hypothetical problem shown in Figure 3.15. An embankment of 2.5 m high is constructed over a 5 m thick deposit of fibrous peat. The groundwater table is assumed to coincide with the ground surface. The embankment is constructed of sand fill over a geotextile layer so that uniform settlement can be expected. The soil is improved by application of surcharge preloading in which the ratio of surcharge of one. The problem and the properties of fibrous peat deposit are given in Figure 4.13. The design life of the structure is 30 years.

4.8.1 Time – Compression Curve

The settlement of the embankment constructed directly on the soil by five layers of 0.5 m will induce a stress increment of 50 kPa to the soil. The overburden stress at the middle of peat layer is 25 kPa. Thus the primary consolidation settlement is:

$$S_c = c_c \frac{H}{1+e_o} \log \frac{\sigma'_o + \Delta\sigma}{\sigma'_o} = 3.128 \frac{5}{1+8.193} \log \frac{25+50}{25} = 0.75 \text{ m}$$

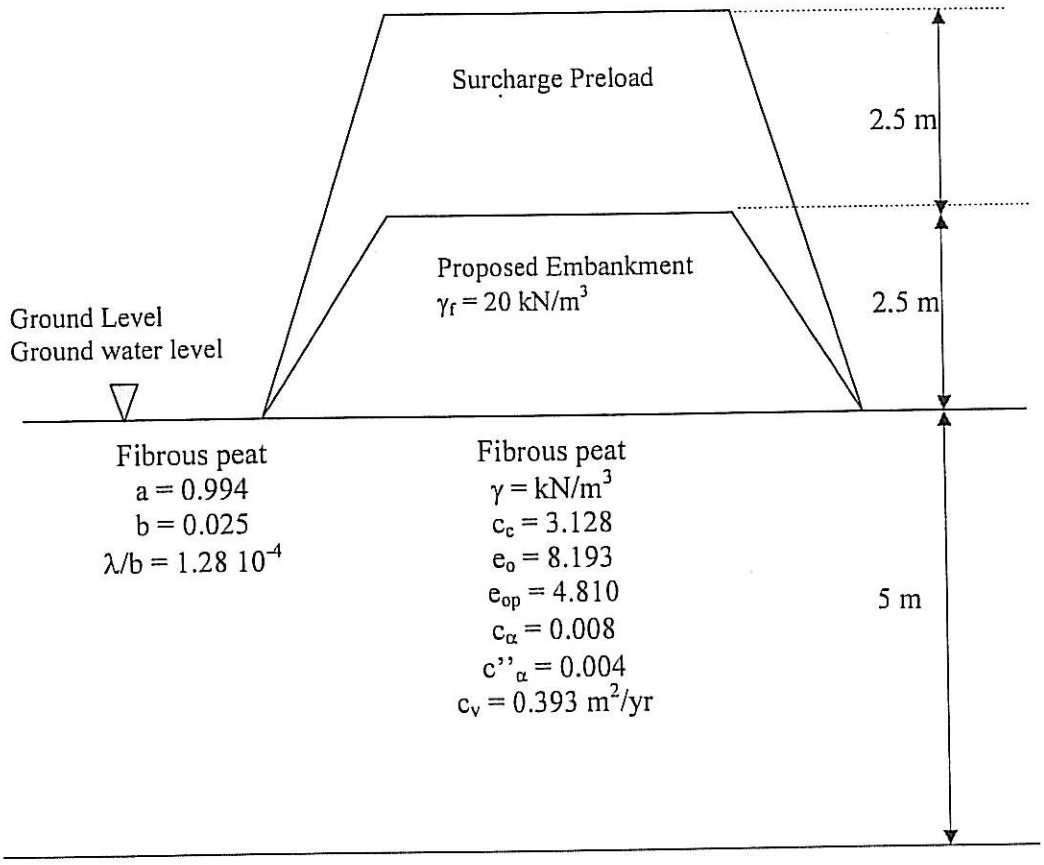

Figure 4.13 Geometry and soil properties for the hypothetical problem

Assume that the water can flow in two directions and the length of drainage path is equal to half of the thickness of the peat deposit or 2.5 m. The time to reach 90% consolidation is:

$$t = \frac{T_v H^2_d}{C_v} = \frac{0.848 \text{ x} (2.5)^2}{0.393} = 13.5 \text{ years}$$

Time required to finish the primary consolidation based on t_p value obtained from laboratory test is about 18 years. The secondary settlement of the peat layer after the end of primary consolidation until the completion of design life of 30 years is:

$$S_s = c_\alpha \frac{H}{1+e_{op}} \log \frac{t}{t_p} = 0.08 \frac{5}{1+4.810} \log \frac{30}{18} = 0.001845 \text{ m} = 1.845 \text{ mm}$$

Thus the total settlement of the embankment at the end of design life of 30 years is about 0.75 m. In this case the effect of secondary settlement is very small.

The application of an additional surcharge of 50 kPa which yield an additional stress of 100 kPa will results in total settlement of:

$$S_c = c_c \frac{H}{1+e_o} \log \frac{\sigma'_o + \Delta\sigma}{\sigma'_o} = 3.128 \frac{5}{1+8.193} \log \frac{25+100}{25} = 1.20 \text{ m}$$

The 90% total settlement of the actual embankment is 67.5 cm occurs at 55% degree of consolidation of the soil with surcharge load. And the time to reach this consolidation is:

$$t = \frac{T_v H^2_d}{C_v} = \frac{0.238 \text{ x} (2.5)^2}{0.393} = 3.78 \text{ years}$$

The primary rebound after removal of surcharge t_{pr} is 2.5 years, and the ratio of elapsed time at which the secondary compression reappear to the time of primary rebound after surcharge removal (t_l/t_p) for effective surcharge ratio R'_s of 1 is 10.

The secondary settlement with application of surcharge is

$$S_s = c''_\alpha \frac{H}{1+e_{op}} \log \frac{t}{t_1} = 0.004 \frac{5}{1+4.810} \log \frac{30}{(10 \text{x} 2.5)+3.78}$$

$$= 0.0000612 \text{ m} = 0.0612 \text{ mm}$$

The application of surcharge in this case will reduce the secondary settlement significantly, however negligible compared to primary settlement.

4.8.2 Rheological model

The settlement of peat under the embankment load was also analyzed using the rheological model. In this case, the increase in stress is 50 kPa, and the parameters for stress increment of 50 kPa as given in Figure 4.13 yields a settlement of:

$$\varepsilon(t)=\Delta\sigma\left[a-b\left(1-e^{(-\lambda/b)t}\right)\right]$$

$$\varepsilon(t)=50\left[0.994-0.025\left(1-e^{(-0.000128)30}\right)\right]$$

$$\varepsilon(t) = 49.4 + 1.6 = 51 \text{ mm} = 0.51 \text{ m}$$

From this calculation, we can see that the primary compressibility take a large portion of settlement as compared to the secondary part. The primary consolidation settlement is 49.4 mm while the secondary consolidation is 1.6 mm. Mokhtar (1997) recommends that the coefficient of secondary compressibility obtained from laboratory should be corrected for the field condition by using a curve in Figure 4.14.

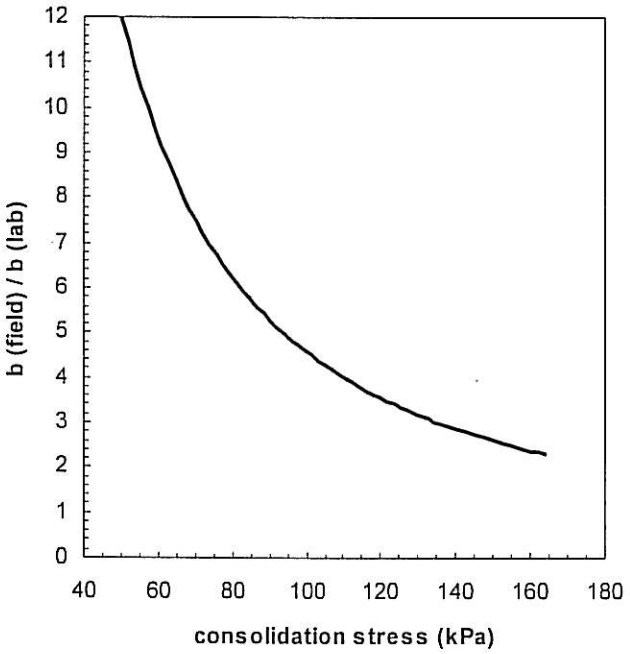

Figure 4.14 Correction for b parameters for field condition (Mokhtar, 1997)

From Figure 4.14, the correction for field condition with consolidation pressure of 50 kPa is 12. Then b value can be corrected as 0.025 x 12 = 0.3. Thus the corrected secondary settlement is $\varepsilon(t)=50\left[0.3\left(1-e^{(-0.000128)30}\right)\right]$ = 15.3 mm. This yields a total settlement of 64.7 cm.

4.9 Discussion

This research was conducted to gain a better understanding on the compression behavior peat soil by using samples of peat from Kampung Bahru Pontian, a location of peat deposit closed to UTM. The generalization of the research data was not attempted in this research since it is fully understood that the properties of peat soil are unique to location.

The preliminary study on the index properties of the peat and the comparisons with published data show that the peat obtained from this location is typical of peat in Malaysia with a high water content (608%), and a very high organic and fiber content (97% and 90% respectively). Based on the classification test, the soil can be grouped as fibrous peat soil with low to medium degree of composition (H_4).

Since the ground water level was found at depth of 1 m, and the sampling was therefore done at depths of between 1 and 2 m. The sampling process was designed and conducted carefully as to avoid disturbance as much as possible. The fact that the extraction of fully undisturbed sample is almost impossible, thus attention was focused on reducing the disturbance by adding sharp edges to cut the soil and to prepare two layers of wooden plate to keep the sample from falling out of the sampler. Attention to reduce the disturbance are also given to transportation and storing the samples.

Initial permeability of the peat is very high and it is comparable to sand. However, the data also showed that the permeability is highly affected by compression or reduction in void ratio. The in-situ shear strength of the soil is very low, thus the construction on such deposit requires the use of a platform. The shear strength obtained from the direct shear test showed that the friction was derived from fibers and the results are comparable to published data.

A series of standard consolidation test was conducted to get a basis for starting pressure for the large strain consolidation. The data obtained from this test was also used for comparison purposes. Table 4.6 presents the compressibility

parameters obtained from the results of standard consolidation test (oedometer cell) and hydraulic consolidation test (Rowe cell).

Table 4.6 Compressibility parameters obtained from oedometer and Rowe tests for consolidation pressure of 50 kPa.

Consolidation Parameters	Oedometer	Rowe
Compression index, c_c	3.706	3.128
Pre consolidation pressure σ_c' (kPa)	45	41
Coef. of vol. compressibility m_v	0.003	0.003
End of primary consolidation, t_p (min)	23	40
End of secondary consolidation, t_s (min)	2900	1130
Coef. of rate of consolidation c_v (m^2/yr)	1.821	0.393
Coef of secondary compression c_α	0.002	0.006

It can be concluded from Table 4.6 that both tests gave a comparable values except for the coefficient of rate of consolidation. This may be due to the coefficient adopted for calculation of c_v from the results of consolidation test using Rowe cell. The coefficient of secondary consolidation obtained from Rowe cell is higher than that obtained from oedometer, may be due to the size of the sample. Referring to the discussion by Mokhtar (1997) for secondary compressibility of peat, this difference suggested that the results of large strain consolidation test (Rowe cell) are less susceptible to the effect disturbance and thus more reliable.

While the results of oedometer tests are analyzed with Cassagrande methods only, the results of Rowe test in term of time compression was analyzed using four different methods including Cassagrande's. The results shown in Table 4.4 suggested that Cassagrande method gives the lowest coefficient of rate of consolidation in under consolidation pressure. Both Cassagrande and Sridharan & Prakash yield almost the same value for the beginning of secondary consolidation (t_p) because both methods are based on the inflection point. However, analysis using Robinson methods shows that the secondary compression can starts as early as about

15 minutes or at degree of consolidation of 65%. This method is based on the plot of pore-water pressure dissipation.

The evaluation of logarithmic of strain – log time curves (rheological model) for three different stress increment of consolidation based on the results of hydraulic consolidation test reveals that the primary compression parameter (a) does not affected by the stress increment while the secondary compression parameter (b) and so the rate of secondary consolidation increase as consolidation pressure increases.

The comparison of c_α value and λ/b, both represent the rate of secondary consolidation, showed that the higher rate of secondary consolidation was predicted using the time – compression curve. The c_α value obtained from the large strain consolidation test is even higher that that obtained from the oedometer test. This also shows that the secondary consolidation can be better observed from the large strain consolidation.

The coefficient of permeability decreases drastically as consolidation increases. The initial permeability is 1.2×10^{-4} m/s, while the coefficient of permeability under consolidation pressure of 200 kPa is found as 2.36×10^{-10} m/s. The lower coefficient of permeability was assessed from the results of consolidation test through c_v values. For this case, the coefficients of rate of consolidation c_v are 1.41×10^{-11} m/s 0.91×10^{-11} m/s for the consolidation pressure of 100 and 200 kPa respectively.

The laboratory assessment on the effect of surcharge showed that the effect of loading–unloading–reloading sequence reduces the coefficient of secondary compression to 13%, while the post-surcharge secant secondary consolidation only reduce the coefficient of secondary consolidation by 50%.

The settlement analysis made on the hypothetical example of an embankment on the fibrous peat deposit showed that even-though laboratory test showed that the secondary consolidation is dominant in the settlement of fibrous peat, the actual settlement takes a very small portion of the settlement. Primary settlement still makes a large portion of the settlement. Thus a method that can speed up primary

consolidation such as preloading with sand column is good for construction on fibrous peat soil. Once the shear strength of the soil is gained through consolidation process, then the construction can be performed with fewer problems. The application of surcharge does not give meaningful improvement in terms of secondary settlement. Stage loading could be a better alternative because this method improves shear strength of the soil and at the same time improve the consolidation characteristics of the soil.

The use of large strain consolidation test to evaluate consolidation characteristics of soil exhibiting secondary consolidation is advantageous because it enable long term observation of deformation of fibers and the resulting strain can be easily observed. The pore water pressure measurement made on the large strain consolidation test enables the elimination of the effect of secondary compression on the evaluation of primary consolidation, thus the evaluation of secondary settlement can be made separately from the primary settlement especially that occurs before the completion of pore water pressure dissipation.

CHAPTER 5

CONCLUSIONS

5.1 Conclusions

This research was conducted to gain a better understanding on the compression behavior peat soil found in Kampung Bahru Pontian, West Johore. It started with the identification of the type of peat as well as index properties and engineering characteristics of the soil. The research was followed with a more extensive study on the compressibility characteristic of the soil through a series of large strain consolidation tests.

The analysis of the test results showed that the peat deposit in Kampung Bahru Pontian, West Johore is a fibrous peat with low to medium degree of decomposition (H4 in von Post scale) and of very high organic and fiber content. The literature study indicated that this is a typical of peat found in West Malaysia.

Fibrous peat is considered as problematic soil because it exhibits unusual compression behavior. The compression behavior was studied through a series of large strain consolidation test using 150 mm diameter Rowe cell. The results showed that the soil has a high compressibility with significant secondary compression stage, which is not constant with the logarithmic of time in some cases. Even though it is observed that the duration of primary consolidation is short, it yields in a significant settlement due to high initial void ratio.

It can be concluded from the test results that the behavior of fibrous peat under study was in accordance with the c_α/c_c concept derived from time-compression curve. The c_α/c_c ratio obtained from this study is 0.025 which is in the lower end of the range suggested by previous researchers. This showed that the secondary settlement was not a dominant part for settlement of the peat under study. The rheological model did not actually capture the secondary consolidation of the peat because it was quite small compared to the primary consolidation. Furthermore, the evaluation of the beginning of tertiary consolidation from test results showed that this compression would occur after a long time compared to design life of a structure, thus negligible.

The comparison between the results of large strain consolidation and the results of the oedometer test showed that the use of Rowe cell for the evaluation of the consolidation characteristics of soil exhibiting secondary consolidation is advantageous because it enables long term observation of deformation of fibers and the resulting strain can be easily observed. The pore water pressure measurement made by the large strain consolidation test enables the elimination of the effect of the secondary compression on the evaluation of the primary consolidation. By using the pore water pressure measurement, the actual beginning of secondary compression can be evaluated using Robinson's method that yields a higher c_v value. The evaluation of c_v value based on this method is preferred because it is based purely on primary consolidation with the secondary compression separated from the total compression during the dissipation of excess pore water from the soil.

The effect of surcharge on secondary compression was studied through loading–unloading–reloading stage on hydraulic consolidation test. The test showed a significant reduction in the coefficient of secondary consolidation. The settlement analysis on the hypothetical problem showed the improvement is negligible because the large part of settlement occurs during primary consolidation stage. The stage loading could be a better alternative because this method improves shear strength of the soil and at the same time improves the consolidation characteristics of the soil. Use of sand column is also a better alternative because it improves the strength of the soil and at the same time speed up the preliminary consolidation.

5.2 Recommendation for Future Study

The results of the study have shown that the compressibility characteristics of fibrous peat soil obtained from Kampung Bahru, Pontial consists of primary and secondary consolidation. The effect of secondary consolidation on the primary consolidation is significant, therefore: it is recommended to perform large strain consolidation test on Rowe cell for fibrous peat and keep the consolidation time for each loading increment accordingly to remove the effect of secondary consolidation.

The laboratory evaluation on the application of surcharge can improve the compressibility characteristic of the fibrous peat, however; the time to complete the primary consolidation is relatively long. Therefore: application of surcharge pre-loading method renders an economic consideration with regard to time. The application of surcharge pre-load is also complicated by the low shear strength of the soil, thus: stage loading may be more suitable for construction on such soil.

An evaluation on the increase in shear strength due to application of consolidation pressure and draining process is recommended as an extension of this research to study the application of stage loading as one improvement method for fibrous peat. The method should be combined with confinement because the most critical problem involving peat soil is lateral spreading of the soil.

In depth study on the suitability of sand column as a means of vertical drains is recommended for future study because this method has been applied successfully for peat soil deposits in Japan and many other countries. The method has the advantage of increasing shear strength and at the same time increasing the rate of primary consolidation process.

It is also recommended that further study involving field investigation on the fibrous peat soil need to be done to justify the laboratory investigation on the soil from this study. Field investigation on the soil is beyond scope of this study. Regardless of the type of soil investigation performed on fibrous peat soil, the consolidation theory should be emphasized since it provides a reliable basis of economic considerations of soil improvement.

REFERENCES

Adams, J. (1965). The Engineering Behavior of a Canadian Muskeg. *Proc., 6th Int. Conf. Soill and Found. Engrg.* Montreal, Canada, 1: 3-7.

Ajlouni, M.A. (2000) *Geotechnical Properties of Peat and RelatedEengineering Problems.* Thesis. University of Illinois at Urbana-Champaign.

American Society for Testing and Materials. (1994) *Annual Book of ASTM Standard.* Vol. 04.08 and 04.09

Barden, L. (1965). Consolidation of Clay with non-linear Viscosity. *Geotechnique* , London, England, 15(4): 345-362.

Barden, L. (1968). Primary and Secondary Consolidation of Clay and Peat. *Geotechnique*, London, England, 18(l): 1-24.

Berry, P. L. (1983). Application of Consolidation Theory for Peat to the Design of a Reclamation Scheme by Preloading. Q. *J. Eng. Geol.*, London, 16(9): 103-112.

Berry, P. L. and Vickers, B. (1975). Consolidation of Fibrous Peat." *J. Geotech. Engrg.*, ASCE, 101(8): 741-753.

Berry, P. L. and Poskitt, T. J. (1972). The Consolidation of Peat. *Geotechnique*, London, England, 22(l): 27-52.

British Standards Institution. (1981). *Methods of Test for Soils for Civil Engineering Purposes*. London, BS 1377.

Colley, B. E. (1950). Construction of Highways Over Peat and Muck Areas. *American Highway,* 29(1): 3-7.

den Hann, E. J. (1994). Vertical Compression of Soils. Ph.D. thesis, Delft University of Technology, Delft, The Netherlands.

den Hann, E. J. (1996). An Investigation of Some Physical Properties of Peat. *Geotechnique*, London, England, 46(l): 1-16.

den Hann, E.J. (1996). A Compression Model for non-brittle Soft Cays and Peat, *Geotechnique*, 46(1):1-16.

Dhowian, A. W. and Edil, T. B. (1980). Consolidation Behavior of Peats. *Geotech. Testing J.*, 3(3): 105-114.

Edil, T.B. and A. W. Dhowian. (1979). Analysis of long-term Compression of Peats. *Geotechnical Engineering*. Vol.10.

Edil, T.B. and A. W. Dhowian. (1981). At-rest Lateral Pressure of Peat Soils. *Conf. on Sedimentation and Consolidation Model*, ASCE, San Fransisco, 411 – 424.

Edil, T. B. and Mochtar, N. E. (1984). Prediction of Peat Settlement. *Proc. Sedimentation Consolidation Models Symp. Prediction and Validation,* ASCE, San Fransisco. California, 411-424.

Edil, T.B. (2001) Site Characterization in Peat and Organic Soils. In *Proceeding of the International Conference on In Situ Measurement of Soil Properties and Case Histories*, 49-59, Bali, Indonesia.

Edil, T.B. (2003). Recent Advances in Geotechnical Characterization and Construction Over Peats and Organic Soils. *Putrajaya (Malaysia): 2nd International Conferences in Soft Soil Engineering and Technology.*

Gibson, R.E., and Lo, K.Y. (1961). A Theory of Consolidation for Soils Exhibiting Secondary Compression, *Acta Polytexch, Scandinavia*, v. 10, 296.

Hanrahan, E. T. (1954). An Investigation of Some Physical Properties of Peat." *Geotechnique,* London, England, 4(2): 108-123.

Hanrahan, E. T. (1964). A Road Failure on Peat. *Geotechnique* , London, England, 14(3): 185-202.

Hartlen, J. and J. Wolski. (1996). Embankments on Organic Soils. *Developemnet in Geotechnical Engineering, Elsevier.* 425.

Hansbo, S. (1991). Full-scale Investigations of the Effect of Vertical Drains on the Consolidation of a Peat Deposit Overlying Clay. *De Mello Volume,* Published by Editoria Edgard Bldcher LTDA, Caixa Postal 5450, 01051 SAo Paolo-sp Brasil.

Head, K.H., (1981). *Manual of Soil Laboratory Testing*, Volume 1,2, and 3. Pentech Press, London.

Head, K.H. (1982). *Manual of Soil Laboratory Testing,* Volume 2: Permeability, Shear Strength and Compressibility Tests. London: Pentech Press Limited.

Head, K.H. (1986). *Manual of Soil Laboratory Testing*, Volume 3: Effective Stress Tests. London: Pentech Press Limited.

Huat, Bujang, B.K., (2004) *Organic and Peat Soil Engineering*. Univ. Putra Malaysia Press.

Hobbs, N. B. (1986). Mire Morphology and the Properties and Behaviour of Some British and Foreign Peats. Q. *I Eng. Geol.*, London, 19(1): 7-80.

Holtz, R.D. and Kovacs, W.D. (1981). *An Introduction to Geotechnical Engineering*. Prentice-Hall, Inc., Englewood Cliffs, New Jersey.

Johson, S.J. (1977). Foundation Precompression with Vertical Sand Draines. *JSMFE, ASCE,* GT4, 103:355-356.

Jones, D. B., Beasley, D. H. and Pollock, D. J. (1986). Ground Treatment by Surcharging on Deposits of Soft Clays and Peat. *Proc. Conf. on Building on Marginal and derelict land, L C. E.*, Glasgow, 679-695.

Jorgenson, M. B. (1987). Secondary Settlement of 4 Danish Road Embankments on Soft Soils. *Proc. 9th. European Conf. Soil Mech. Found. Engrg.*, 2: 577-560.

Keene, P., and Zawodniak, C. D. (1968). Embankment Construction on Peat Utilizing Hydraulic Fill. *Proc., Advances in Peatlands Engineering,* Ottawa, Canada, 45-50.

Kogure, K. and Ohira, Y.,(1977). Statistical Forecasting of Compressibility of Peaty Ground. *Can. Geotech. J.*, Ottawa, Canada, 14(4): 562-570.

Lan, L. T. (1992). A Model for One Dimensional Compression of Peat. Ph.D. Thesis. University of Wisconsin, Madison, Wisconsin.

Landva, A. O. and La Rochelle, P. (1983). Compressibility and Shear Characteristics of Radforth Peats. *Testing of Peat and Organic Soils, ASTV STP* 820. 157-191.

Landva, A. 0. and Pheeney, P. E. (1980). Peat Fabric and Structure. *Can. Georech. J.*. Ottawa, Canada, 170: 416-435.

Landva, A. O., Pheeney, P. E. and Mersereau, D. E. (1983). Undisturbed Sampling of peat. *Testing of Peat and Organic Soils,* ASTM STP 820, 141-156.

Landva,A.O. and La Rochelle, P. (1983). Compressibility and Shear Characteristics of Radforth Peats, *ASTM STP*, 820: 157-191.

Lea, F.M. (1956). In the Chemistry of Cement and Concrete, ed. Lea and Desch, p.637. London : Edwar Arnold Ltd.

Lea, N., D. and Browner, C. 0. (1963). Highway Design and Construction Over Peat Deposits in the Lower British Colombia. *Highway Research Record,* (7): 1-32.

Lefebre, G. K., Langlois, P., Lupien, C., Lavallde , J. G. (1984). Laboratory Testing and in-situ Behavior of Peat as Embankment Foundation. *Can. Geotech. J.*, Ottawa, Canada, 21(2): 101-108.

Leonards, G.A. and P. Girault. (1961). A Study of The One-dimensional Consolidation Test.*Proceeding 9th ICSMFE*, Paris, 1:116-130.

Levesqe, M., Jacquin, F. and Polo, A. (1980). Comparative Bodegradability of Shagnum and Sedge Peat from France. *Proc., 6th Int. Peat Congress,* Duluth, Minnesota, 584-590.

Lewis, W. A. (1956). The Settlement of the Approach Embankments to a New Road Bridge at Lockford, West Suffolk. *Geotechnique,* London, England, 6(3): 106-114.

Mesri, G. and Choi, Y. K. (1985a). Settlement Analysis of Embankments on Soft Clays. J. *of Geotech. Engrg., ASCE,* 111 (4): 441-464.

Mesri, G. and Choi. Y. K. (1985b). The Uniqueness of the end-of-primary (EOP) Void atio-effective Stress Relationship. *Proc., 11th Int. Conf. on Soil Mech. and Found. Engrg.*, San Francisco, 2: 587-590.

Mesri, G., Lo, D.O. (1986). An Analysis of the Gloucester Test Fill using ILLICON. Gloucester test fill Symposium, National Research Council of Canada, Ottawa, August.

Mesri, G., Lo, D.O. (1991). Field performance of prefabricated vertical drains. *Proc., Int. Conf. on Geotech. Eng. for Coastal Development-Theory to practice,* Yokohama, 1: 231-236.

Mesri, G., Stark, T. D. and Chen, C. S. (1994). C_c/C_α Concept Applied to Compression of Peat. Discussion, J. of *Geotech. Engrg.*, ASCE, 118(8): 764-766.

Mesri, G. and Feng, T. W. (1991). "Surcharging to reduce secondary settlement." Proc., *Int. Conf. Geotech. Engrg. for Coastal Development - Theory to Practice,* Yokohama. Japan, 359-364

Mesri, G., and Rokhsar, A. (1974). Theory of Consolidation for Clays. J. of *Geotech. Engrg.*, ASCE, 100(8): 889-904.

Mesri, G., T.D. Statark, M.A. Ajlouni and C. S. Chen (1997). Secondary Compression of Peat With or Without Surcharging. *J. Geotech. Geoev. Engr.* 123(5): 411-421.

Miyakawa, J. (1960). Soils Engineering Research on Peats Alluvia. Reports 1-3. Civil Engineering Research Institute. Hokkaido Development Bureau Bulletin No. 20

Mokhtar, N.E. (1998). Perbedaan Perilaku Teknis Tanah Lempung dan Tanah Gambut (Peat Soil), *Jurnal Geoteknik*, Himpunan Ahli Teknik Tanah Indonesia, 3(1): 16-34.

Muskeg Engineering Handbook. (1969). I.C. Macfarlane. University of Toronto Press.

Muttalib, A.A. et.al. (1991). Characterization, Distribution, and Utilization of Peat in Malaysia, In *Proceedings of the International Symposium on Tropical Peatland,* ed. Aminuddid, Kuching, Sarawak. 7-16.

Nakayama, M., Yamaguchi, H. and Kougra, K. (1990). Changes in Pore Size Distribution of Fibrous Peat Under Various one-dimensional Consolidation Conditions. *Memories on The Defense Academy,* 30(1): 1-27.

Ng, S. Y. and Eischens, G.R. (1983). Repeated short-term Consolidation of Peats. *Testing of Peat and Organic Soils, ASTM STP 820,* 192-206.

Nurly Gofar and Yulindasari Sutejo. (2005). Engineering Properties of Fibrous Peat, *Proc. Seminar Penyelidikan Kej. Awam (SEPKA)*, Johor Bahru. 119-129.

Noto, Shigeyuki. (1991). *Peat Engineering Handbook.* Civil Engineering Research Institute, Hokkaido development Agency, Prime Minister's Office, Japan.

Olson. R.E. and Mesri, G. (1970). Mechanisms Controlling Compressibility of Clays. *J. of Soil Mechanics and Foundations Division, ASCE, 96* (SM6), 1863-1878.

Robinson, R. G. (1997). Determination of Radial Coefficient of Consolidation by the Inflection Point Method, *Geotechnique*, 47(5): 1079-1081.

Robinson, R. G. (2003). A Study on the Beginning of Secondary Compression of Soils. *Journal of Testing and Evaluation.* 31(5): 1-10.

Rowe, P.W. and Barden, L. (1966). A New Consolidation Cell. *Geotechnique.* 16: 162-169.

Samson , L. (1985). Postconstruction Settlement of an Expressway Constructed Over Peat by Precompression. *Can. Geotech. J.,* Ottawa, Canada, 22(2): 1-9.

Samson , L. and La Rochelle, P. (1972). Design and Performance of an Expressway Constructed Over Peat by Preloading. *Can. Geotech. J.,* Ottawa, Canada, 9: 447-466.

Sridharan, A., and Prakash, K. (1998). Secondary Compression Factor. *Geotechnical Engineering*. 131(2): 96-103.

Termaat, R. and Topolnicki, M. (1994). Biaxial Tests with Natural and Artificial Peat. *Proc., International Workshop on Advances in Understanding and Modeling the Mechanical Behavior of Peat, Delft,* Netherlands, 241-251.

Weber, W. G. (1969). Performance of Embankments Constructed Over Peat. J. *Soil Afech. Found Div.,* ASCE, 95(l): 53-76.

Yamaguchi, H. (1990). Physicochernical and Mechanical Properties of Peats and Peaty Ground. *Proc. 6th. Int. congress Int. Assoc. Eng. Geol.*, Balkema, Rotterdam, 521-526.

Yamaguchi, H., Ohira, Y., Kogure, k. and Mori, S. (1985a). Deformation and Strength Properties of Peat. *Proc., 11th Int. Conf. on Soil Mech. and Found Engrg.,* San Francisco, 2: 2461-2464.

Yamaguchi, H. Ohira, Y., Kogure, k. and Mori, S. (1985b). Undrained Shear Characteristics of Normally Consolidated Peat Under Triaxial Compression and Extension Conditions. *Japanese Society of Soil Mich. and Found. Engrg.*, 25(3): 1-18.

Yamaguchi, H., Yamauchi, K. and Kawano, K. (1987). Simple Shear Properties of Peat. *Proc. 6th. Int. Symp. Geotech. Engrg. Soft Soils,* Ciudad, Mexico, 163-170.

APPENDIX A

Sampling Procedure

The procedures for sampling of peat :

1. Excavate soil to a depth below ground water level by using hoe. Clean the base and throw away the twigs and roots.

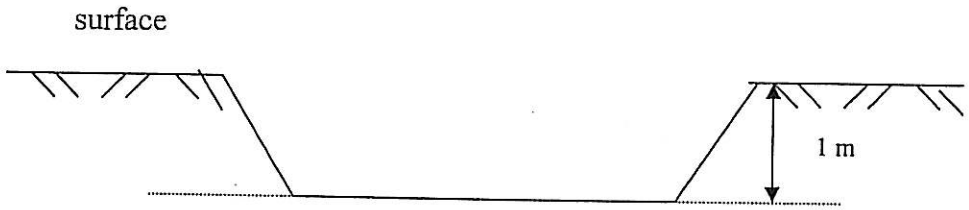

2. Push a 300 mm diameter and 300 mm height tube into the soil carefully to get a sample (Figure A1). The sharpness of the tube has to be ensured to cut the fiber from blocking the tube and to control the quality of the sample. Sharp knife was used to help cutting any fiber from outside the tube when needed.

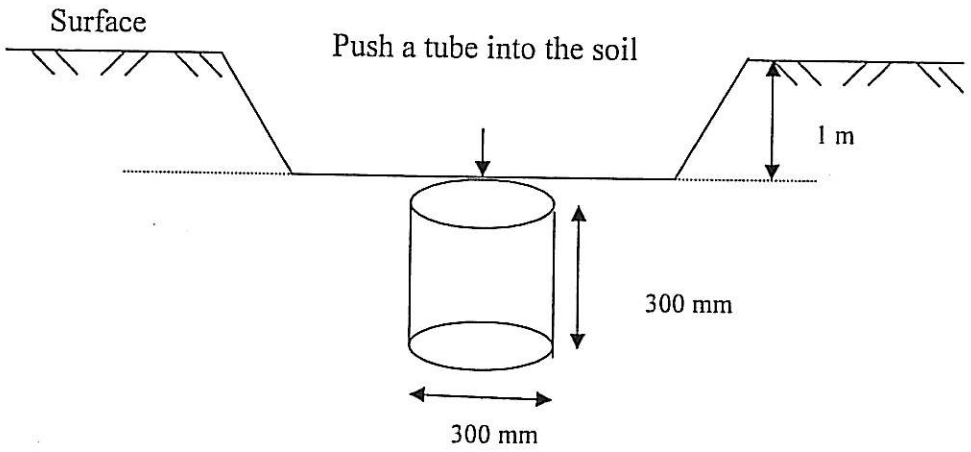

3. Excavate the surrounding of the tube then cut the base of sample using a sharp knife.

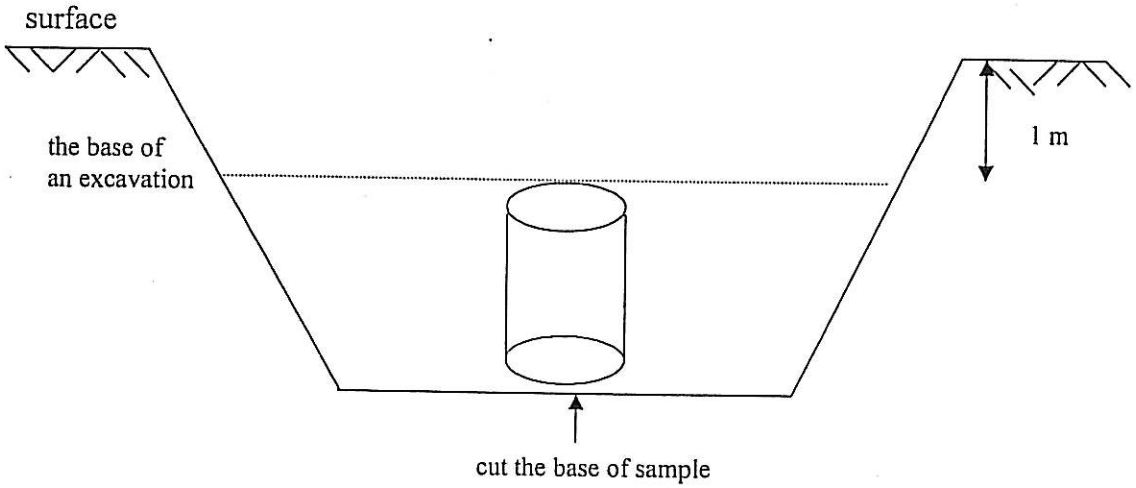

4. Insert a piece of cylindrical wood plate below the sample and keep the sample still in by blocking the top and bottom of the tube using a wood piece which of the same diameter with the inside of the tube (Figure A2).

5. Take the tube out carefully and put on a safe place. Cover the top and bottom of the tube with wax to maintain the moisture of soil (Figure A2).

6. Cover again the top and bottom of the using square wood plate (500 mm x 500 mm) and secure it with ropes to stabilize the tube during transportation (Figure A3).

7. Arrange two sample tubes in one wooden box (Figure A3). Cover the wall of the wooden box and fill the voids with layers of sponge to minimize the effect of vibration during transportation from site to Geotechnical Laboratory at UTM.

8. A thin wall fixed piston sampler (Figure A5 and A6) was also used to take samples horizontally and vertically for checking the quality of samples, water content determination, and constant head permeability test

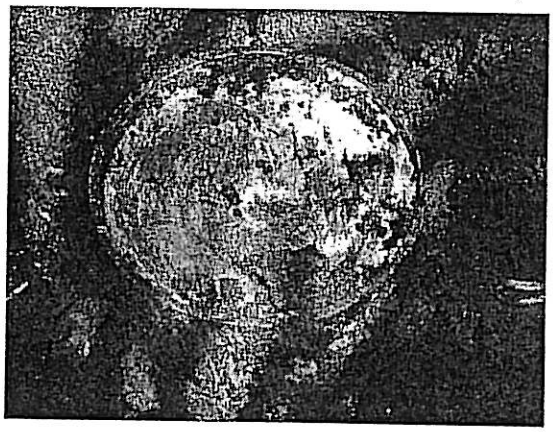

Figure A1: A block sampler was manually pushed into the bottom of a test pit

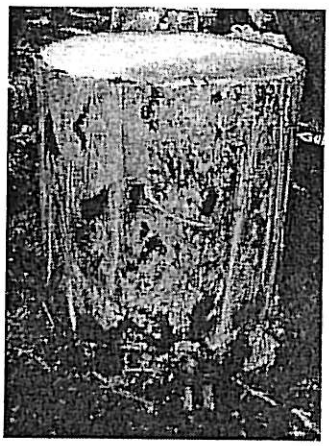

Figure A2: A peat block was covered with 2 cylindrical pieces of wood, and sealed with melted candles, which hardened at normal temperature to preserve the natural moisture content

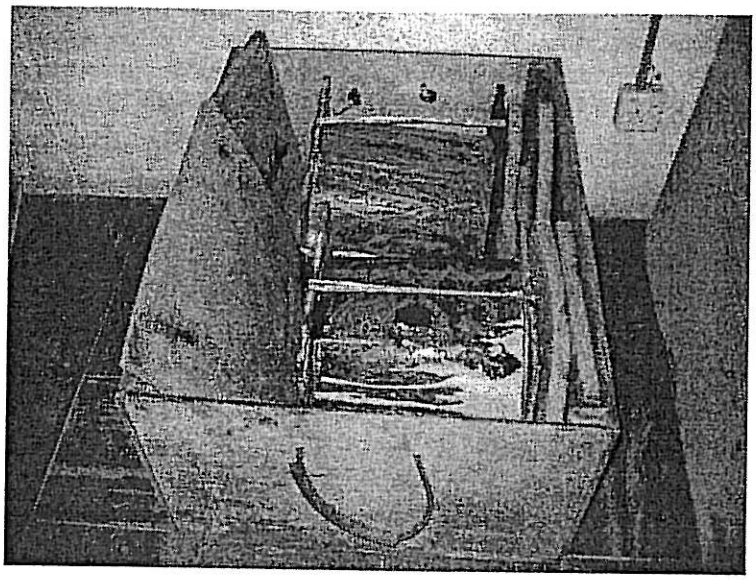

Figure A3: Each peat block was covered with 2 pieces of wood, tied with ropes, and then put into a wooden box to prevent the soil sample from moving during transportation and then transported and kept in the laboratory

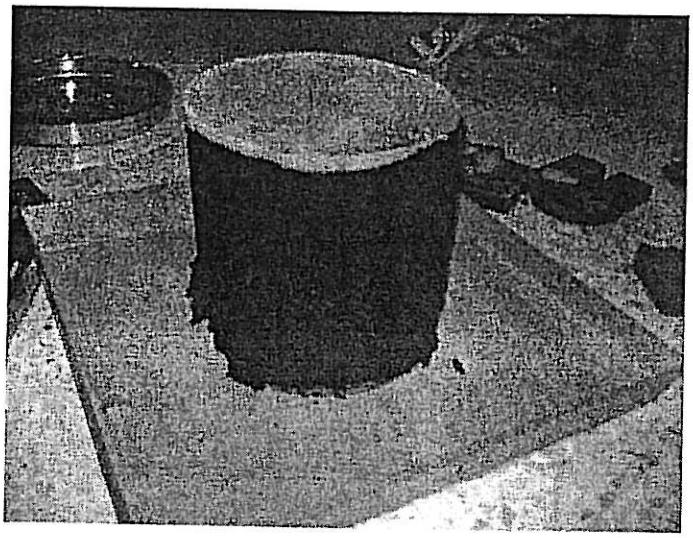

Figure A4: The fibrous peat soil block sample

Figure A5: A thin wall fixed piston samplers was manually pushed and carved from the bottom of a test pit to obtain vertical undisturbed fibrous peat soil samples

Figure A6: A thin wall fixed piston sampler was sealed with moisture-resistant plastic covers to preserve the moisture content of undisturbed fibrous peat soil sample in the sampler

APPENDIX B

Index Tests and Classification

1. Natural Moisture Content

Typical Test Sheet

Location : Geotechnical Laboratory			Job ref.	
			Bore hole/ Pit no.	
Soil Description : PEAT			Sample no.	1
			Depth	1-2 m
Test method ASTM D2216-92 / BS 1377 : Part 2:1990 : 3.2			Date	14/01/2005
Related test				
Speciment ref.		1	2	3
Container no.		A1-1	A1-2	A1-3
Mass of wet soil + container (m_2)	g	543	471	481
Mass of dry soil + container (m_3)	g	312	248	259
Mass of container (m_1)	g	276	214	222
Mass of moisture (m_2-m_3)	g	231	223	222
Mass of dry soil (m_3 –m_1)	g	36	34	37
Moisture content $w = \frac{m_2 - m_3}{m_3 - m_1} x100$	%	641.167	655.882	600
		Average	w = 632.349 %	

No	Moisture Content (w %)
Test 1-1	641.167
Test 1-2	655.882
Test 1-3	600
Test 2-1	621.490
Test 2-2	601.714
Test 2-3	631.298
Test 3-1	555.717
Test 3-2	577.973
Test 3-3	584.219
AVERAGE	**608**

2. Specific Gravity (Gs)

Typical Test Sheet

Location : Geotechnical Laboratory		Job ref.	
		Bore hole/ Pit no.	
Soil Description : PEAT		Sample no.	1
		Depth	1-2 m
Test method ASTM D854-92 / BS 1377 : Part 2 : 1990 : 8.3 / 8.4		Date	08/02/2005
Method of preparation : pycnometer method			
Small/Large pycnometer			
Speciment references		1	
Pycnometer number		1567	1459
Mass of bottle + soil +water (m_3)	g	137.745	137.924
Mass of bottle + soil (m_2)	g	46.642	47.489
Mass of bottle full of water (m_4)	g	135.273	135.245
Mass of bottle (m_1)	g	35.476	36.556
Mass of soil ($m_2 - m_1$)	g	11.166	10.933
Mass of water in full bottle ($m_4 - m_1$)	g	99.797	98.689
Mass of water used ($m_3 - m_2$)	g	91.103	90.435
Volume of soil particles ($m_4 - m_1$)- ($m_3 - m_2$)	mL	8.694	8.254
Specific gravity Gs = $\frac{m_2 - m_1}{(m_4 - m_1) - (m_3 - m_2)}$	Mg/m^3	1.284	1.325
		Average **Gs = 1.305**	

No	Specific Gravity (Gs)
Test 1-1	1.284
Test 1-2	1.325
Test 2-1	1.442
Test 2-2	1.439
Test 3-1	1.513
Test 3-2	1.510
Test 4-1	1.482
Test 4-2	1.534
Test 5-1	1.509
Test 5-2	1.543
Test 6-1	1.544
Test 6-2	1.486
AVERAGE	**1.468**

3. Initial void ratio

Based on Average moisture content & Average Specific Gravity,

$$e_0 = \frac{Gs \times w}{\gamma_w} = \mathbf{8.925}$$

4. Organic Content and Ash Content

Typical Test Sheet

Location : Saint Laboratory		Job ref.	
		Bore hole/ Pit no.	
Soil Description : PEAT		Sample no.	1
		Depth	1-2 m
Test method ASTM D1997-91 / BS 1377 : Part 3:1990 : 4.3		Date	22/02/2005
Related test			
Speciment ref.		1	
Crucible no.		C_{40}	C_{14}
Mass of crucible (m_1)	g	32.3868	34.7537
Mass of crucible + soil (m_2)	g	37.3868	39.7537
Mass of crucible + soil after ignition (m_3)	g	32.8248	34.8945
Organic Content OC = $\frac{m_2 - m_3}{m_2 - m_1} x100$	%	91.240	97.184
		average OC = **94.212**	
Ash Content AC = 100 % - OC	%	**AC = 5.788**	

5. Fiber Content

Typical Test Sheet

Location : Geotechnical Laboratory		Job ref.	
		Bore hole/ Pit no.	
Soil Description : PEAT		Sample no.	A-1
		Depth	1-2 m
Test method ASTM D1997-91		Date	04/02/2005
Related test			
Speciment ref.		1	
Cointainer no.		1	2
Mass cointainer	g	9.641	9.873
Mass of dry soil of fibers retained #100sieve (m_1)	g	45.201	44.162
Mass of dry soil of fibers retained #100sieve after ignition (m_2)	g	40.814	39.880
Fiber Content FC = $\frac{m_2}{m_1} x100$	%	90.294	90.304
		Average FC = **90.299**	

No	Organic content (%)	Ash Content (%)	Fiber Content (%)	pH
Test 1	94.212	5.788	90.299	3.04
Test 2	98.52	1.48	90.435	3.26
Test 3	98.542	1.458	89.621	3.42
AVERAGE	**97.091**	**2.909**	**90**	**3.24**

5. Sieve Analysis

Typical Test results

Graph TEST 1: SIEVE APARTURE SIZE vs CUMULATIVE (%) PASSED

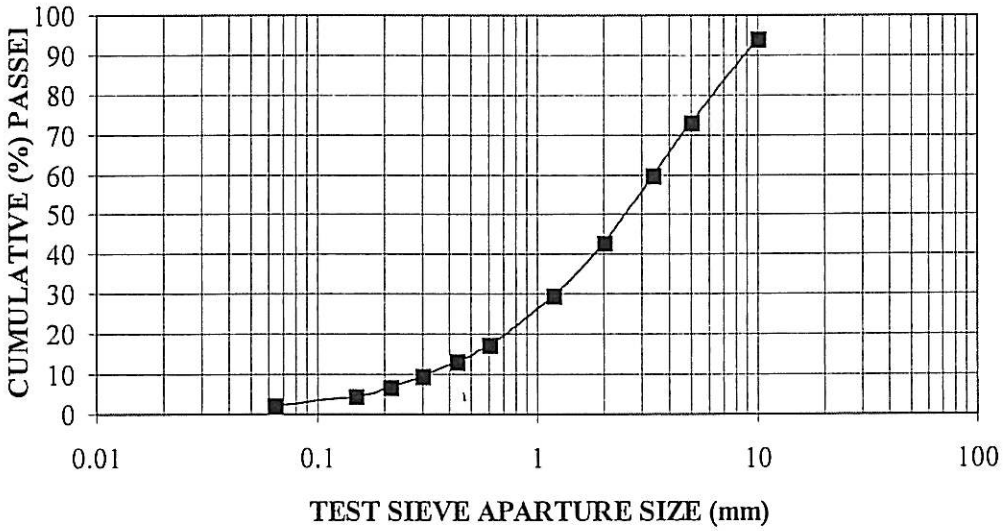

Test No	Sieve Size (mm)	Mass Passing (g)	Percentage Passing Cumulative (%)
1	0.063	9	2.26
2	0.063	11	2.74
3	0.063	13	3.23
AVERAGE			**2.74**

Appendix C

Shear Strength and Initial Permeability

1. Field Vane Shear Test

Date : 09/01/2005										
Sample No	1		2		3		4		5	
Blad NR Page No	1/2	2/2	1/2	2/2	1/2	2/2	1/2	2/2	1/2	2/2
Djup Depth (m)	1	2	1	2	1	2	1	2	1	2
Vinge Vane	ϕ 65 x H130 mm									
Vane Factor (Vc)	1.01									
Undisturbed M_1 (Nm)	14	11.1	13.9	15.5	8.6	12.3	10.7	7.7	15.8	18.4
Remoulded Sample M_3 (Nm)	49	4.8	4.0	9.6	2.0	5.1	3.8	6.4	6.8	9.6
Rod Friction M_{2A} (Nm)	2.1	5.5	2.0	11	1.8	2.5	1.3	3.9	1.7	3.5
Rod Friction M_{2B} (Nm)	3.8	3.4	1.7	5.3	1.4	2.5	3.5	3.8	1.5	4.3
Torque $M_U = M1-M_{2A}$ (Nm)	11.9	5.6	11.9	4.5	6.8	9.8	9.4	3.8	14.1	14.9
Torque $M_r = M1-M_{2B}$ (Nm)	1.1	1.4	2.3	4.3	0.6	2.6	0.30	2.6	5.3	5.3
Shearing Strengths $\tau_{fu} = \frac{M_u}{V_c}$ (kPa)	11.78	5.54	11.78	4.46	6.73	9.7	9.31	3.76	13.96	14.75
Shearing Strengths $(\tau_{fu})_r = \frac{M_r}{V_c}$ (kPa)	1.09	1.39	2.28	4.26	0.59	2.57	0.30	2.57	5.25	5.25
Sensitivity $S_t = \frac{\tau_{fu}}{(\tau_{fu})_r}$	10.81	3.99	5.17	1.05	11.41	3.77	31.03	1.46	2.66	2.81

For 1 m depth :

$$\tau_{fu} = \frac{53.56}{5} = 10.712$$

$$(\tau_{fu})_r = \frac{9.51}{5} = 1.902$$

$$S_t = \frac{27.93}{3} = 9.130$$

For 2 m depth :

$$\tau_{fu} = \frac{38.21}{5} = 7.642$$

$$(\tau_{fu})_r = \frac{16.04}{5} = 3.208$$

$$S_t = \frac{10.57}{3} = 3.523$$

2. Shear Box Test

Typical Test Results

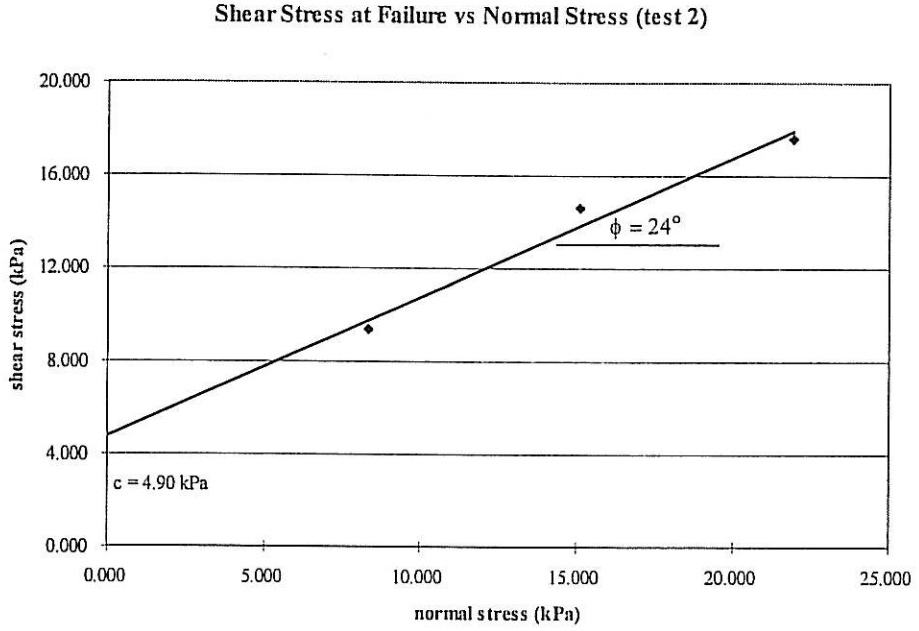

Test 1			
Load (kg)	0.25	0.50	0.75
Normal stress σ_n (kPa)	8.315	15.127	21.940
Shear stress τ (kPa)	8.200	10.300	18.100
Test 2			
Load (kg)	0.25	0.50	0.75
Normal stress σ_n (kPa)	8.315	15.127	21.940
Shear stress τ (kPa)	9.400	14.600	17.600
Test 3			
Load (kg)	0.25	0.50	0.75
Normal stress σ_n (kPa)	8.315	15.127	21.940
Shear stress τ (kPa)	8.700	11.800	17.200

Shear Strength Parameters	**Test 1**	**Test 2**	**Test 3**	**AVERAGE**
Cohesion, c' (kPa)	1.80	4.90	3.25	**3.32**
Friction, ϕ (^{0})	27	24	25	**25**

3. Constant Head Permeability Test

Sample No.1 :

Date of testing the sample: 28th May 2005
Measuring beaker capacity: 1000 ml
Mass of sample + mould: 2295 g
Mass of mould: 1349 g
Mass of sample: 946 g

Hydraulic gradient, i	*Vertical rate of flow, q (ml/ min.)*	*Vertical rate of flow, q (m^3/s)*	*Vertical flow velocity, v (m/ s)*
3.34	85.67	0.00000143	0.00016365
4.99	142.92	0.00000238	0.00027301
6.64	214.62	0.00000358	0.00040997
7.47	237.77	0.00000396	0.00045419
7.88	255.03	0.00000425	0.00048716
8.29	274.67	0.00000458	0.00052467

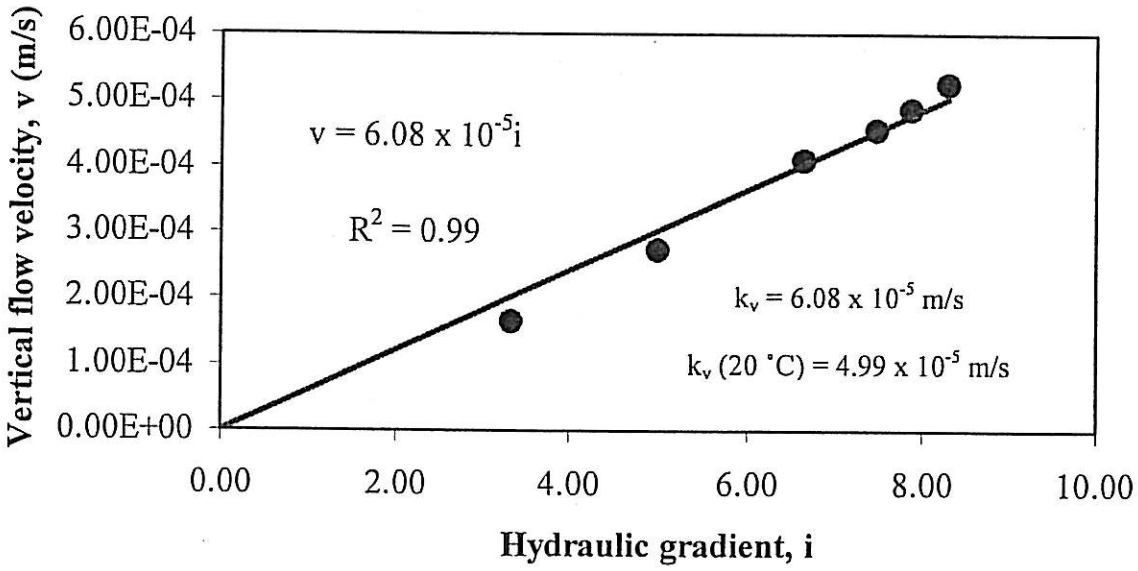

Sample No.2 :

Date of testing the sample: 2nd June 2005
Measuring beaker capacity: 1000 ml
Mass of sample + mould: 1941 g
Mass of mould: 985 g
Mass of sample: 956 g

Hydraulic gradient, i	*Vertical rate of flow, q (ml/min.)*	*Vertical rate of flow, q (m^3/s)*	*Vertical flow velocity, v (m/s)*
2.10	422.82	0.00000705	0.00080767
2.52	432.12	0.00000720	0.00082543
2.93	441.78	0.00000736	0.00084389
3.34	462.57	0.00000771	0.00088360
3.75	462.80	0.00000771	0.00088404
4.17	504.63	0.00000841	0.00096394

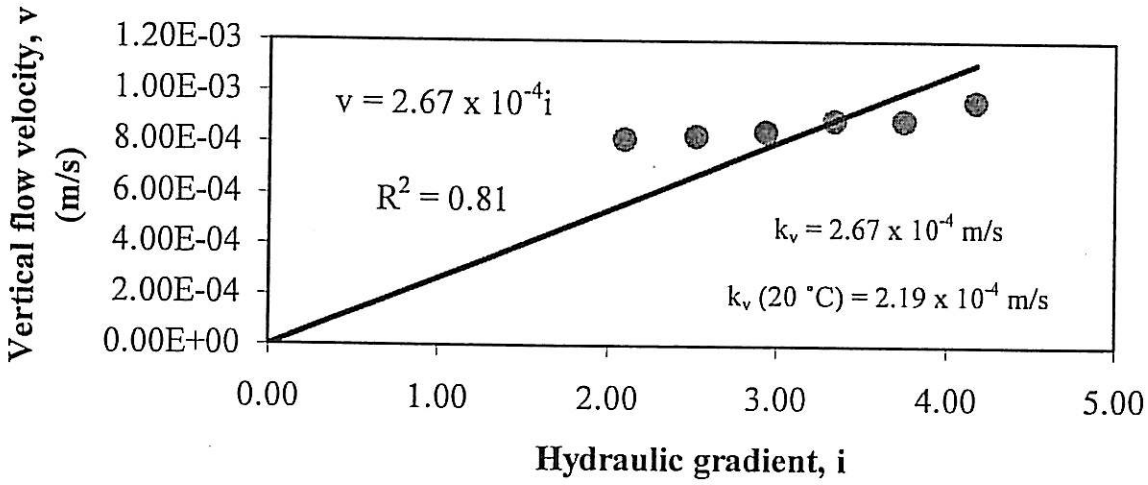

Sample No.3 :

Date of testing the sample: 2nd June 2005
Measuring beaker capacity: 1000 ml
Mass of sample + mould: 2334 g
Mass of mould: 1345 g
Mass of sample: 989 g

Hydraulic gradient, i	*Vertical rate of flow, q (ml/min.)*	*Vertical rate of flow, q (m^3/s)*	*Vertical flow velocity, v (m/s)*
3.34	254.20	0.00000424	0.00048557
4.99	337.89	0.00000563	0.00064544
6.64	398.64	0.00000664	0.00076148
7.47	430.84	0.00000718	0.00082299
7.88	432.29	0.00000720	0.00082576
8.29	437.65	0.00000729	0.00083600

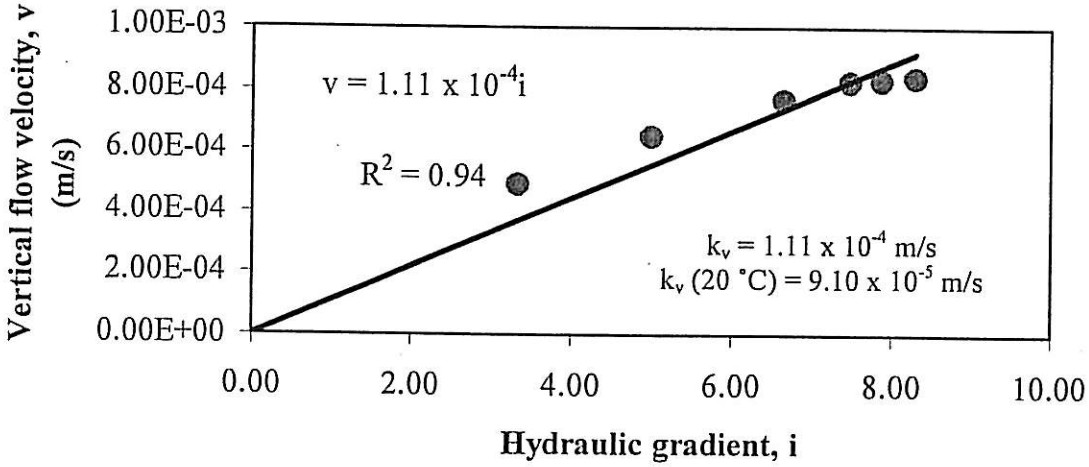

Data of coefficient of permeability at 20°C, *k (20 °C)* for Fibrous Peat Soil :

Vertical sample no.	**Total mass of initial soil sample, M_T (kg)**	**Total volume of initial sample, V_T (m^3)**	**Bulk density, ρ (kg/m^3)**	**Moisture content, *w* (%)**	**Dry density, ρ_d (kg/m^3)**	**Initial void ratio, e_o**	**Coefficient of permeability at 20°C, k_v (20°C) (m/s)**
1	0.946	0.0010574838	894.58	526.68	142.75	9.62	0.00004990
2	0.956	0.0010574838	904.03	578.02	133.33	10.37	0.00021900
3	0.989	0.0010574838	935.24	679.16	120.03	11.63	0.00091000

Average vertical coefficient of permeability at 29 °C, k_v = **1.46 x 10^{-4} m/s**

Average vertical coefficient of permeability at 20 °C, k_v **(20 °C) = 1.20 x 10^{-4} m/s**

APPENDIX D

Standard Consolidation Tests

Typical Time-Compression Curve

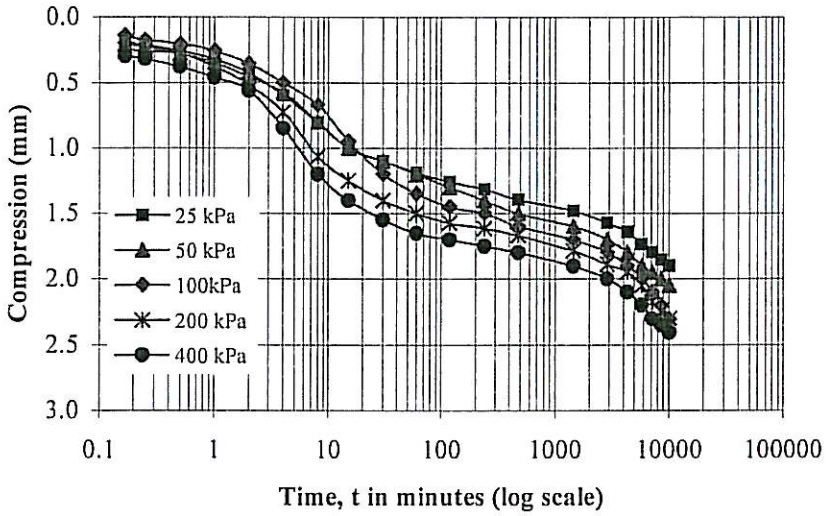

1. Analysis of Time-Compression curve (based onCassagrande)

Test 1		**25 kPa**	**50 kPa**	**100 kPa**	**200 kPa**	**400 kPa**
Soil compression parameter	t_p (minutes)	28	27	26	24	22
	t_s (minutes)	3000	2800	3100	4500	3100
	$c_{\alpha 1}$	0.003	0.003	0.003	0.001	0.001
	$c_{\alpha 2}$	0.004	0.004	0.007	0.013	0.008
	$c_v(m^2/year)$	3.187	2.026	1.366	0.844	0.702
Test 2		**25 kPa**	**50 kPa**	**100 kPa**	**200 kPa**	**400 kPa**
Soil compression parameter	t_p (minutes)	29	25	25	30	23
	t_s (minutes)	3000	2400	2800	2900	2800
	$c_{\alpha 1}$	0.001	0.002	0.018	0.001	0.012
	$c_{\alpha 2}$	0.004	0.004	0.010	0.005	0.004
	$c_v(m^2/year)$	1.558	1.290	1.154	0.574	0.369
Test 3		**25 kPa**	**50 kPa**	**100 kPa**	**200 kPa**	**400 kPa**
Soil compression parameter	t_p (minutes)	15	18	20	17	12
	t_s (minutes)	3500	3500	3500	3400	3000
	$c_{\alpha 1}$	0.001	0.001	0.001	0.001	0.001
	$c_{\alpha 2}$	0.001	0.001	0.001	0.002	0.001
	$c_v(m^2/year)$	3.273	2.147	1.514	1.289	1.094
AVERAGE		**25 kPa**	**50 kPa**	**100 kPa**	**200 kPa**	**400 kPa**
Soil compression parameter	t_p (minutes)	**24**	**23**	**24**	**24**	**19**
	t_s (minutes)	**3167**	**2900**	**3133**	**3600**	**2967**
	$c_{\alpha 1}$	**0.002**	**0.002**	**0.007**	**0.001**	**0.005**
	$c_{\alpha 2}$	**0.003**	**0.003**	**0.003**	**0.001**	**0.004**
	$c_v(m^2/year)$	**2.673**	**1.821**	**1.345**	**0.902**	**0.722**

Typical e-p' and e-log p' curve

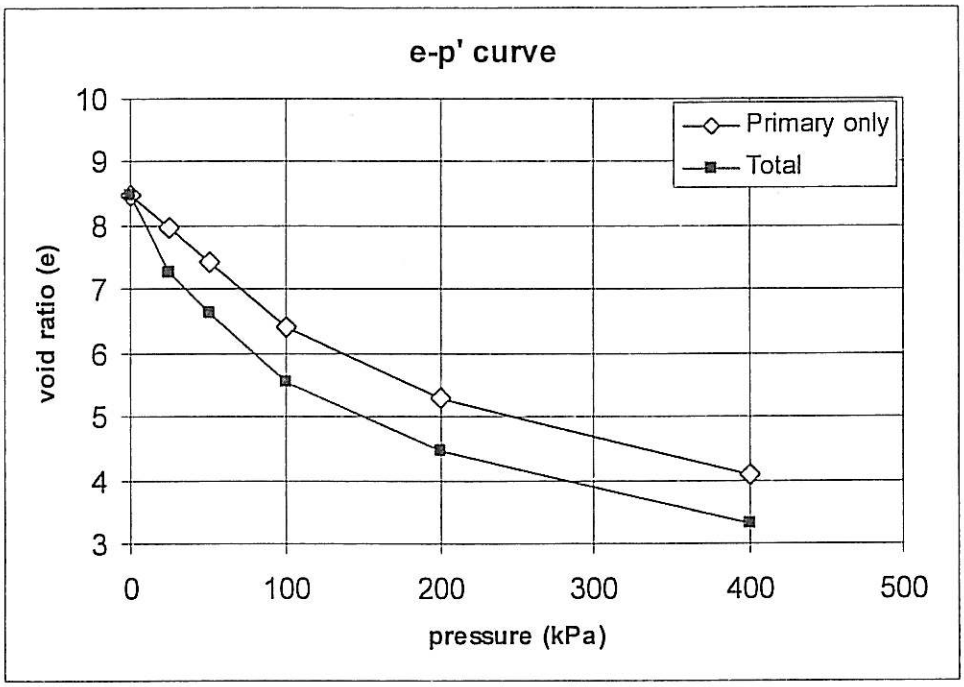

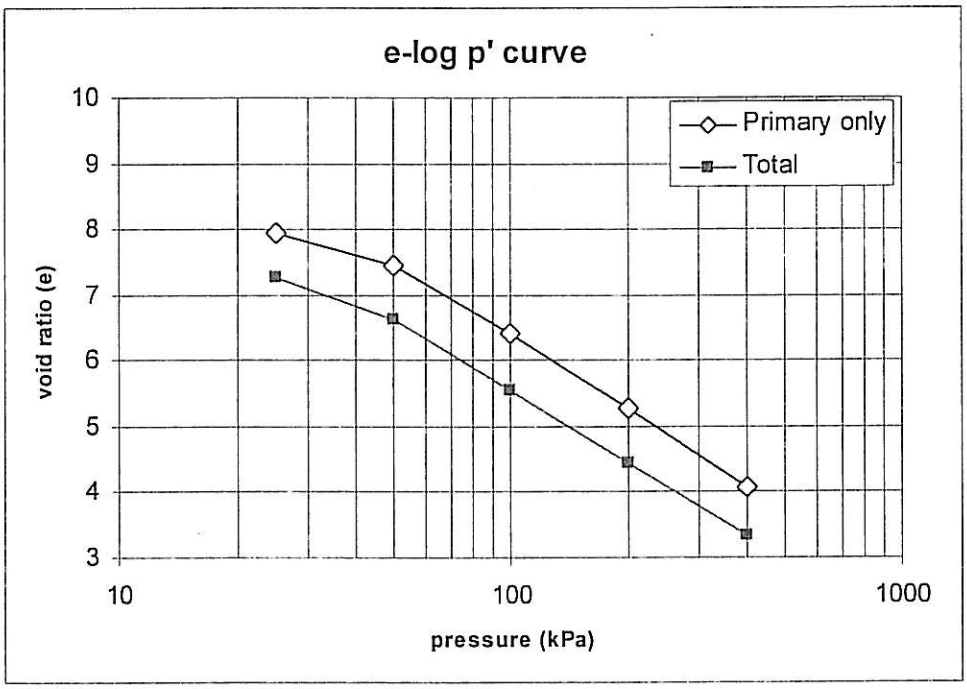

2. Analysis e-log p' curve from Oedometer Tests

Test 1	(p+s)	(p)
Initial void ratio (e_o)	8.471	
Compression index (C_c)	3.571	3.488
Preconsolidation pressure ($\sigma'p$)	47	46
Test 2	(p+s)	(p)
Void ratio (e_o)	11.664	
Compression index (C_c)	5.642	5.547
Preconsolidation pressure ($\sigma'p$)	43	40
Test 3	(p+s)	(p)
Void ratio (e_o)	10.702	
Compression index (C_c)	2.104	2.084
Preconsolidation pressure ($\sigma'p$)	51	50
AVERAGE	(p+s)	(p)
Void ratio (e_o)	**10.270**	
Compression index (C_c)	**3.772**	**3.706**
Preconsolidation pressure ($\sigma'p$)	**47**	**45**

3. Analysis of Permeability based on Primary Consolidation

Test 1	Consolidation Pressure				
	25 kPa	50 kPa	100 kPa	200 kPa	400 kPa
Coefficient of compressibility (a_v)	0.021	0.021	0.021	0.011	0.006
Coefficient of volume compressibility (m_v)	0.00218	0.00218	0.00218	0.00119	0.00063
Coefficient of rate of consolidation (c_v)	3.187	2.026	1.366	0.844	0.702
Vertical coefficient of permeability (k_v)	6.953×10^{-3}	4.420×10^{-3}	2.980×10^{-3}	1.004×10^{-3}	4.438×10^{-4}
Test 2	Consolidation Pressure				
	25 kPa	50 kPa	100 kPa	200 kPa	400 kPa
Coefficient of compressibility (a_v)	0.047	0.037	0.035	0.018	0.009
Coefficient of volume compressibility (m_v)	0.00374	0.00292	0.00275	0.00145	0.00077
Coefficient of rate of consolidation (c_v)	1.558	1.290	1.154	0.574	0.369
Vertical coefficient of permeability (k_v)	5.827×10^{-3}	3.772×10^{-3}	3.171×10^{-3}	8.323×10^{-4}	2.852×10^{-4}
Test 3	Consolidation Pressure				
	25 kPa	50 kPa	100 kPa	200 kPa	400 kPa
Coefficient of compressibility (a_v)	0.027	0.021	0.011	0.006	0.004
Coefficient of volume compressibility (m_v)	0.00234	0.00178	0.00097	0.00054	0.00030
Coefficient of rate of consolidation (c_v)	3.273	2.147	1.514	1.289	1.094
Vertical coefficient of permeability (k_v)	7.674×10^{-3}	3.826×10^{-3}	1.475×10^{-3}	6.968×10^{-4}	3.266×10^{-4}
Average	Consolidation Pressure				
	25 kPa	50 kPa	100 kPa	200 kPa	400 kPa
Coefficient of compressibility (a_v)	**0.032**	**0.026**	**0.022**	**0.011**	**0.006**
Coefficient of volume compressibility (m_v)	**0.00275**	**0.00229**	**0.00197**	**0.00106**	**0.00050**
Coefficient of rate of consolidation (c_v)	**2.673**	**1.821**	**1.345**	**0.902**	**0.722**
Vertical coefficient of permeability (k_v)	$\mathbf{6.818\times10^{-3}}$	$\mathbf{4.006\times10^{-3}}$	$\mathbf{2.542\times10^{-3}}$	$\mathbf{5.130\times10^{-4}}$	$\mathbf{3.519\times10^{-4}}$

APPENDIX E

Hydraulic Consolidation Tests (Rowe Cell)

1. Analysis of Time Compression Curve

1.a. Casagrande Method

Test 1

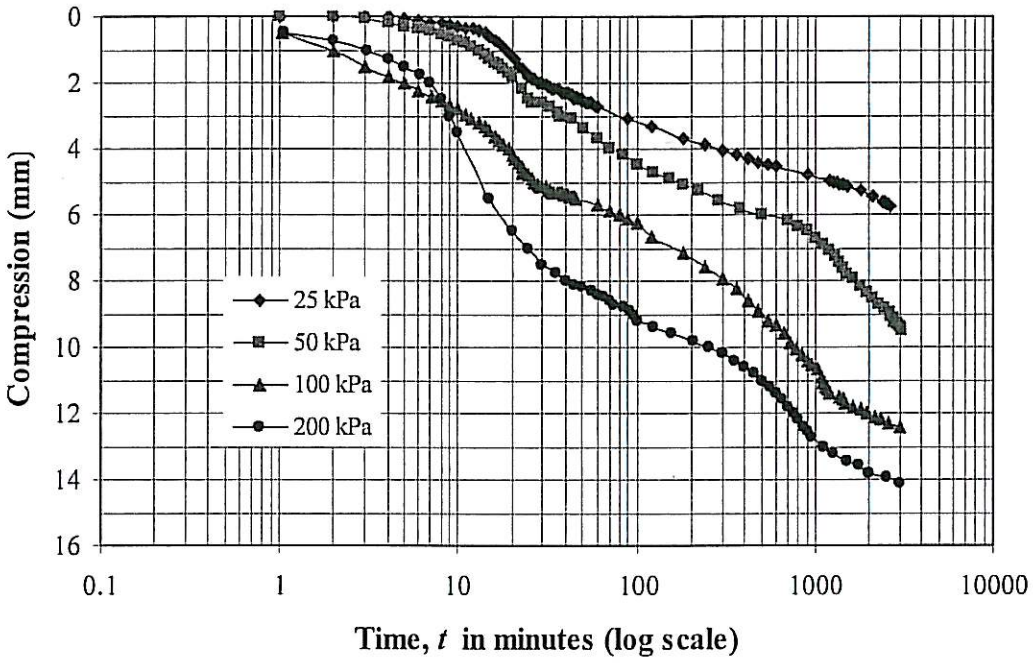

Test 1: Casagrande Test Results					
Consolidation pressure		**25 kPa**	**50 kPa**	**100 kPa**	**200 kPa**
Soil compression parameter	t_p (minutes)	29	28	28	22
	t_s (minutes)	1500	1100	1200	900
	$c_{\alpha 1}$	0.008	0.011	0.010	0.006
	$c_{\alpha 2}$	0.011	0.014	0.010	0.009
	$c_v(m^2/year)$	0.812	0.454	0.491	0.419

Average for Casagrande Test Results					
Consolidation pressure		**25 kPa**	**50 kPa**	**100 kPa**	**200 kPa**
Soil compression parameter	t_p (minutes)	41	40	40	38
	t_s (minutes)	1180	1130	860	800
	$c_{\alpha 1}$	0.004	0.006	0.021	0.011
	$c_{\alpha 2}$	0.009	0.015	0.017	0.018
	$c_v(m^2/year)$	0.573	0.393	0.327	0.209

Test 2

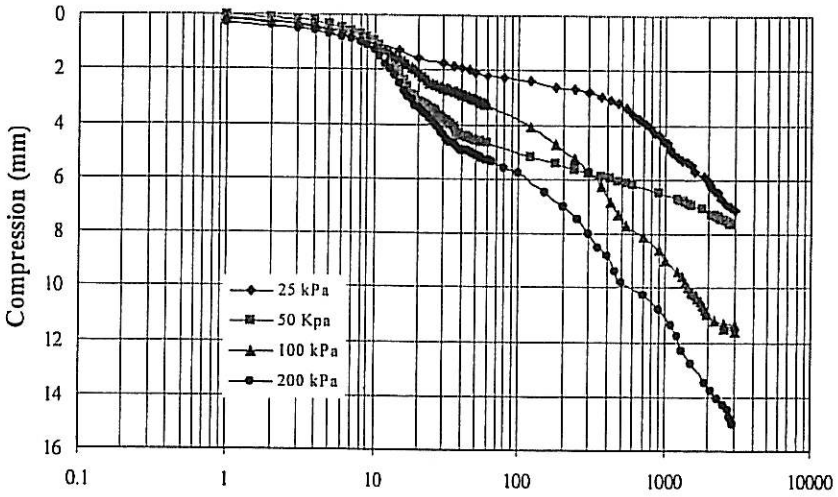

Test 2: Casagrande Test Results					
Consolidation pressure		**25 kPa**	**50 kPa**	**100 kPa**	**200 kPa**
Soil compression parameter	t_p (minutes)	30	28	25	25
	t_s (minutes)	900	900	600	550
	$c_{\alpha 1}$	0.003	0.006	0.008	0.006
	$c_{\alpha 2}$	0.021	0.007	0.015	0.009
	$c_v(m^2/year)$	0.951	0.515	0.447	0.271

Test 3

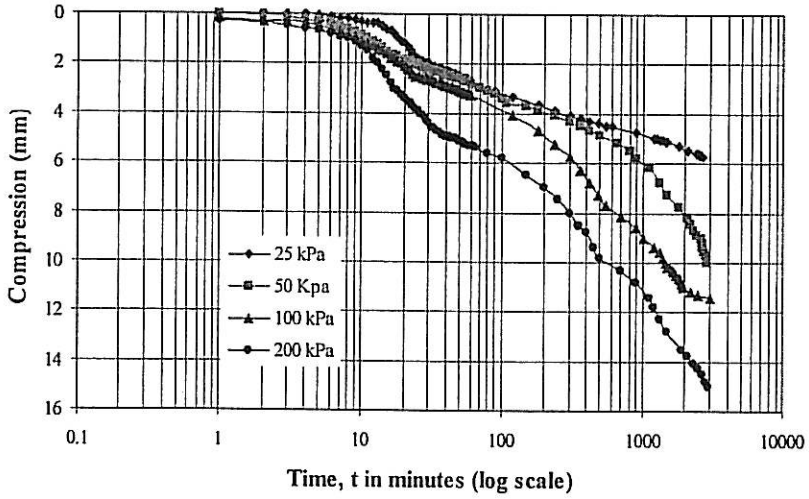

Test 3: Casagrande Test Results					
Consolidation pressure		**25 kPa**	**50 kPa**	**100 kPa**	**200 kPa**
Soil compression parameter	t_p (minutes)	28	27	25	25
	t_s (minutes)	1700	1600	500	500
	$c_{\alpha 1}$	0.007	0.007	0.008	0.009
	$c_{\alpha 2}$	0.007	0.014	0.022	0.019
	$c_v(m^2/year)$	0.571	0.509	0.364	0.154

Test 4

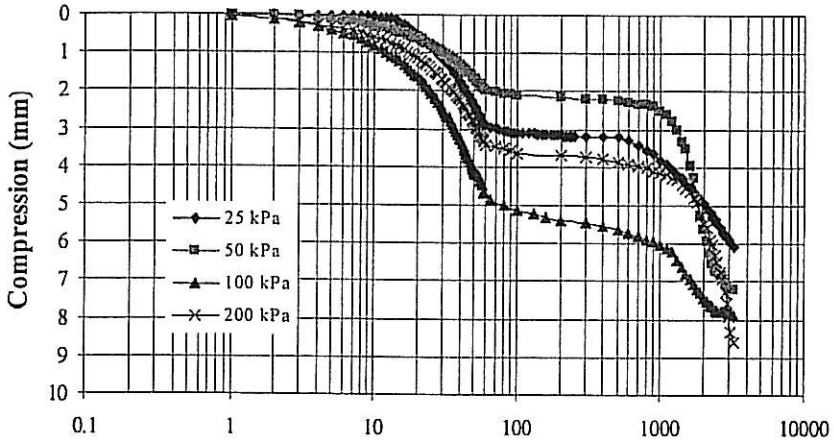

Test 4: Casagrande Test Results					
Consolidation pressure		**25 kPa**	**50 kPa**	**100 kPa**	**200 kPa**
Soil compression parameter	t_p (minutes)	60	60	60	60
	t_s (minutes)	900	1200	1100	1200
	$c_{\alpha 1}$	0.001	0.001	0.002	0.002
	$c_{\alpha 2}$	0.001	0.032	0.011	0.026
	c_v(m^2/year)	0.225	0.225	0.130	0.080

Test 5

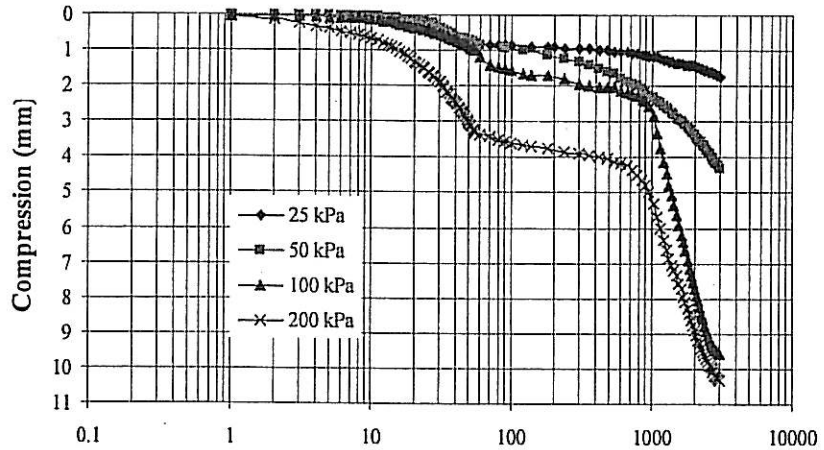

Test 5: Casagrande Test Results					
Consolidation pressure		**25 kPa**	**50 kPa**	**100 kPa**	**200 kPa**
Soil compression parameter	t_p (minutes)	60	55	60	58
	t_s (minutes)	900	850	900	850
	$c_{\alpha 1}$	0.001	0.003	0.003	0.003
	$c_{\alpha 2}$	0.003	0.006	0.029	0.026
	c_v(m^2/year)	0.306	0.261	0.204	0.120

1.b. Taylors Method

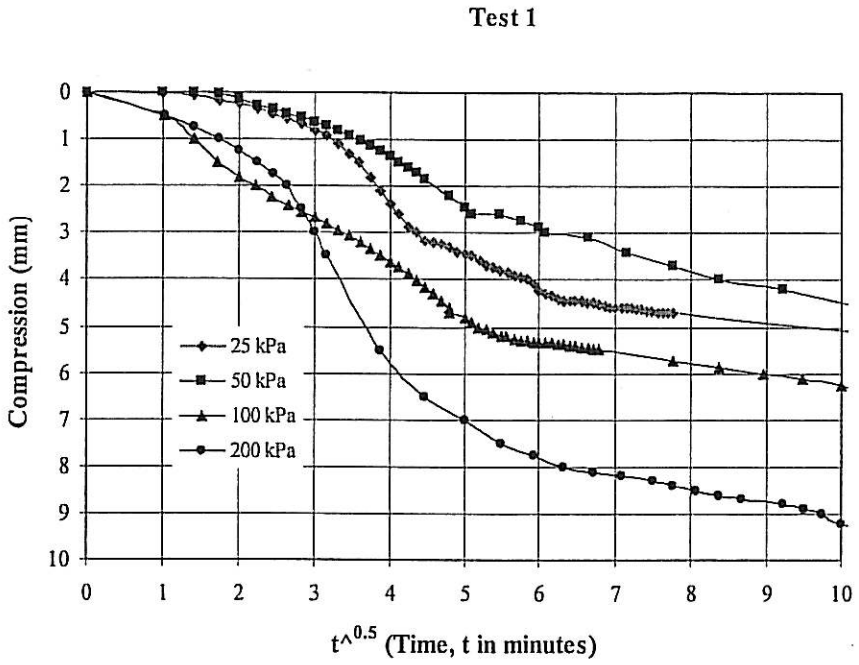

Test 1: Taylors Test Results					
Consolidation pressure		25 kPa	50 kPa	100 kPa	200 kPa
Soil compression parameter	c_v (m^2/year)	1.249	1.127	0.952	0.670

Average for Taylors Test Results					
Consolidation pressure		25 kPa	50 kPa	100 kPa	200 kPa
Soil compression parameter	c_v (m^2/year)	0.718	0.636	0.431	0.292

Test 2

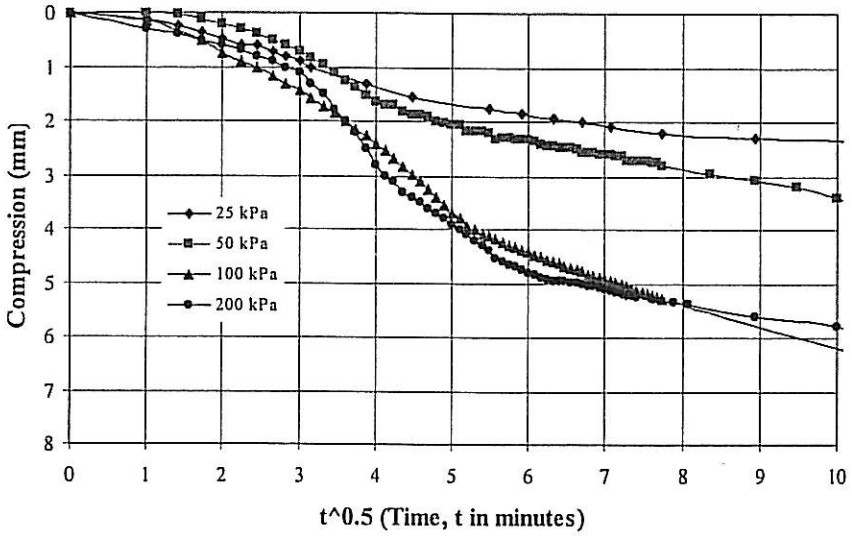

Test 2: Taylors Test Results					
Consolidation pressure		25 kPa	50 kPa	100 kPa	200 kPa
Soil compression parameter	c_v (m^2/year)	0.872	0.808	0.410	0.286

Test 3

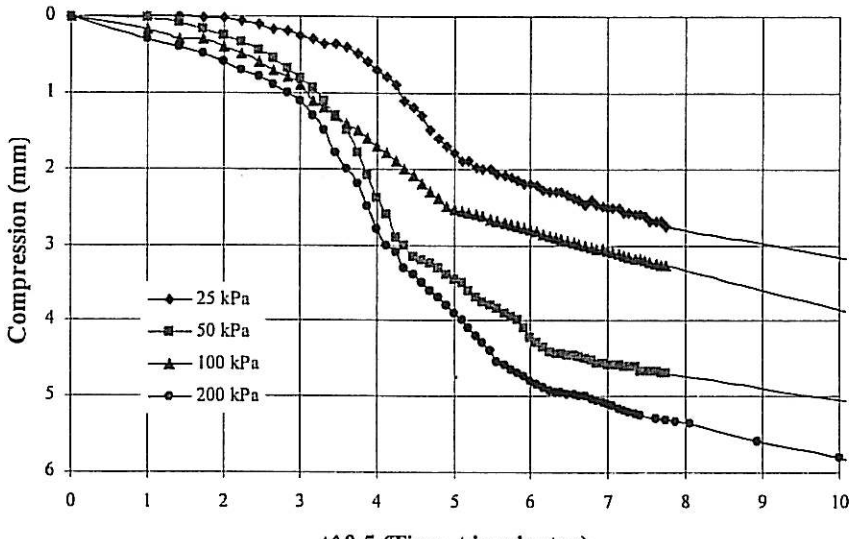

Test 3: Taylors Test Results					
Consolidation pressure		25 kPa	50 kPa	100 kPa	200 kPa
Soil compression parameter	c_v (m^2/year)	0.596	0.528	0.390	0.217

Test 4

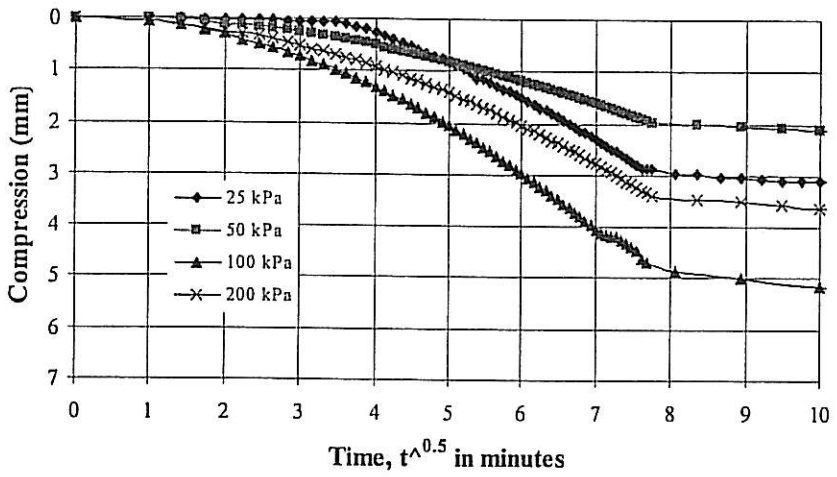

Test 4: Taylors Test Results					
Consolidation pressure		25 kPa	50 kPa	100 kPa	200 kPa
Soil compression parameter	c_v (m^2/year)	0.418	0.311	0.187	0.117

Test 5

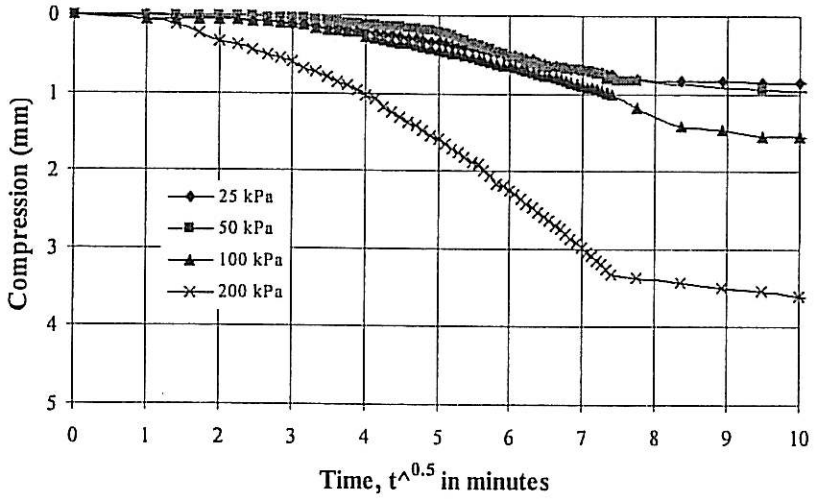

Test5: Taylors Test Results					
Consolidation pressure		25 kPa	50 kPa	100 kPa	200 kPa
Soil compression parameter	c_v (m^2/year)	0.456	0.406	0.215	0.169

1.c. Sridharan and Prakash Method

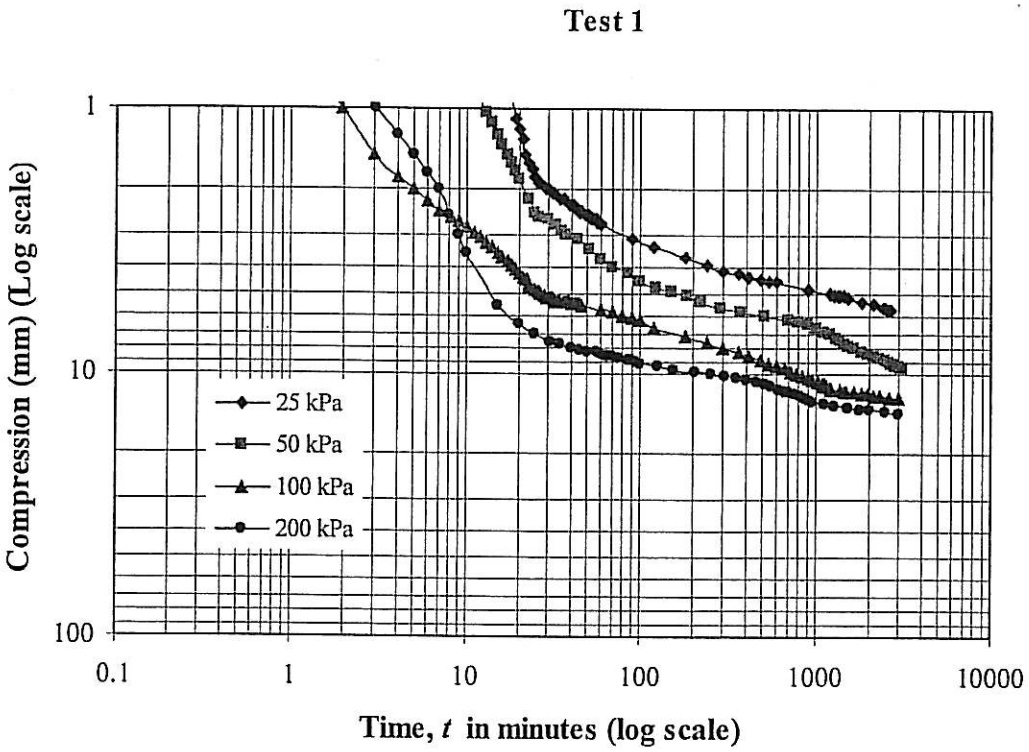

Test 1: Sridharan & Prakash Test Results					
Consolidation pressure		**25 kPa**	**50 kPa**	**100 kPa**	**200 kPa**
Soil compression parameter	t_p (minutes)	30	27	25	18
	c_α	0.007	0.006	0.010	0.004
	c_v(m^2/year)	1.064	1.057	0.932	0.742

Average for Sridharan & Prakash Test Results					
Consolidation pressure		**25 kPa**	**50 kPa**	**100 kPa**	**200 kPa**
Soil compression parameter	t_p (minutes)	42	38	37	34
	c_α	0.003	0.004	0.006	0.005
	c_v(m^2/year)	1.222	0.950	0.691	0.464

Test 2

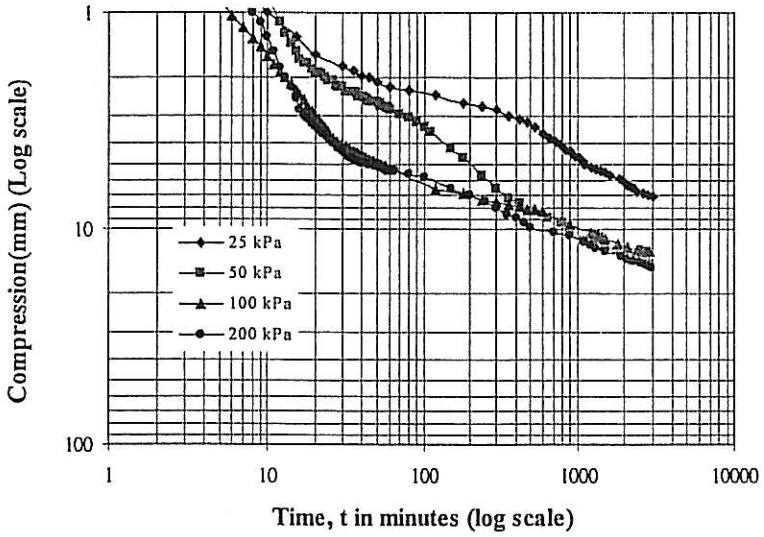

Test 2: Sridharan & Prakash Test Results					
Consolidation pressure		**25 kPa**	**50 kPa**	**100 kPa**	**200 kPa**
Soil compression parameter	t_p (minutes)	29	23	23	22
	$c\alpha$	0.001	0.005	0.005	0.005
	c_v(m^2/year)	1.483	1.438	1.018	0.632

Test 3

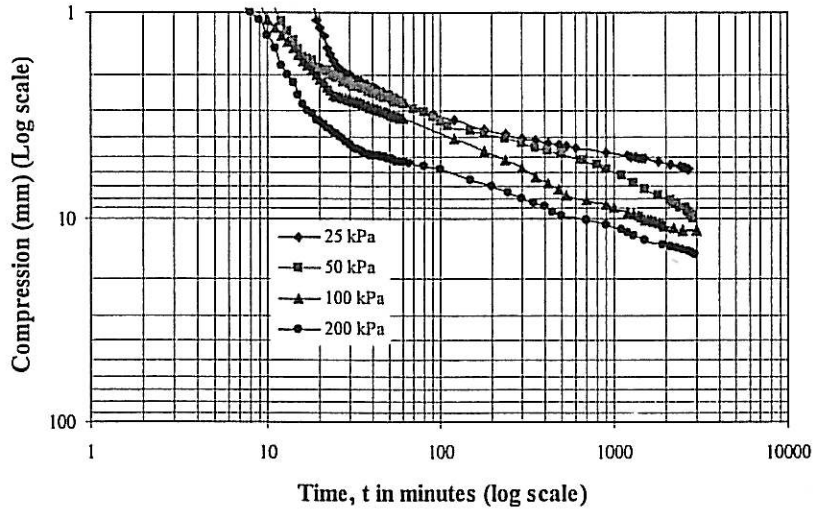

Test 3: Sridharan & Prakash Test Results					
Consolidation pressure		**25 kPa**	**50 kPa**	**100 kPa**	**200 kPa**
Soil compression parameter	t_p (minutes)	29	28	26	23
	$c\alpha$	0.006	0.005	0.009	0.009
	c_v(m^2/year)	2.277	1.153	0.769	0.519

Test 4

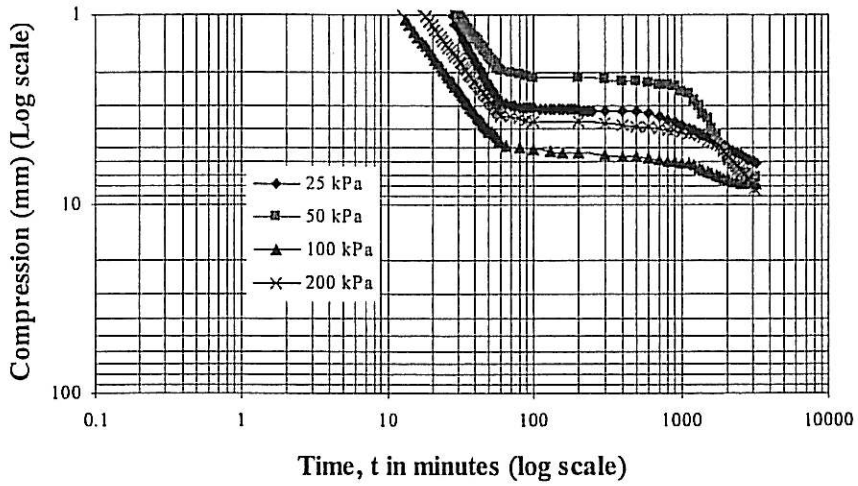

Test 4: Sridharan & Prakash Test Results					
Consolidation pressure		25 kPa	50 kPa	100 kPa	200 kPa
Soil compression parameter	t_p (minutes)	60	60	50	50
	$c\alpha$	0.001	0.001	0.003	0.003
	c_v(m^2/year)	0.603	0.448	0.312	0.179

Test 5

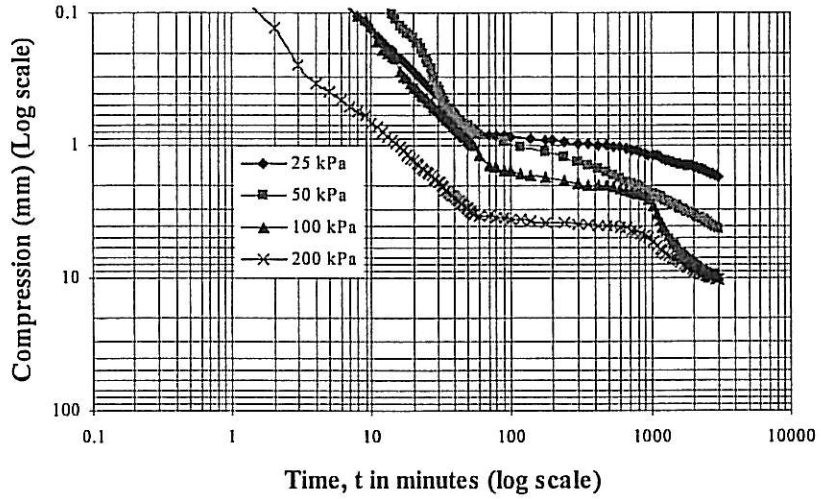

Test 5: Sridharan & Prakash Test Results					
Consolidation pressure		25 kPa	50 kPa	100 kPa	200 kPa
Soil compression parameter	t_p (minutes)	60	50	60	55
	$c\alpha$	0.002	0.002	0.002	0.002
	c_v(m^2/year)	0.684	0.656	0.422	0.248

1.d. Robinson Method

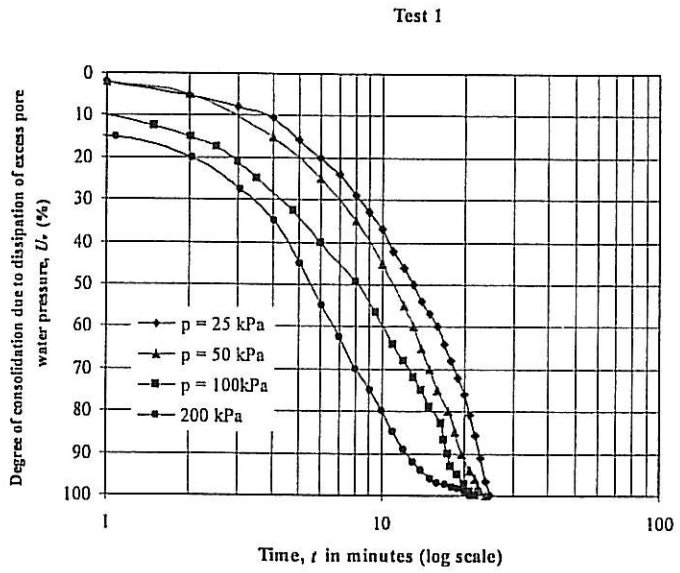

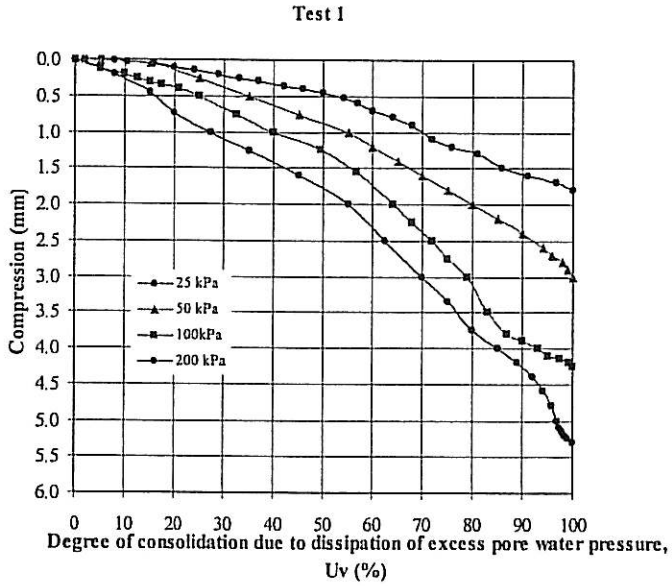

Test 1 : Robinson Test Results					
Consolidation pressure		**25 kPa**	**50 kPa**	**100 kPa**	**200 kPa**
Soil compression parameter	t_p (100) (minute)	25	24	23	22
	U_v (%)	60	60	58	55
	t_p (minutes)	16.5	14	9.5	6
	c_v(m^2/year)	1.053	1.052	1.168	1.158

Average for Robinson Test Results					
Consolidation pressure		**25 kPa**	**50 kPa**	**100 kPa**	**200 kPa**
Soil compression parameter	t_p (100) (minute)	27	26	23	23
	U_v (%)	61	65	68	69
	t_p (minutes)	18	15	13	13
	c_v(m^2/year)	0.676	0.685	0.631	0.540

Test 2

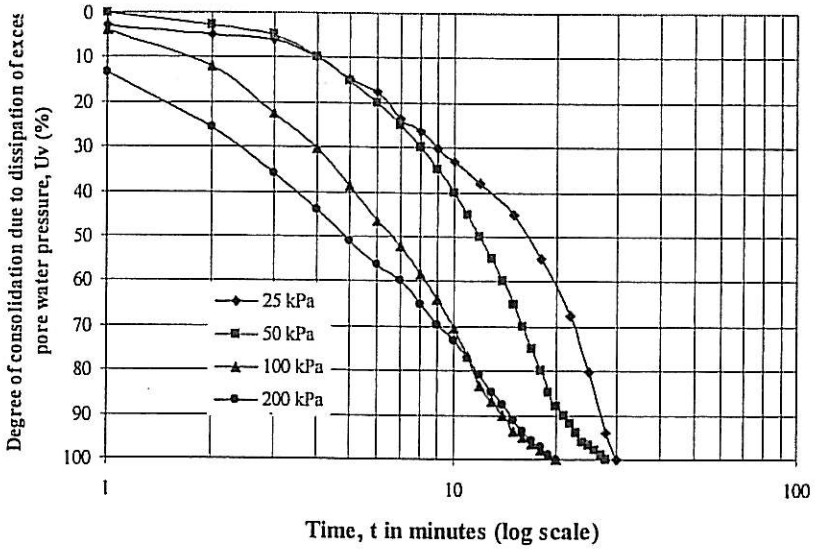

Test 2

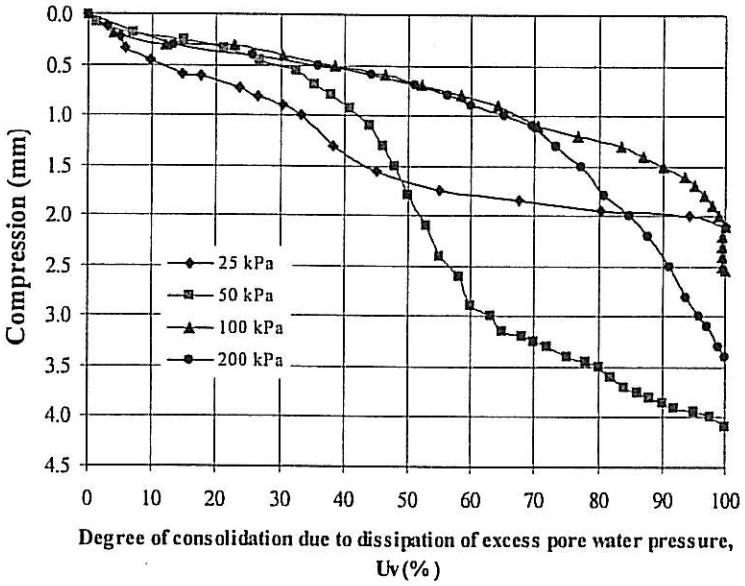

Test 2 : Robinson Test Results					
Consolidation pressure		**25 kPa**	**50 kPa**	**100 kPa**	**200 kPa**
Soil compression parameter	t_p (100)(minute)	30	28	20	20
	U_v (%)	68	85	70	70
	t_p (minutes)	22	19	10	9
	c_v(m^2/year)	0.535	0.534	0.596	0.609

Test 3

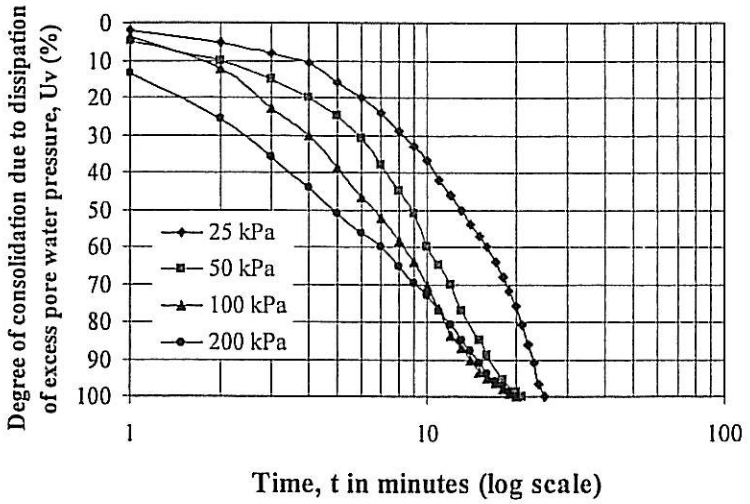

Test 3

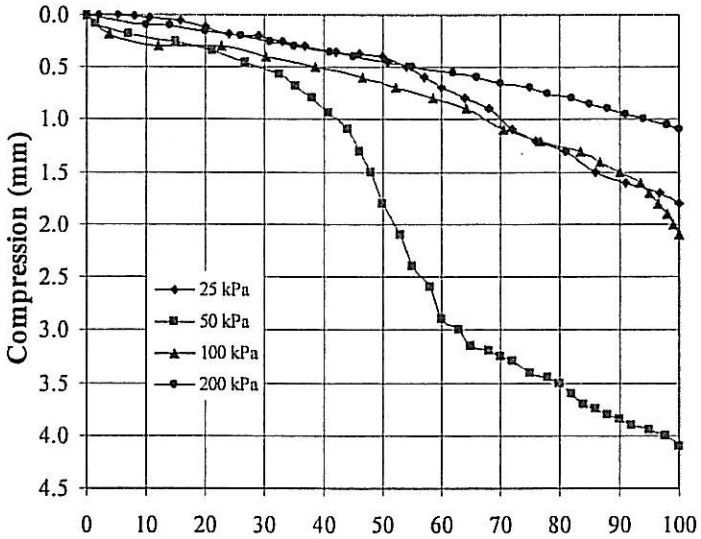

Test 3 : Robinson Test Results					
Consolidation pressure		**25 kPa**	**50 kPa**	**100 kPa**	**200 kPa**
Soil compression parameter	t_p (100)	25	21	20	20
	U_v (%)	50	50	64	70
	t_p (minutes)	13	9	9	9
	c_v(m^2/year)	0.615	0.909	0.672	0.524

Test 4

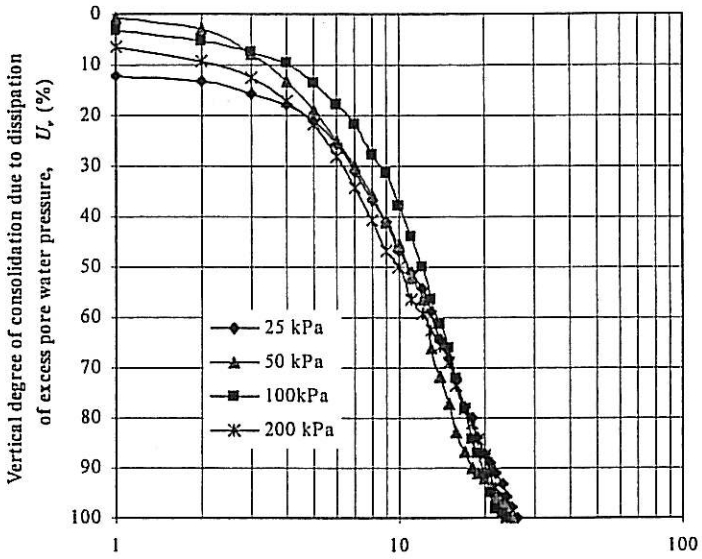

Time, t in minutes (log scale)

Test 4

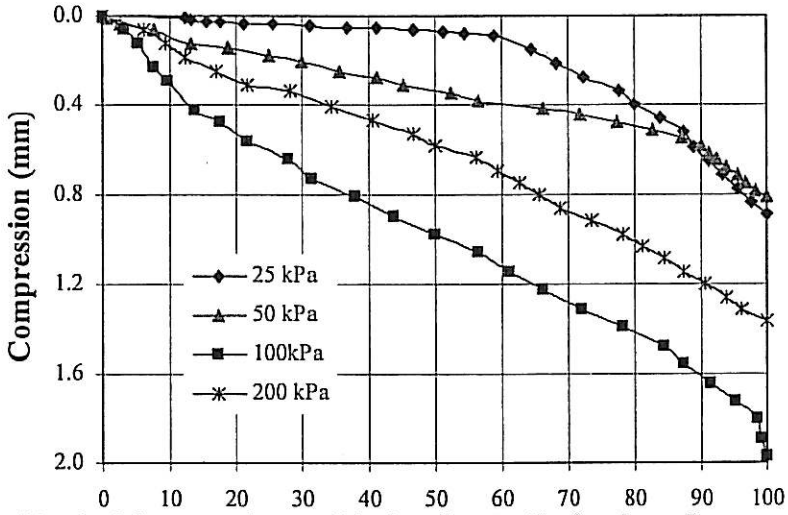

Vertical degree of consolidation due to dissipation of excess pore water pressure, Uv (%)

Test 4 : Robinson Test Results					
Consolidation pressure		25 kPa	50 kPa	100 kPa	200 kPa
Soil compression parameter	t_p (100) (minute)	26	25	24	24
	U_v (%)	60	58	80	85
	t_p (minutes)	14	13	17	18
	c_v(m^2/year)	0.715	0.508	0.326	0.187

Test 5

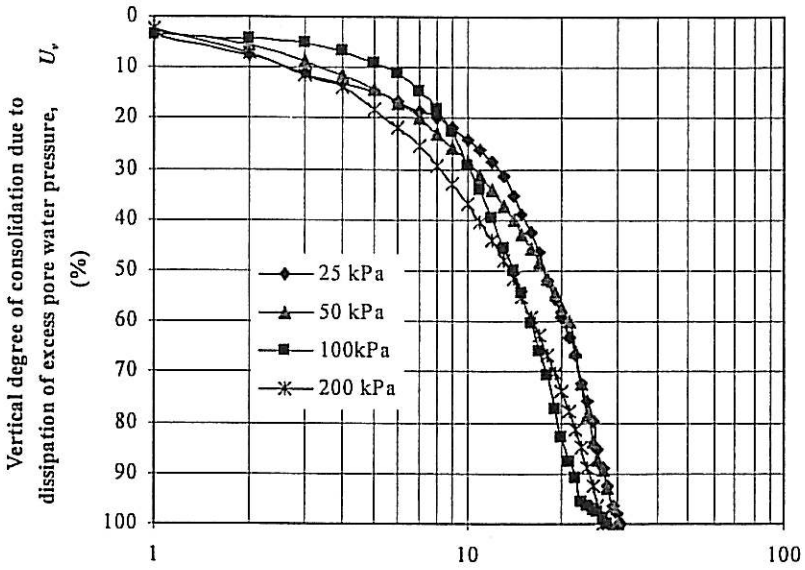

Test 5

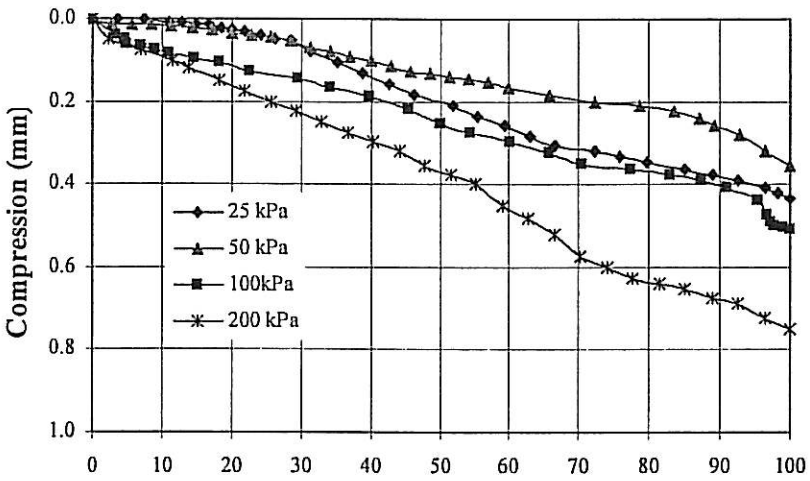

Test 5 : Robinson Test Results					
Consolidation pressure		**25 kPa**	**50 kPa**	**100 kPa**	**200 kPa**
Soil compression parameter	t_p (100) (minutes)	31	30	28	27
	U_v (%)	68	72	70	67
	t_p (minutes)	23	22	19	18
	c_v(m^2/year)	0.464	0.421	0.393	0.222

2.a. Analysis e-log P curve from Rowe Cell Tests

e-Log P curve of Test 1 (P+S)

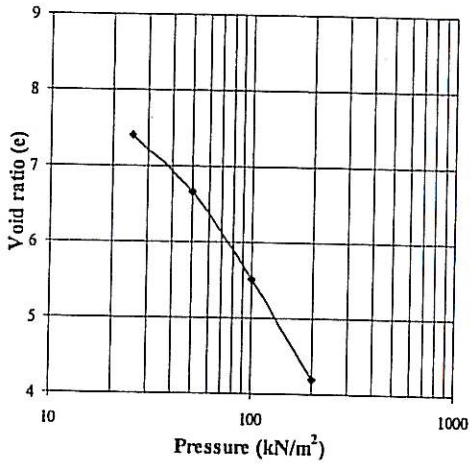

e-Log P curve of Test 1 (P)

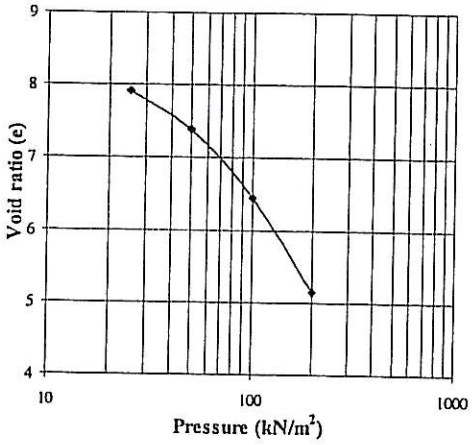

e-Log P Test 1 Rowe Cell Results		
Compressibility characteristics	(p+s)	(p)
Compression index (C_c)	4.272	4.146
Preconsolidation pressure (σ'p)	43	42

e-Log P curve of Test 2 (P+S)

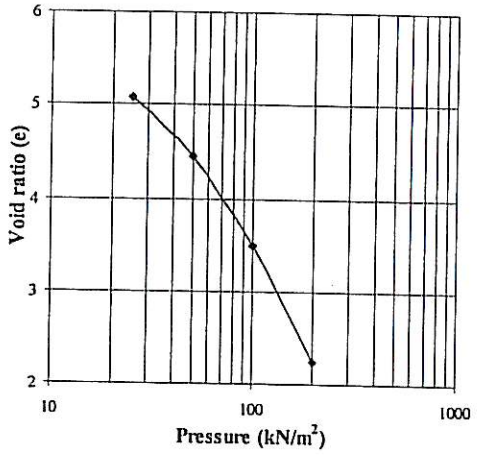

e-Log P curve of Test 2 (P)

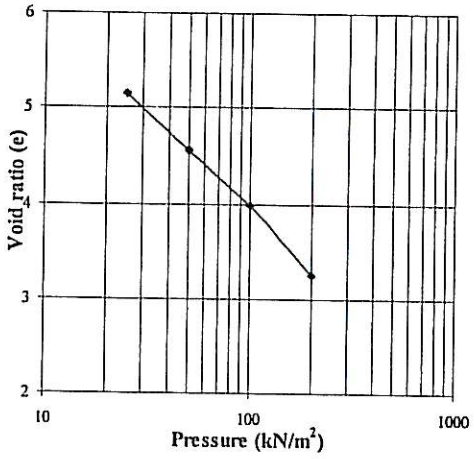

e-Log P Test 2 Rowe Cell Results		
Compressibility characteristics	(p+s)	(p)
Compression index (C_c)	3.838	2.199
Preconsolidation pressure (σ'p)	44	42

e-Log P curve of Test 3 (P+S)

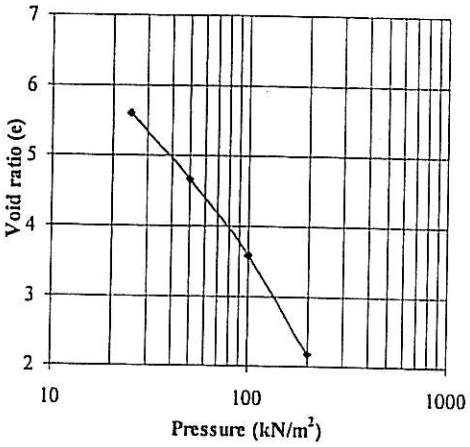

e-Log P curve of Test 3 (P)

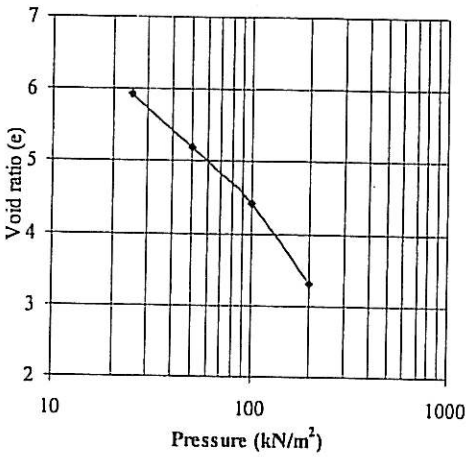

e-Log P Test 3 Rowe Cell Results		
Compressibility characteristics	(p+s)	(p)
Compression index (C_c)	4.496	3.016
Preconsolidation pressure ($\sigma'p$)	41	40

e-Log P curve of Test 4 (P+S)

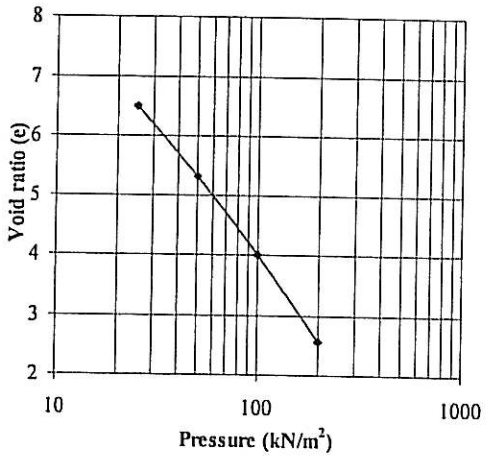

e-Log P curve of Test 4 (P)

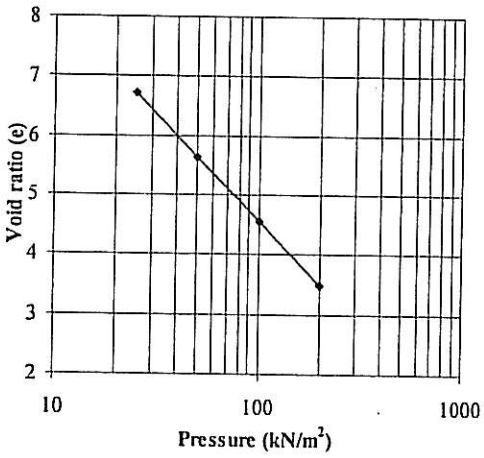

e-Log P Test 4 Rowe Cell Results		
Compressibility characteristics	(p+s)	(p)
Compression index (C_c)	4.649	3.986
Preconsolidation pressure ($\sigma'p$)	42	40

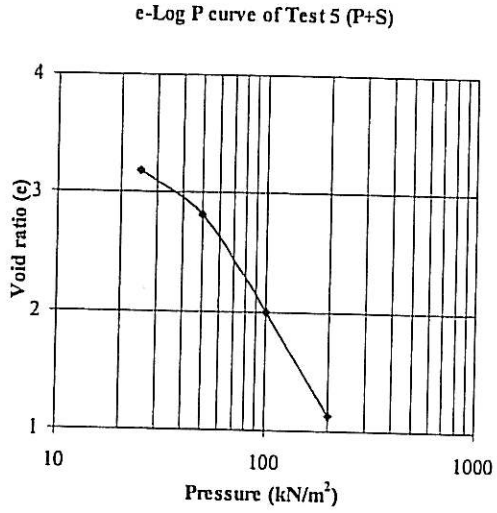

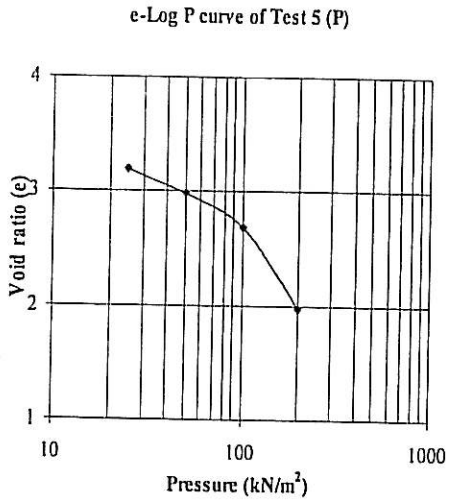

e-Log P Test 5 Rowe Cell Results		
Compressibility characteristics	(p+s)	(p)
Compression index (C_c)	2.869	2.292
Preconsolidation pressure ($\sigma'p$)	44	42

Average for e-Log P Rowe Cell Results		
Compressibility characteristics	(p+s)	(p)
Compression index (C_c)	4.025	3.128
Preconsolidation pressure ($\sigma'p$)	43	41

2.b. Analysis e-P' curve from Rowe Cell Tests

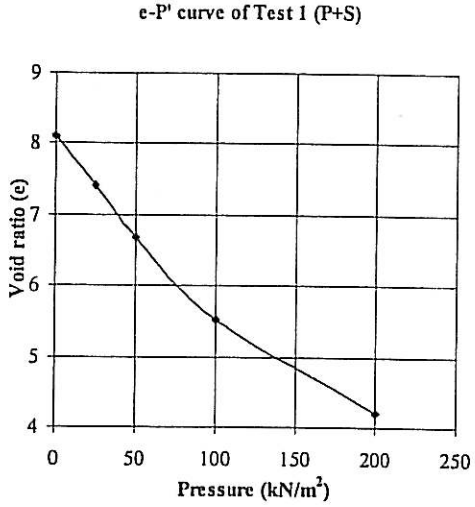

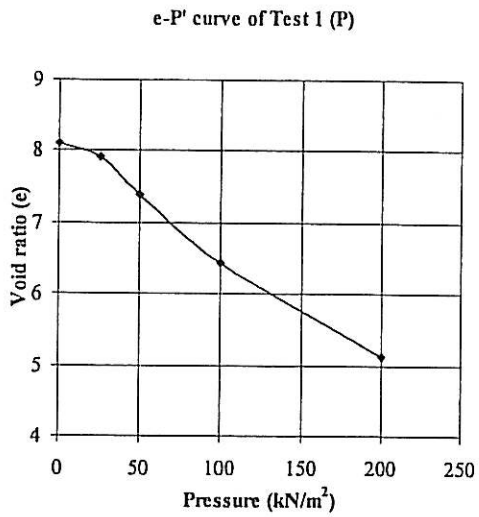

e-P' Test 1 Rowe Cell Results						
Consolidation pressure			**25 kPa**	**50 kPa**	**100 kPa**	**200 kPa**
Soil compression parameter	e_o		8.092			
	a_v	(p+s)	0.027	0.030	0.023	0.013
		(p)	0.007	0.021	0.019	0.0133
	m_v	(p+s)	0.00297	0.00330	0.0025	0.00143
		(p)	0.00077	0.00231	0.00209	0.00143

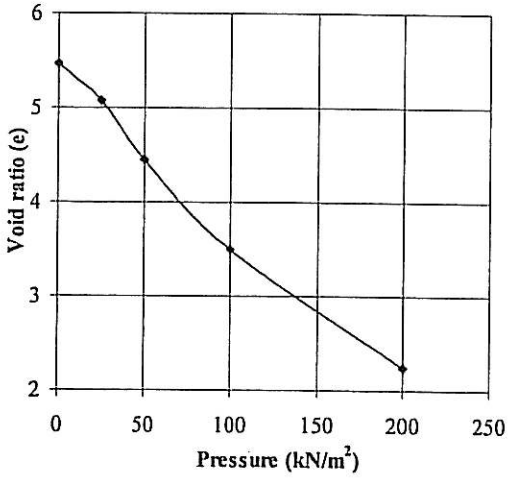

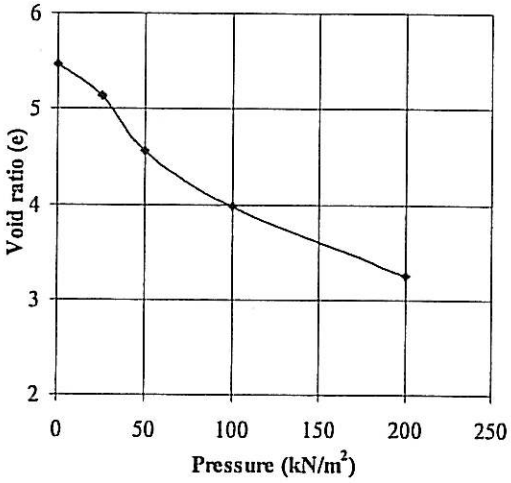

e-P' Test 2 Rowe Cell Results						
Consolidation pressure			**25 kPa**	**50 kPa**	**100 kPa**	**200 kPa**
Soil compression parameter	e_o		5.469			
	a_v	(p+s)	0.016	0.026	0.019	0.012
		(p)	0.013	0.024	0.011	0.007
	m_v	(p+s)	0.00241	0.00396	0.00294	0.00193
		(p)	0.00204	0.00365	0.00176	0.00113

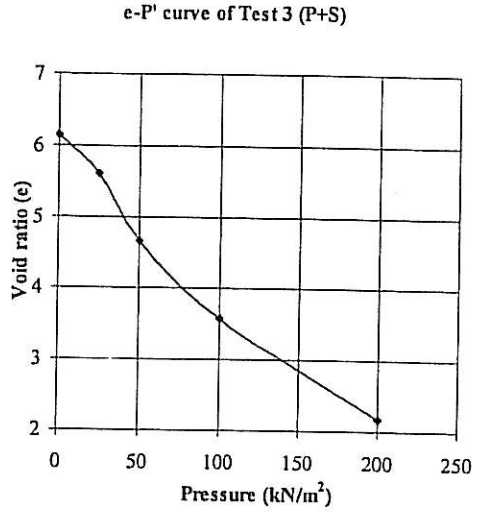

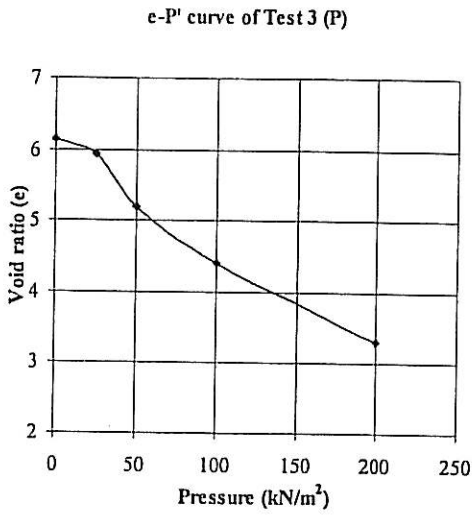

e-P' Test 3 Rowe Cell Results						
Consolidation pressure			**25 kPa**	**50 kPa**	**100 kPa**	**200 kPa**
Soil compression parameter	e_o		6.147			
	a_v	(p+s)	0.022	0.038	0.022	0.014
		(p)	0.009	0.030	0.022	0.014
	m_v	(p+s)	0.00302	0.00532	0.00302	0.00197
		(p)	0.00126	0.00420	0.00224	0.00154

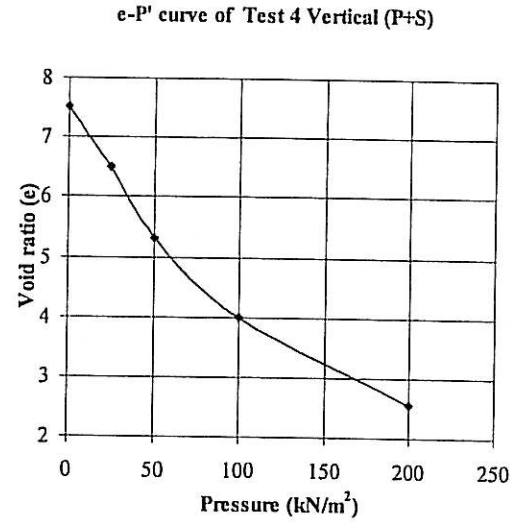

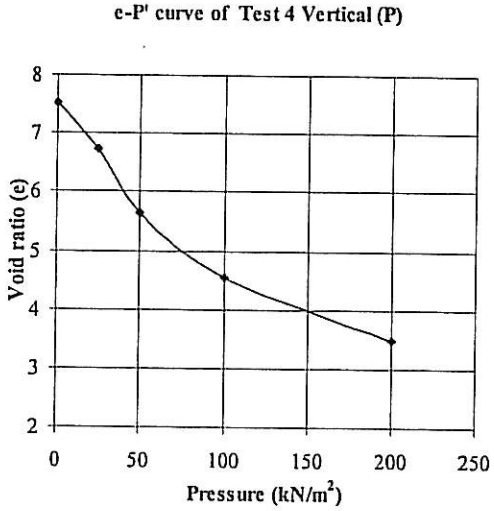

e-P' Test 4 Rowe Cell Results						
Consolidation pressure			**25 kPa**	**50 kPa**	**100 kPa**	**200 kPa**
Soil compression parameter	e_o		7.513			
	a_v	(p+s)	0.040	0.048	0.026	0.014
		(p)	0.032	0.043	0.022	0.011
	m_v	(p+s)	0.00470	0.00564	0.00305	0.00164
		(p)	0.00376	0.00505	0.00258	0.00129

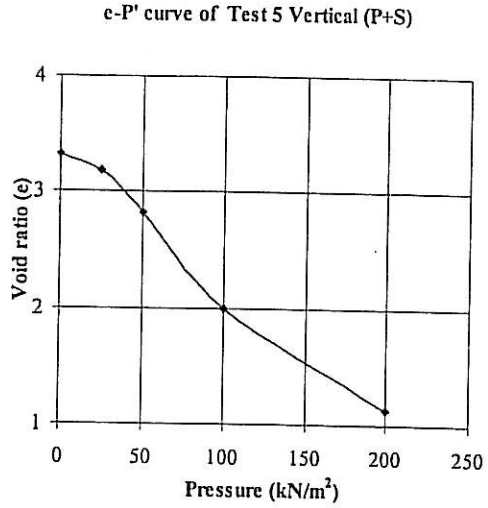

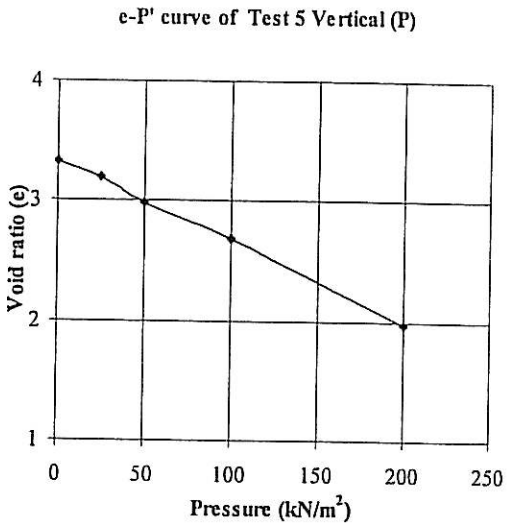

e-P' Test 5 Rowe Cell Results						
Consolidation pressure			**25 kPa**	**50 kPa**	**100 kPa**	**200 kPa**
Soil compression parameter	e_o		3.324			
	a_v	(p+s)	0.006	0.007	0.016	0.009
		(p)	0.005	0.009	0.006	0.007
	m_v	(p+s)	0.00139	0.00162	0.00370	0.00208
		(p)	0.00116	0.00208	0.00139	0.00162

Average e-P' Test Rowe Cell Results						
Consolidation pressure			**25 kPa**	**50 kPa**	**100 kPa**	**200 kPa**
Soil compression parameter	e_o		6.109			
	a_v	(p+s)	0.022	0.030	0.021	0.012
		(p)	0.013	0.025	0.015	0.010
	m_v	(p+s)	0.00290	0.00387	0.00834	0.00181
		(p)	0.00180	0.00283	0.00201	0.00140

3. Gibson and Lo Method

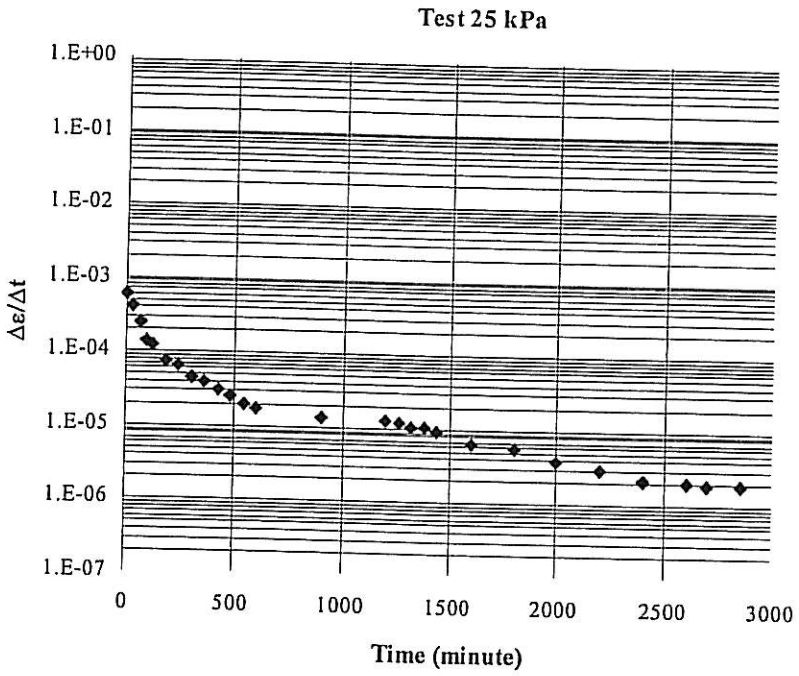

Typical data for stress increment 25 kPa				
Test No.	Rheological Parameter for Stress Incerement 25 kPa			
	a	b	λ	λ/b
1.	0.997	0.015	$1.4x10^{-6}$	$0.96x10^{-4}$
2.	0.995	0.015	$2.2x10^{-6}$	$1.47x10^{-4}$
3.	0.994	0.012	$3.2x10^{-6}$	$2.67x10^{-4}$
4.	0.997	0.014	$1.1x10^{-6}$	$0.80x10^{-4}$
5.	0.998	0.016	$1.0x10^{-6}$	$0.62x10^{-4}$
6.	0.994	0.013	$3.2x10^{-6}$	$2.46x10^{-4}$
7.	0.997	0.009	$1.3x10^{-6}$	$1.42x10^{-4}$
8.	0.990	0.018	$5.2x10^{-6}$	$2.89x10^{-4}$
9.	1.000	0.006	$0.1x10^{-6}$	$0.17x10^{-4}$
10.	1.000	0.001	$1.4x10^{-6}$	$0.14x10^{-4}$
Average	0.996	0.012	$2.01x10^{-6}$	$1.36x10^{-4}$

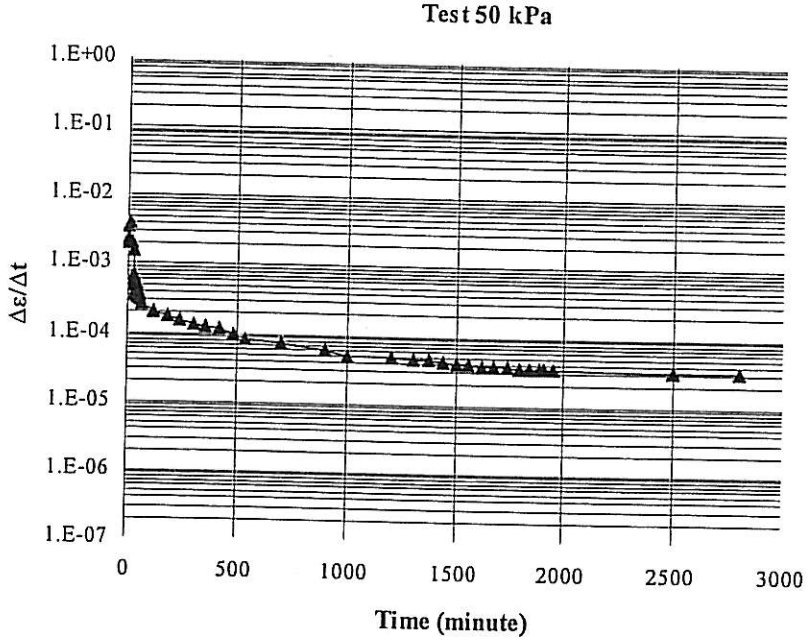

Typical data for stress increment 50 kPa				
Test No.	Rheological Parameter for Stress Incerement 50 kPa			
	a	b	λ	λ/b
1.	0.994	0.016	$3.7x10^{-6}$	$2.31x10^{-4}$
2.	0.994	0.027	$3.6x10^{-6}$	$1.33x10^{-4}$
3.	0.995	0.028	$2.6x10^{-6}$	$0.92x10^{-4}$
4.	0.997	0.027	$1.2x10^{-6}$	$0.44x10^{-4}$
5.	0.992	0.026	$3.6x10^{-6}$	$1.38x10^{-4}$
Average	0.994	0.025	$2.94x10^{-6}$	$1.28x10^{-4}$

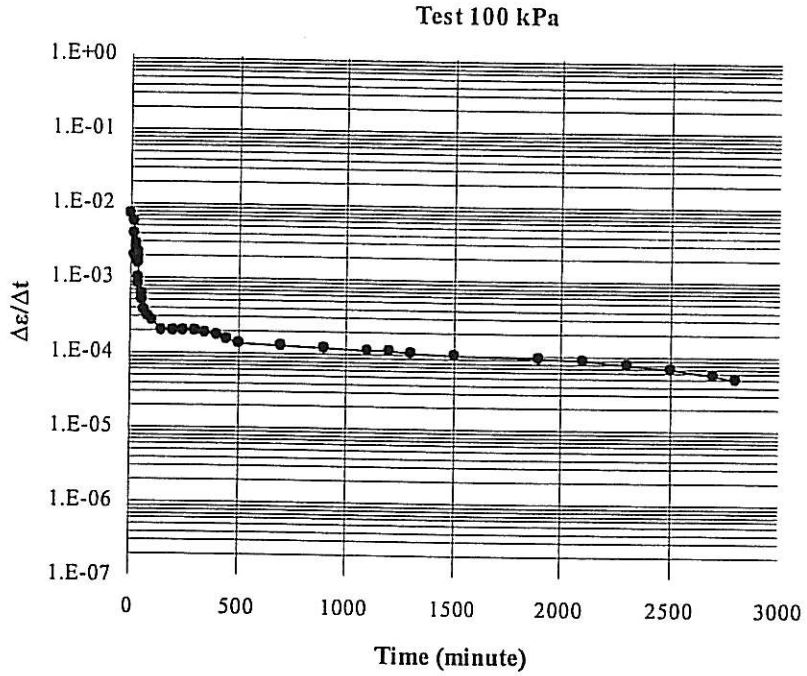

Typical data for stress increment 100 kPa				
Test No.	Rheological Parameter for Stress Incerement 100 kPa			
	a	b	λ	λ/b
1.	0.999	0.050	$7.1x10^{-6}$	$1.29x10^{-4}$
2.	0.994	0.027	$3.6x10^{-6}$	$1.33x10^{-4}$
3.	0.996	0.064	$1.8\ x10^{-6}$	$0.28x10^{-4}$
4.	0.997	0.064	$1.3\ x10^{-6}$	$0.20x10^{-4}$
5.	0.995	0.055	$1.9\ x10^{-6}$	$0.34x10^{-4}$
Average	0.996	0.052	$3.14x\ 10^{-6}$	$0.67x10^{-4}$

4. Hydraulic Consolidation Test for The Effect of Surcharge

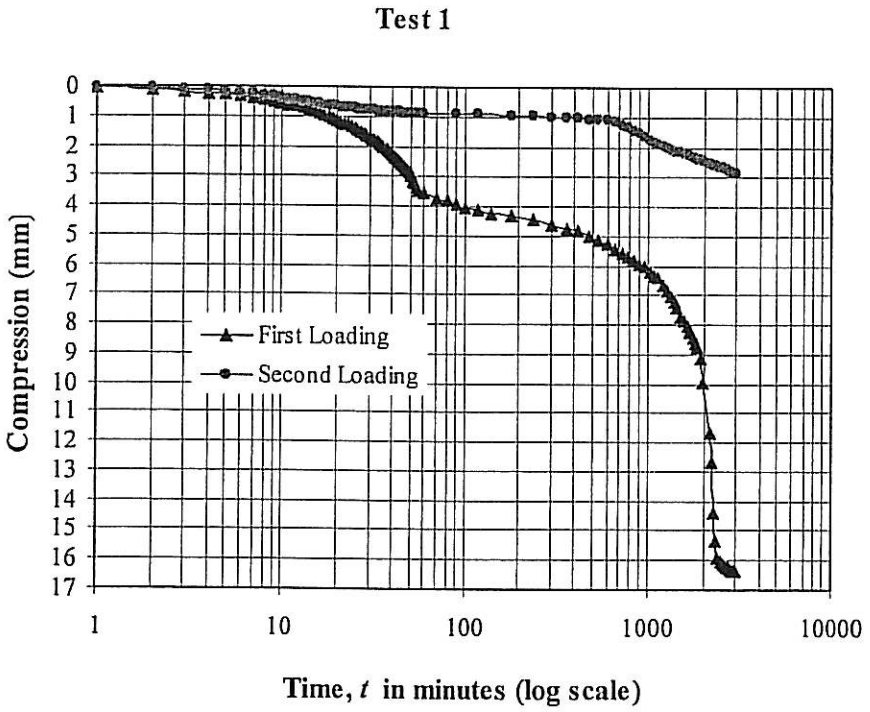

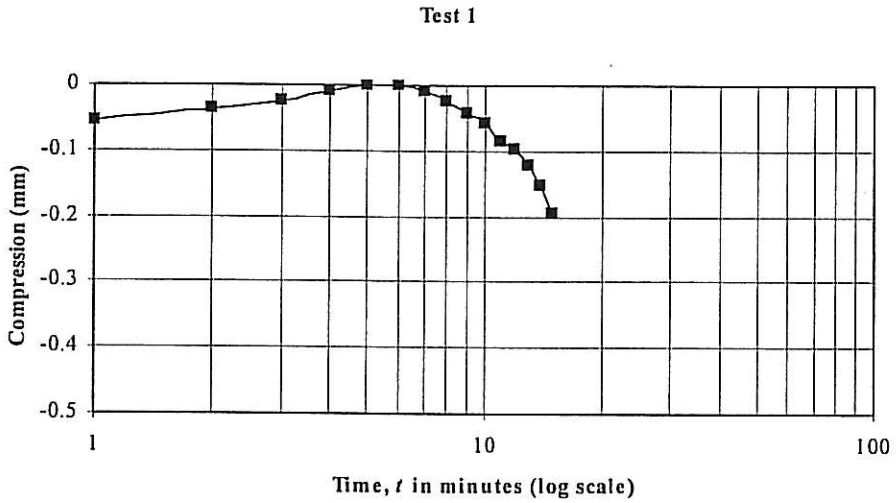

Results of Hydraulic Consolidation Test 1 for The Effect of Surcharge		
Soil compression parameter	First Loading	Second Loading
t_p (minutes)	60	40
c_α	0.004	0.001
c''_α	0.0044	
e_o (at t_p)	4.326	
e_o	8.308	

Test 2.

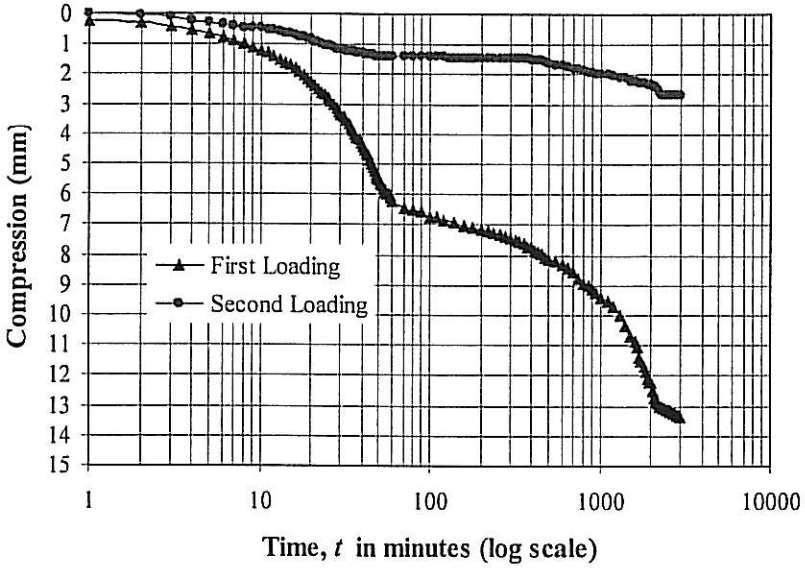

Test 2

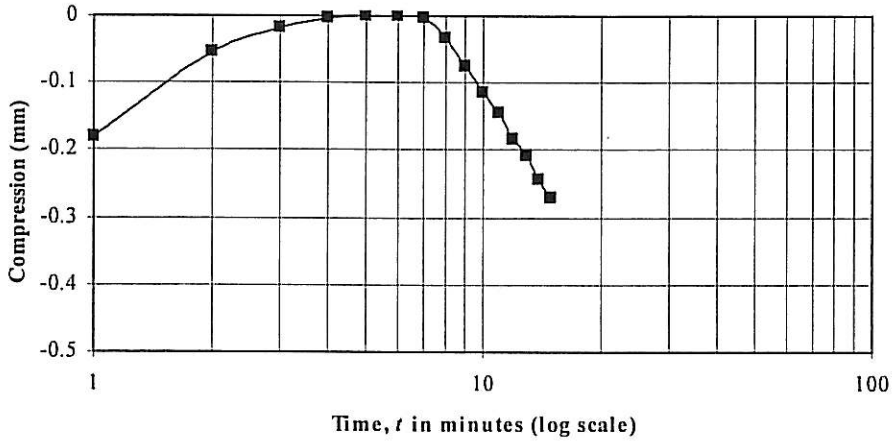

Results of Hydraulic Consolidation Test 2 for The Effect of Surcharge		
Soil compression parameter	First Loading	Second Loading
t_p (minutes)	58	48
c_α	0.008	0.001
c''_α	0.0038	
e_o (at t_p)	5.175	
e_o	8.181	

Test 3

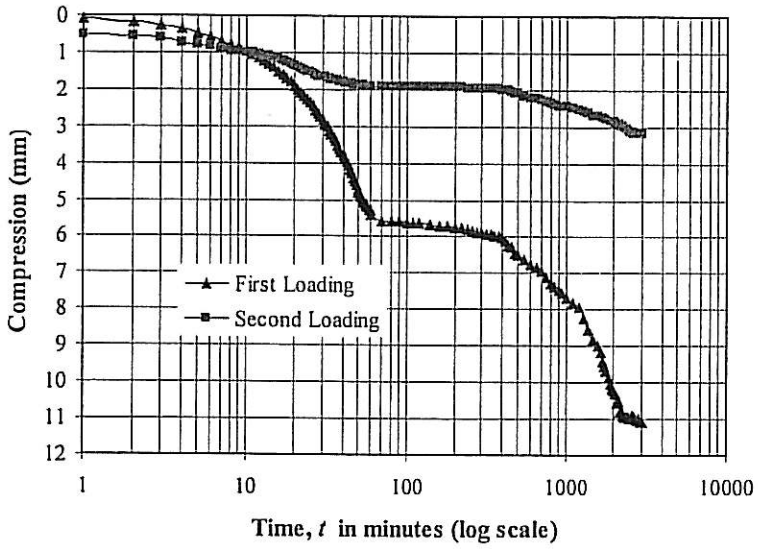

Test 3

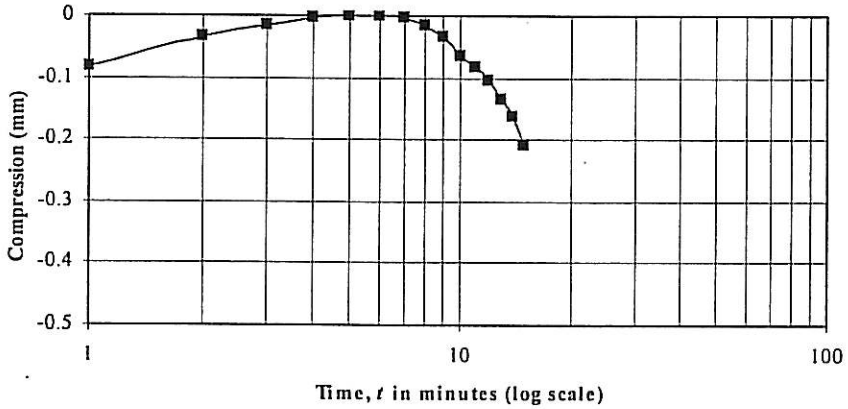

Results of Hydraulic Consolidation Test 3 for The Effect of Surcharge		
Soil compression parameter	First Loading	Second Loading
t_p (minutes)	60	55
c_α	0.010	0.001
c''_α	0.0032	
e_o (at t_p)	4.930	
e_o	8.092	

Average of Hydraulic Consolidation Test for The Effect of Surcharge		
Soil compression parameter	First Loading	Second Loading
t_p (minutes)	59	48
c_α	0.008	0.001
c''_α	0.0038	
e_o (at t_p)	4.810	
e_o	8.193	

5. Hydraulic Permeability Test

Type of permeability test	Hydraulic permeability test	Consolidation Pressure (kPa)	Coefficient of permeability at 20° C
Double Vertical Drainage	Test 1	200	k_v (20°C) = 2.36×10^{-10} m/s
	Test 2	200	k_v (20°C) = 8.82×10^{-10} m/s
	Test 3	200	k_v (20°C) = 3.43×10^{-9} m/s
	Test 4	200	k_v (20°C) = 1.54×10^{-9} m/s
	Test 5	200	k_v (20°C) = 4.02×10^{-10} m/s
Average			k_v (20°C) = 1.30×10^{-9} m/s

Apparatus

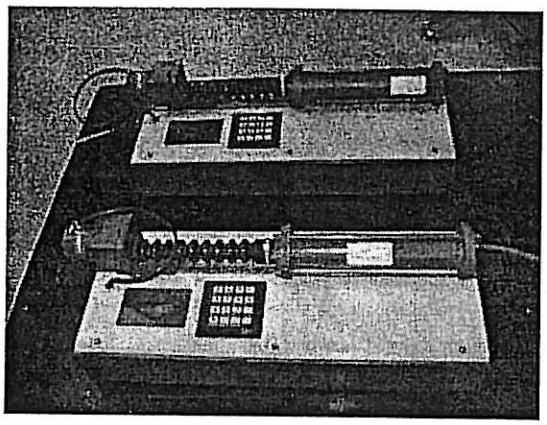

Figure C1: Two independently controlled water pressure systems, giving maximum pressure up to 1000 kPa used for hydraulic consolidation and permeability tests in laboratory

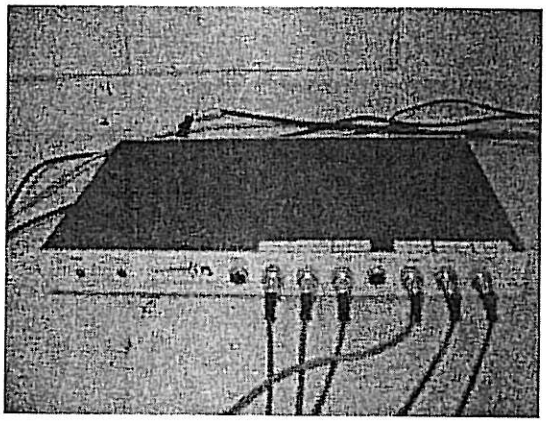

Figure C2: Power supply and readout unit for the electric pore pressure transducer

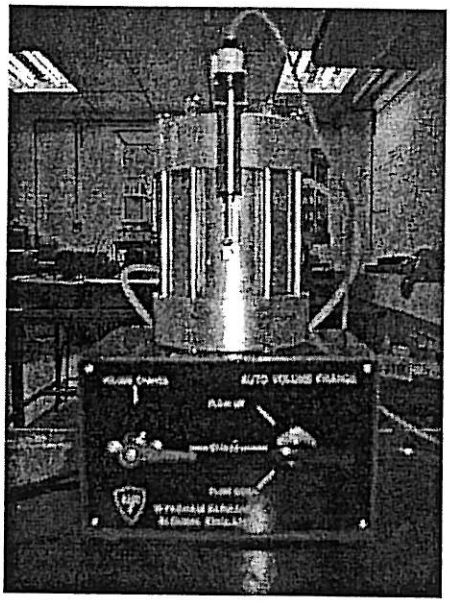

Figure C3: Volume change gauge

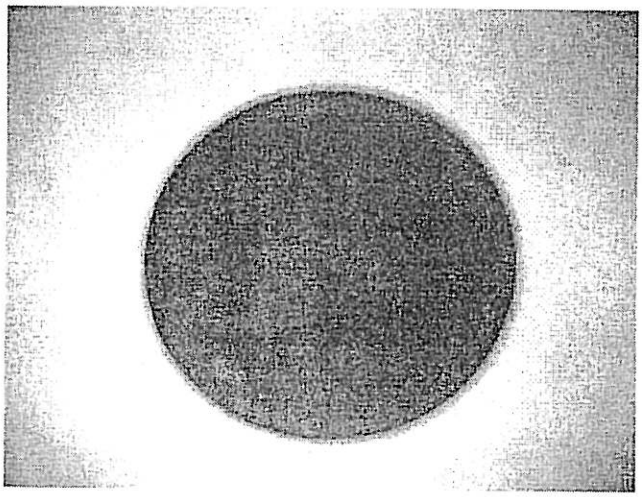

Figure C4: Sintered bronze disc of 4 mm thickness

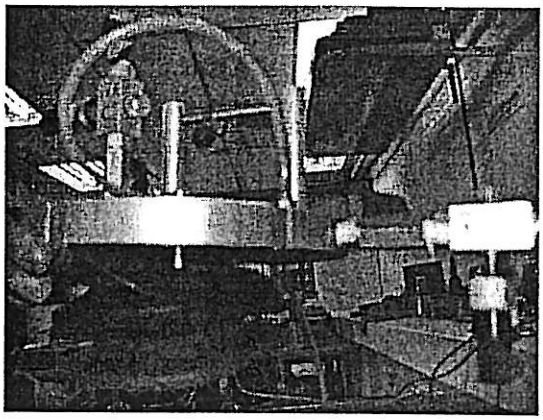

Figure C5: Rowe cell top attached to diaphragm

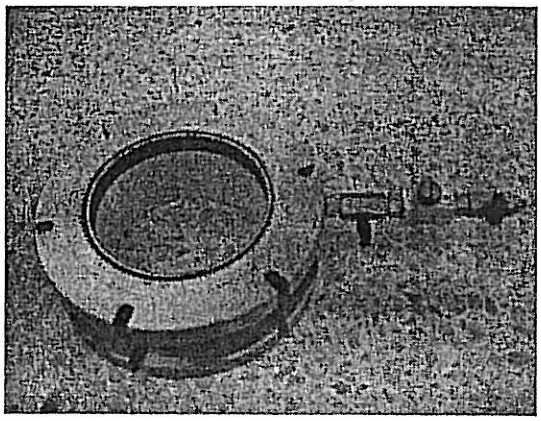

Figure C6: Rowe cell body of 151.4 mm internal diameter

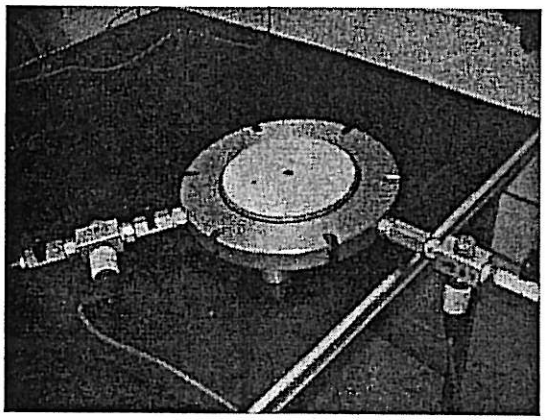

Figure C7: Rowe cell base

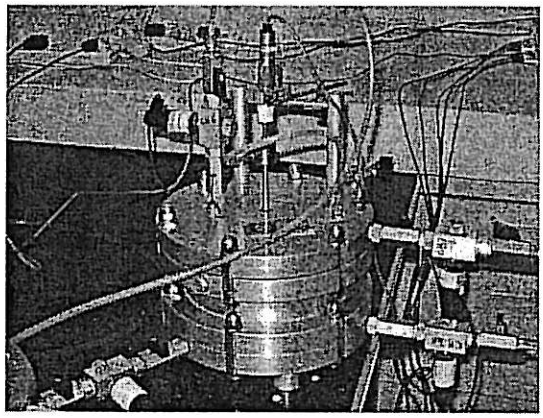

Figure C8: Bolt tightened Rowe cell connected to linear transducer

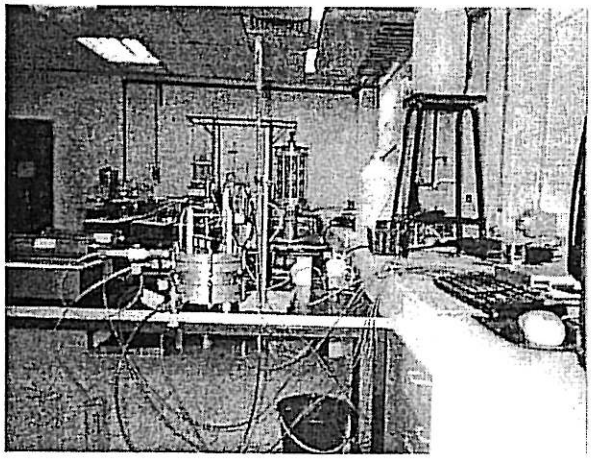

Figure C9: A burette connected to Rowe consolidometer for hydraulic permeability test

APPENDIX F

Steps for various methods used for settlement evaluation

1. Casagrande's method based on settlement curve

For a typical consolidation pressure, the settlement of soil is plotted against the logarithmic of time. A typical consolidation curve of Casagrande's method based on settlement curve is shown in Figure F1. The following steps with reference to Figure F1 are needed to evaluate vertical or horizontal coefficient of consolidation (c_v) and coefficient of secondary compression (c_α) of soil:

Step 1: Project the straight portions of the primary consolidation and secondary compression to intersect at A. The ordinate of A, d_{100}, is the settlement for 100% primary consolidation.

Step 2: For the initial portion of the consolidation curve, which is parabolic in shape, select times, t_A and t_B with their corresponding settlements (d_A and d_B) such that the initial settlement for 0% primary consolidation, d_0 is defined as follows:

$$d_0 = \frac{d_A\sqrt{t_B} - d_B\sqrt{t_A}}{\sqrt{t_B} - \sqrt{t_A}}$$

Note that the selected times, t_A and t_B must be within the time corresponding to average degree of consolidation, $U < 60\%$.

Step 3: Calculate the ordinate for 50% primary consolidation as $d_{50} = (d_0 + d_{100})/2$. Draw a horizontal line through this point to intersect the curve at B. The abscissa of point B is the time for 50% primary consolidation, t_{50}.

Step 4: With equal strain loading condition, the theoretical time factors for 50% primary consolidation for one-dimensional two-way vertical and drainage is 0.197 (Table 3.1) and the vertical coefficient of rate consolidation (c_v) for the soil :

$$c_v = \frac{T_{50}\,H^2}{t_{50}} = \frac{0.197\,H^2}{t_{50}}$$

and the coefficient of secondary compression is :

$$c_\alpha = \frac{\Delta H_s / H_o}{\mathrm{Log}(t_2/t_1)}$$

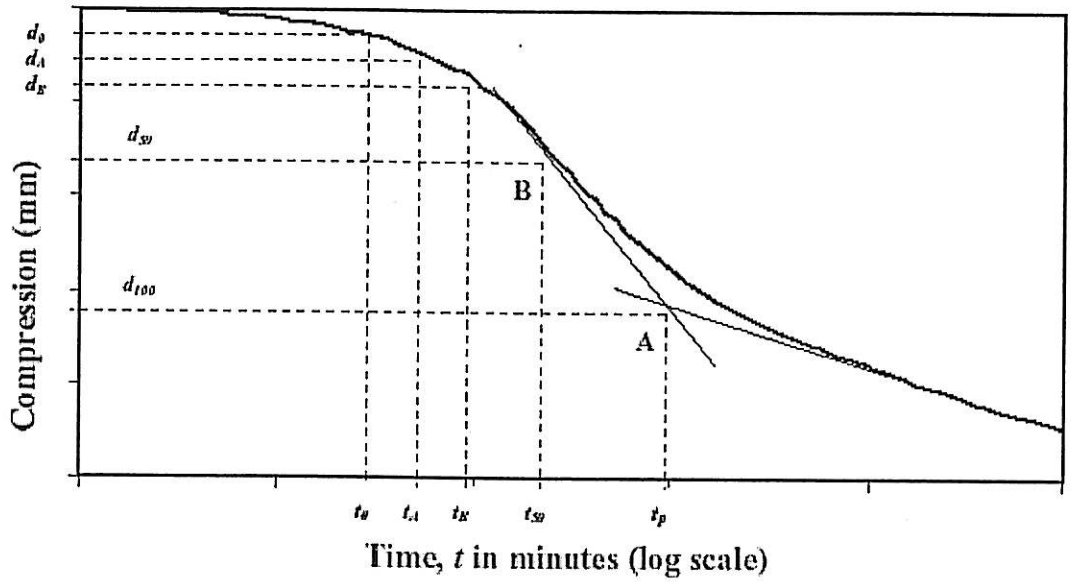

Figure F1: A typical consolidation curve of the fibrous peat soil analyzed by Casagrande's method based on settlement

2. Taylor's method

In this method, a plot of settlement versus the square root of time is drawn for a typical consolidation pressure as shown in Figure F2. The steps to determine the vertical coefficient of rate of consolidation (c_v) of soil for Taylor's method with reference to Figure F2 are as follows:

Step 1: Plot the settlements versus square root of times.

Step 2: Draw the best straight line through the initial part of the curve intersecting the ordinate at O and the abscissa ($\sqrt{}$time) at A. Note that the ordinate at O is defined as the beginning of initial compression based on Taylor's method.

Step 3: The time at point A is noted as $\sqrt{t_A}$.

Step 4: Locate a point B, 1.15 $\sqrt{t_A}$, on the abscissa.

Step 5: Join OB.

Step 6: The intersection of the line OB with the curve, point C, gives the settlement and the time for 90% degree of consolidation (t_{90}). It should be noted that the value read off the abscissa is $\sqrt{t_{90}}$ and as such, when the average degree of consolidation, U is equal to 90%, the theoretical factors for one-dimensional two-way vertical consolidation with equal strain loading condition is 0.848 respectively (Table 3.1). Thus, the coefficient of rate of consolidation for the soil are defined by :

$$c_v = \frac{0.848\ H^2}{t_{90}}$$

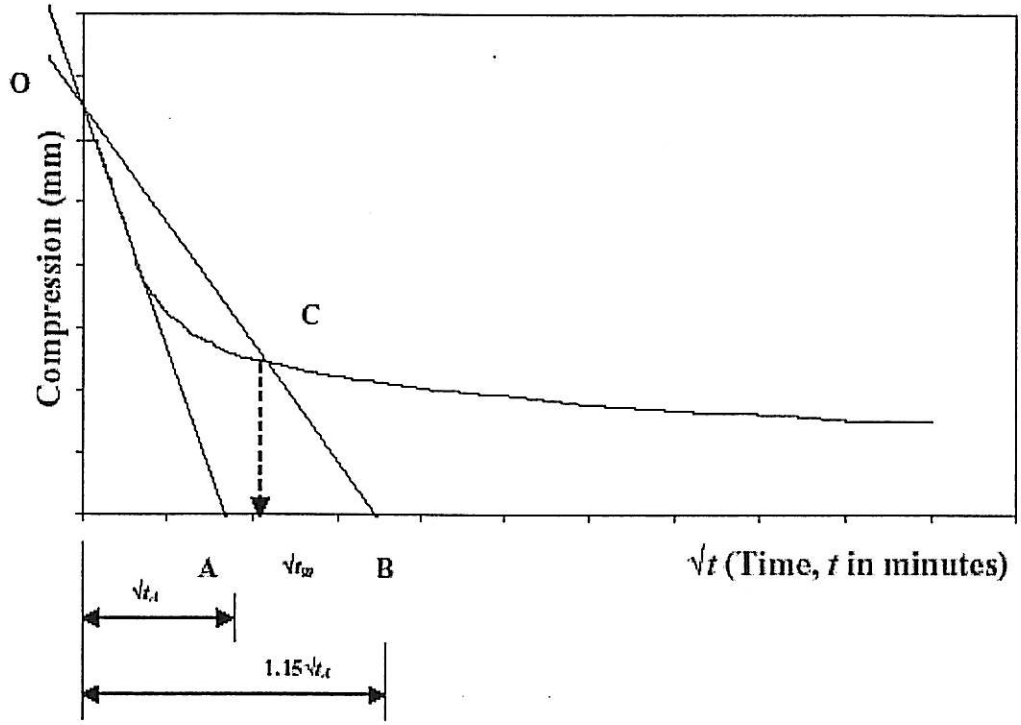

Figure F2: A typical consolidation curve of the fibrous peat soil analyzed by Taylor's method

3. Extended Casagrande's method

This method is suitable to evaluate the log time-compression curve when tertiary compression is evident in addition to secondary compression as part of long-term compression of soil. With reference to Figure F4, steps for evaluating the vertical coefficient of consolidation (c_v) and coefficient of secondary compression (denoted as $c_{\alpha 1}$) of soil are similar to those of Casagrande's method based on settlement curve with addition to the following step:

Step 1: Project the straight portions of the secondary compression and the tertiary compression to intersect at C. The ordinate at C is the point that signifies the end of secondary compression and the beginning of tertiary compression (t_s) of soil. Corresponding to the point, coefficient of tertiary compression ($c_{\alpha 2}$) of soil is defined as :

$$c_{\alpha 2} = \frac{\Delta H_t / H_o}{\text{Log}(t_s/t_p)}$$

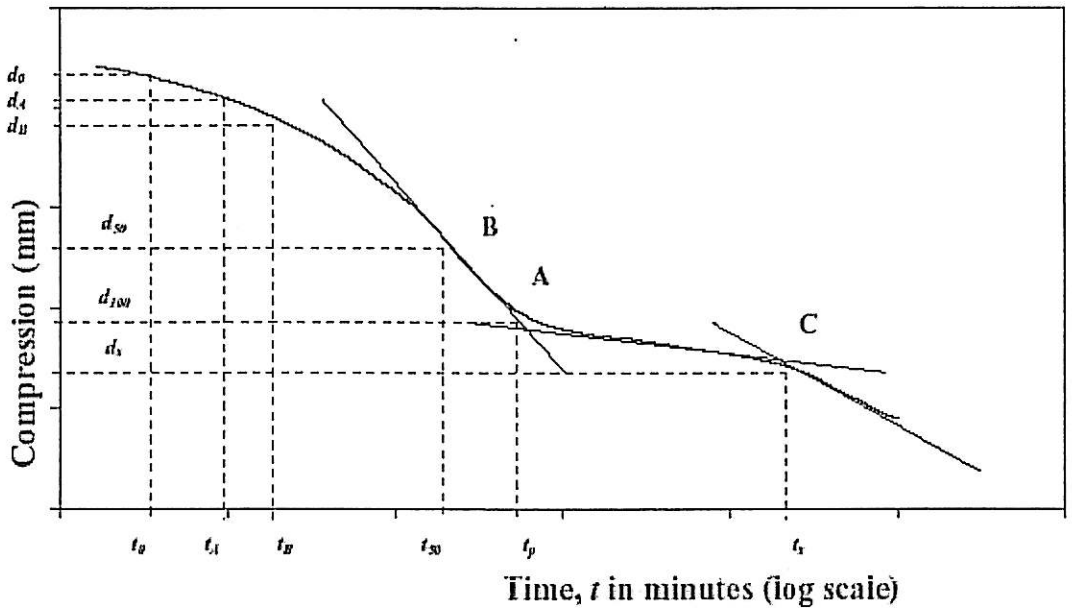

Figure F3: A typical consolidation curve of the fibrous peat soil analyzed by extended Casagrande's method

4. Sridharan and Prakash's method

For a typical consolidation pressure, the method considers a relationship between logarithmic of compression and logarithmic of time of soil as shown in Figure F4a. Such method can only be used to evaluate vertical coefficient of consolidation (c_v) and coefficient of secondary compression (c_α) of soil since Sridharan and Prakash (1998) only developed the theoretical curve using the method for one-dimensional vertical consolidation (Figure F4b).

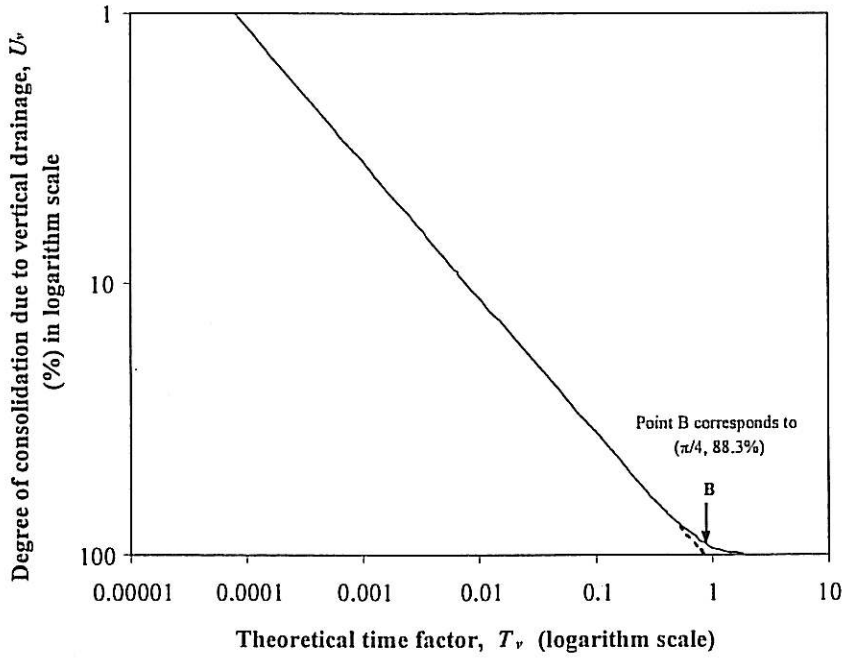

Figure F4b: Theoretical log U_v - log T_v plot (Source: Sridharan and Prakash, 1998)

Using the method, steps for evaluating vertical coefficient of consolidation (c_v) and coefficient of secondary compression (c_α) of soil are as follows:

Step 1: Plot the logarithmic of compression versus the logarithmic of time.

Step 2: Project the straight portions of the primary consolidation and secondary compression to intersect at A. The point of intersection at A between the two linear portions is regarded as the end of primary consolidation and the beginning of secondary compression of soil.

Step 3: The beginning of primary consolidation of soil is determined for the consolidation curve using Casagrande's method based on settlement curve.

Step 4: Calculate the ordinate for 88.3% primary consolidation as $d_{88.3} = (d_0 + d_{100})$ x (88.3/100). Draw a horizontal line through this point to intersect the curve at B. The abscissa of point B is the time for 88.3% primary consolidation, $t_{88.3}$.

Step 5: Using the method, the theoretical factor of 88.3% primary consolidation is $\pi/4$ for one-dimensional vertical consolidation. As such, the vertical coefficient of consolidation of soil is defined as $c_v = (\pi/4) \times H^2 / t_{88.3}$ whereas, the coefficient of secondary compression (c_α) of soil is defined as :

$$m = \frac{\log (\Delta\delta_s / H_0)}{\log (t_2 / t_1)}$$

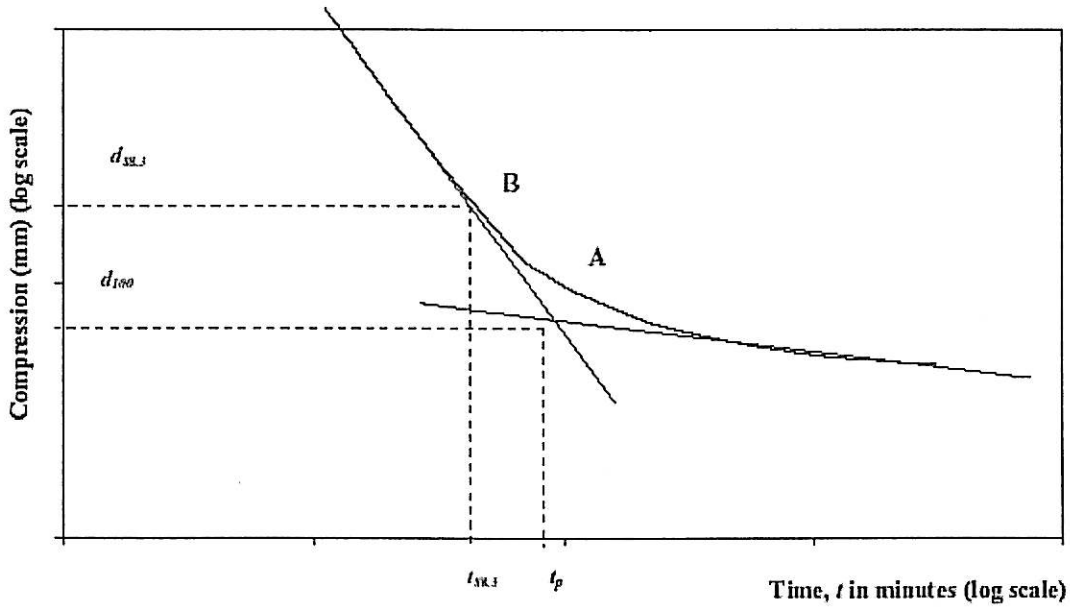

Figure F4a: A typical consolidation curve of the fibrous peat soil analyzed by Sridharan and Prakash's method

5. Robinson (Excess pore water pressure dissipation curve)

In this method, the dissipation of excess pore water pressure measured at the central base of Rowe consolidometer is plotted against the square root of time for a typical consolidation pressure as shown in Figure F5a. Steps for evaluating vertical and horizontal coefficient of consolidation (c_v and c_h) of soil based on pore water pressure measurement are illustrated as follows:

Step 1: Plot the dissipation of excess pore water pressure in percentage versus the logarithmic of time. The dissipation of excess pore water pressure is expressed by the following equation:

$$\mathbf{U\ (\%) = [(u_o - u) / (u_o - u_b)]\ x\ 100}$$

where,

U = dissipation of excess pore water pressure (%)
$\mathbf{u_o}$ = Initial excess pore water pressure
u = Excess pore water pressure at any time
$\mathbf{u_b}$ = Back pressure which is taken as 10 kPa

Step 2: The starting and ending points of the excess pore water pressure dissipation curve are defined as the beginning and ending of primary consolidation of the soil (d_0 and d_{100}) and their corresponding times are denoted by t_0 and t_{100} respectively. Calculate the ordinate for 50% primary consolidation as $d_{50} = (d_0 + d_{100})/2$. Draw a horizontal line through this point to intersect the curve at A. The abscissa of point A is the time for 50% primary consolidation, t_{50}.

Step 3: With equal strain loading condition, the theoretical time factors for 50% primary consolidation for one-dimensional two-way vertical consolidation is 0.197. Therefore based on pore water pressure measurement, vertical coefficient of rate of consolidation (c_v) of soil is defined by :

$$c_v = \frac{0.131\ Tv\ H^2}{t_{50}}$$

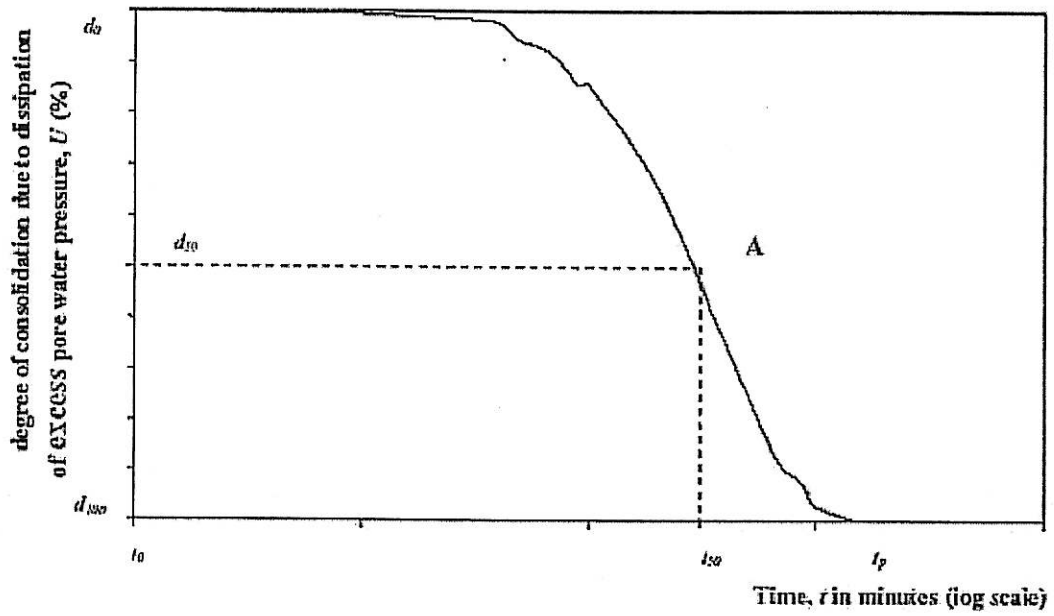

Figure F5a: A typical excess pore water pressure dissipation curve of the fibrous peat soil based on pore water pressure measurement

The method considers that secondary compression actually begins during the dissipation of excess pore water pressure from soil. Using the method, steps for evaluating vertical coefficient of rate of consolidation (c_v) and coefficient of secondary compression (c_α) of soil are as follows:

Step 1: Plot the settlement versus the dissipation of excess pore water pressure (in percentage) of soil as shown in Figure F5b. The point (Point A) where the plot deviates from linearity at the later consolidation stage is regarded as the beginning of secondary compression of soil. With reference to Figure F5b, the deviation from linearity represented by δ_s is the secondary compression during the dissipation of excess pore water pressure from soil.

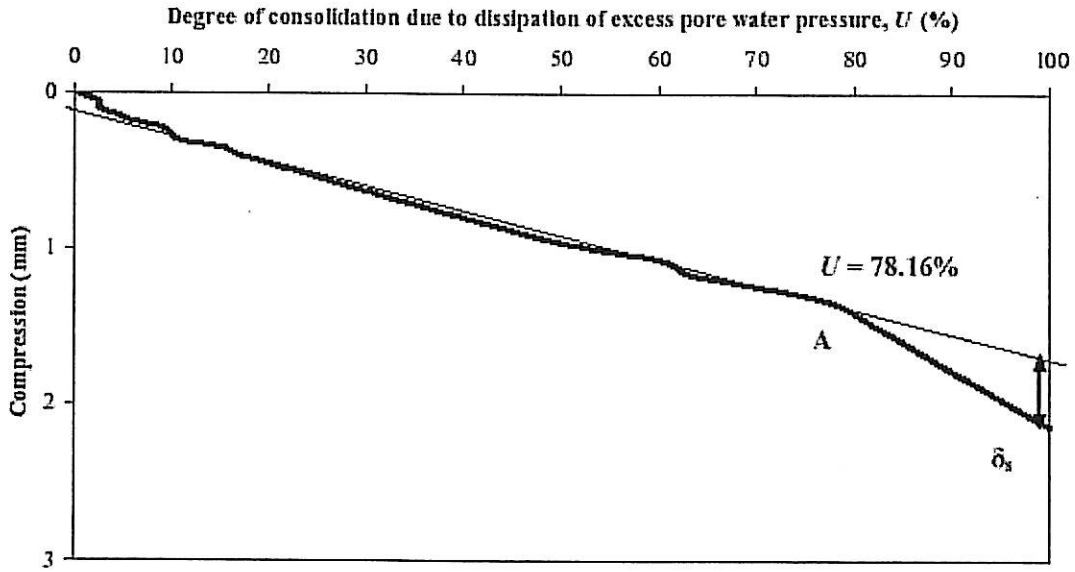

Figure F5b: A typical degree of consolidation due to dissipation of excess pore water pressure (U_b) – compression plot of the fibrous peat soil

Step 2: Plot the total compression corresponding to the dissipation of excess pore water pressure from soil against the logarithmic of time as shown in Figure F5c(1).

Step 3: Subtract the secondary compression (δ_s) during the dissipation of excess pore water pressure from the total compression of soil to give primary consolidation of soil free from the influence of secondary compression.

Step 4: Plot the primary consolidation versus the logarithmic of time of soil as shown in Figure F5c(2). The starting and ending ordinates of the primary consolidation curve are regarded as the beginning and ending of primary consolidation (d_0 and d_{100}) of soil respectively. There corresponding times are denoted by t_0 and t_{100} respectively.

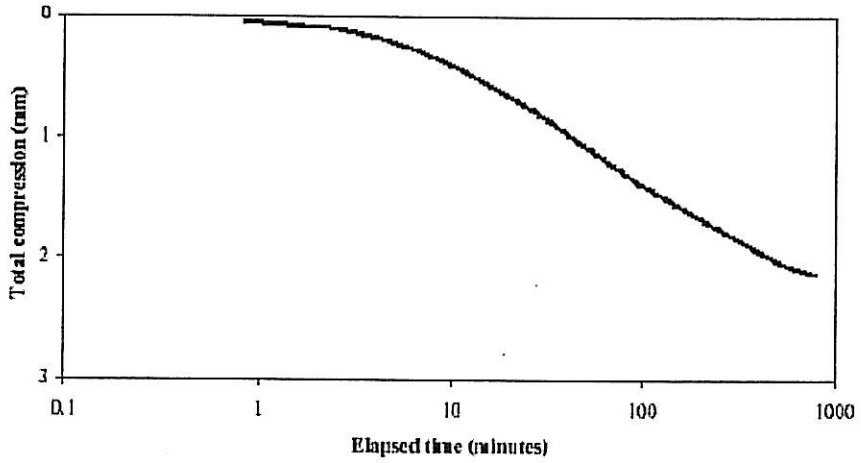

(1)

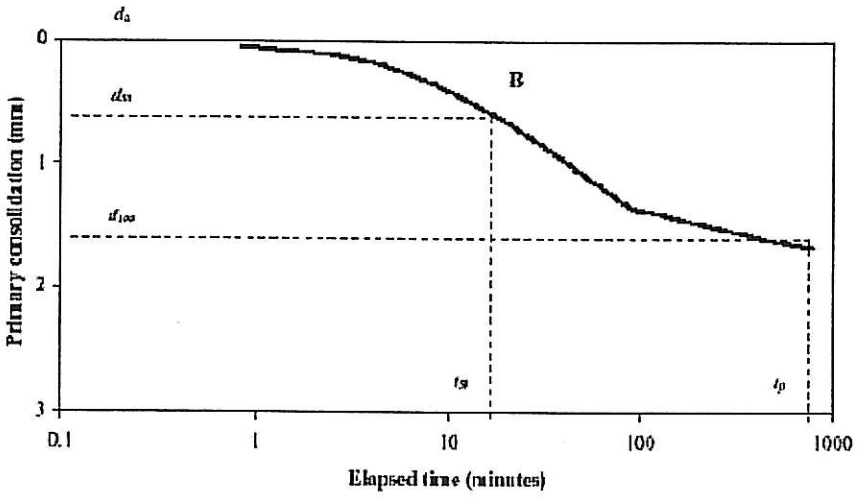

(2)

Figure F5c: A typical graphical plot for the analysis on the beginning of secondary compression of the fibrous peat soil using Robinson's method (1) Log time-total

compression curves (2) Log time-primary consolidation curves after removing the secondary compression

Step 5: With equal strain loading condition, the theoretical time factors for 50% primary consolidation for one-dimensional two-way vertical consolidation is 0.197 and as such, the vertical coefficient of rate of consolidation (c_v) for the soil is defined by :

$$c_v = \frac{0.197\,H^2}{t_{50}}$$

Whereas as the soil's coefficient of secondary compression is defined as :

$$c_\alpha = \frac{\Delta H_s / H_o}{\mathrm{Log}(t_2/t_1)}$$

Step 6: Plot the secondary compression during the dissipation of excess pore water pressure from soil (δ_s) against their corresponding time ($t - t_o$) as shown in Figure F5d. The coefficient of secondary compression of soil (c_α) is determined by dividing the slope of the linear relationship between the secondary compression during the dissipation of excess pore water pressure from soil (δ_s) and their corresponding time ($t - t_o$), by the thickness of the consolidating soil layer, H.

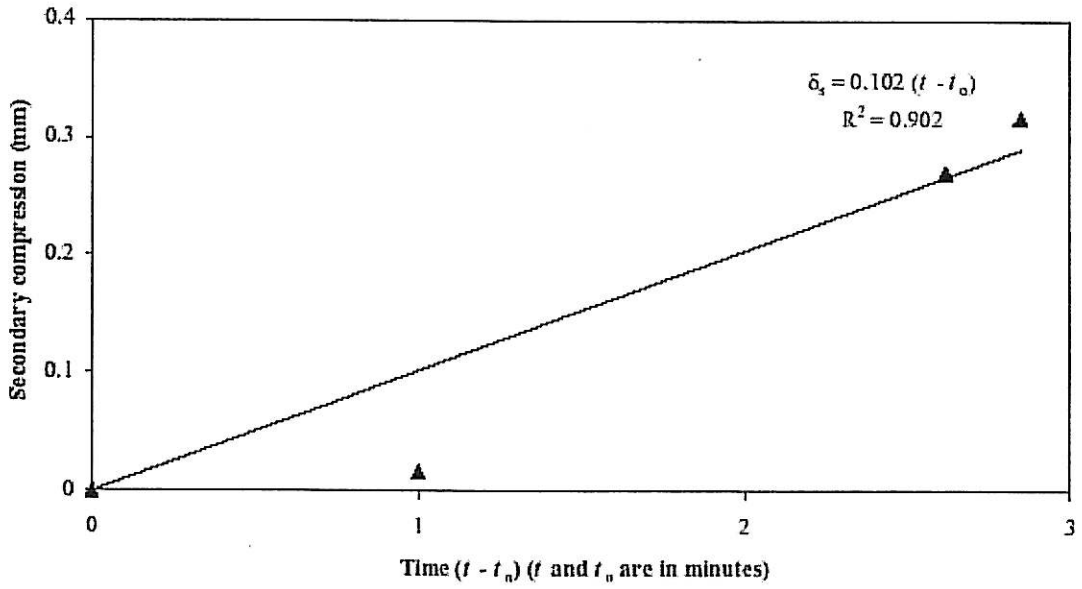

Figure F5d: A typical graphical plot for the determination of coefficient of secondary compression, c_α of the fibrous peat soil analyzed by Robinson's method

6. Gibson and Lo method

Gibson and Lo method was basically developed for estimation of the total settlement of peat. It does not give the values for c_v and t_p. The evaluation is based on curve of time dependent strain vs time as shown in Figure 6.

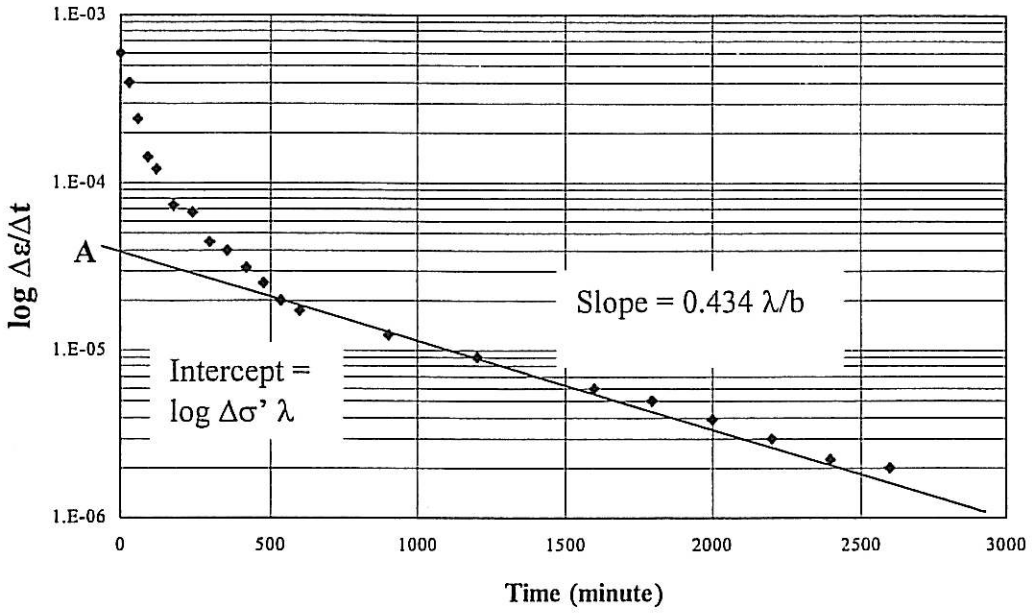

Figure F6: Theoretical log Log Δe/Δt vs t plot (Source: Mokhtar, 1997)

The steps for evaluating the settlement of foundation on peat are as follows:

Step 1: Plot the logarithmic of time dependent strain versus time

Step 2: Project the straight portions of the curve to intersect the ordinate at A. The intercept is equal to log Δσ' λ and the slope of the straight line is equal to 0.434 λ/b.

Step 3: If the pressure increment given to the soil (Δσ) is known, then λ =intercept/Δσ.

Step 4: From the slope and the value of λ, calculate the secondary compression index b.

Step 5: Using the relationship $\varepsilon(t) = \Delta\sigma\left[a - b\left(1 - e^{-(\lambda/b)t}\right)\right]$, estimate the value of *a*:

$$a = \frac{\varepsilon(t)}{\Delta\sigma} - b + b\,e^{-(\lambda/b)t}$$

where ε(t) is the reading at t.